DRAFT

(last updated 25 June 2010)

Technical Description for the Coupled Carbon-Nitrogen Component of the Community Land Model, version 4 (CLM4-CN)

Peter E. Thornton[1], Samuel Levis[2]

[1]Environmental Sciences Division, Oak Ridge National Laboratory,

[2]Climate and Global Dynamics Division, National Center for Atmospheric Research

1 Introduction

This technical note describes the logical structure and numerical implementation of the Community Land Model with prognostic Carbon and Nitrogen cycles (CLM-CN), as implemented within version 4 of the Community Land Model (CLM4). CLM4 is the land surface parameterization component of version 1 of the Community Earth System Model (CESM1). CLM-CN is an optional component of CLM4 which estimates states and fluxes of carbon and nitrogen for vegetation, litter, and soil organic matter, and associated exchange with the atmosphere. When activated, CLM-CN replaces the diagnostic treatment of vegetation structure (e.g. leaf area index and canopy height) in CLM4 with prognostic variables.

Chapter 1 provides background on the development history of CLM-CN, describes the relationship of CLM-CN and this technical note to previous model descriptions, and summarizes the model structure and process representation. Chapter 2 describes the treatment of prognostic vegetation canopy structure. Chapters 3-7 cover the physiological processes controlling states and fluxes of carbon and nitrogen in vegetation. Chapter 8 describes the model structure for litter and soil organic matter pools of carbon and nitrogen, and the controls on decomposition. Chapter 9 describes the sources and sinks of nitrogen, and the supply of and demand and competition for mineral nitrogen (i.e. the nitrogen economy). Chapters 10 and 11 explain the sub-models dealing with fire and anthropogenic landcover change. Chapter 12 describes the implementation of stable carbon isotope (^{13}C) states and fluxes. Chapter 13 explains the mechanism used to ensure mass balance for carbon and nitrogen. Chapter 14 provides theoretical and methodological details on model initialization, and Chapter 15 describes the model input requirements that are unique to CLM-CN. Chapter 16 documents the configuration of and results from a benchmark simulation in which CLM-CN is driven in offline mode with reanalysis surface weather fields for the period 1948-2004. All references are gathered in Chapter 17.

1.1 Model History

This section describes the historical progression of model development that resulted in CLM-CN. Model evaluation studies accompanying major development efforts are also briefly described.

1.1.1 Biome-BGC

Many of the ideas incorporated in CLM-CN derive from the earlier development of the offline ecosystem process model Biome-BGC (Biome BioGeochemical Cycles), originating at the Numerical Terradynamic Simulation Group (NTSG) at the University of Montana, under the guidance of Prof. Steven Running. Biome-BGC itself is an extension of an earlier model, Forest-BGC (Running and Coughlan, 1988; Running and Gower, 1991), which simulates water, carbon, and, to a limited extent, nitrogen fluxes for forest ecosystems. Forest-BGC is designed to be driven by remote sensing inputs of vegetation structure, and so uses a diagnostic (prescribed) leaf area index, or, in the case of the dynamic allocation version of the model (Running and Gower, 1991), prescribed maximum leaf area index.

Biome-BGC expands on the Forest-BGC logic by introducing a more mechanistic calculation of leaf and canopy scale photosynthesis (Hunt and Running, 1992), and extending the physiological parameterizations to include multiple woody and non-woody vegetation types (Hunt et al., 1996; Running and Hunt, 1993). Later versions of Biome-BGC introduced more mechanistic descriptions of belowground carbon and nitrogen cycles, nitrogen controls on photosynthesis and decomposition, sunlit and shaded canopies, vertical gradient in leaf morphology, and explicit treatment of fire and harvest disturbance and regrowth dynamics (Kimball et al., 1997; Thornton, 1998; Thornton et al., 2002; White et al., 2000). Biome-BGC version 4.1.2 (Thornton et al., 2002) provided a point of departure for integrating new biogeochemistry components into CLM.

1.1.2 CLM2.0

At the March 2001 meeting of the CCSM Biogeochemistry Working Group (BGCWG) in Berkeley, CA, preliminary plans were made for the development of new biogeochemistry capabilities in the CCSM land model. At that time development was

underway on a fully-coupled climate-carbon cycle model, building on the CCSM version 1.0 framework (I. Fung and S. Doney). At the same time a new version of the CCSM land model was under development, merging development within the NCAR Land Surface Model (LSM) (Bonan, 1996; Bonan, 1998) and the Common Land Model (Dai et al., 2003; Zeng et al., 2002). This merged land model under development was named the Community Land Model (CLM2.0), which was released to the community in May 2002 (Bonan et al., 2002). One result of the CCSM BGCWG meeting in March 2001 was the identification of the main biogeochemical elements that should be added to CLM2.0, including prognostic leaf area and phenology, carbon-nitrogen coupling, and explicit representation of disturbance.

1.1.3 CLM2.1

At the March 2002 joint meeting of the CCSM BGCWG and Land Model Working Group (LMWG) in Boulder, CO, P. Thornton introduced a new code structure for CLM that included a hierarchical organization of data structures representing sub-grid heterogeneity. Sub-grid levels in the hierarchy are landunits (geomorphically distinct sub-grid regions such as glacier, lake, urban, and vegetation), columns (representing regions of uniform soil properties), and plant functional types (PFTs). The new structure was shown to reproduce exactly the results of CLM2.0, while providing the architecture necessary for a clear representation of the biogeochemistry components identified at the 2001 BGCWG meeting. CLM2.1 did not include coupled carbon and nitrogen cycles, but did introduce the ability for multiple PFTs to coexist on a single soil column, where they compete for water.The joint working groups formed a code review committee (I. Fung, F. Hoffmann, E. Holland, P. Houser, T. King, D. Noone, D. Ojima, P. Thornton (chair), M. Vertenstein, Z.-L. Yang, X. Zeng) to assess the new model structure. The new code was approved by the review committee, adopted as CLM2.1 at the June 2002 CCSM Workshop, and released to the community in February 2003.

1.1.4 CLM3.0 and CLM3.1BGC

A major software engineering re-write of CLM2.1 was performed to allow the code to run efficiently on both scalar and vector compute architectures, and model input and output formats were revised. A number of improvements were made to the

biophysical parameterizations, including corrections for 2 m air temperature and aerodynamic resistances. The belowground competition from CLM2.1 was adopted as the default behavior. This new version, CLM3.0, was released to the community in June 2004, in conjunction with the release of the complete coupled system CCSM3.0. Performance of CLM3.0 when run as a component of CCSM3.0 is documented by Dickinson et al. (2006), and the complete technical description of CLM3.0 is given in Oleson et al. (2004).

CLM3.0 was adopted by the BGCWG as the code base for implementation of coupled carbon-nitrogen cycles (CLM3.1BGC). CLM3.1BGC includes the fundamental carbon-nitrogen coupling mechanisms from Biome-BGC, translated to a sub-daily timestep (Thornton et al., 2002). A significant issue for coupled climate-carbon cycle modeling is the establishment of spun-up (steady-state) conditions with respect to carbon stocks and fluxes. Slow fluxes of nitrogen into and out of terrestrial ecosystems makes this an even more critical problem for coupled carbon-nitrogen-climate modeling. A model spin-up approach designed specifically for a coupled carbon-nitrogen cycle model was implemented (Thornton and Rosenbloom, 2005), significantly reducing the computational cost of initiating a new simulation.

Initial offline experiments with the carbon-nitrogen code revealed that the biophysical canopy integration scheme in CLM3.0 was flawed and was not suitable for the integration of a fully prognostic biogeochemistry model. The treatment of sunlit and shaded canopy radiation interception was revised, and a new algorithm was introduced relating canopy structural and functional characteristics through a parameterized vertical gradient in specific leaf area. The new algorithm greatly improves steady-state canopy photosynthesis, permits realistic development of canopies from very low initial leaf area, and has been validated against observations from multiple sites (Thornton and Zimmermann, 2007).

Further offline experiments highlighted several deficiencies in the hydrology scheme of CLM3.0 which resulted in excessively dry soils, low productivity, and biased partitioning of evapotranspiration. A preliminary set of hydrology modifications was developed and tested by D. Lawrence and P. Thornton and incorporated in both the standard (diagnostic canopy) model version (Lawrence et al., 2007) and in CLM3.1BGC

(Thornton and Zimmermann, 2007). These modifications include scaling of canopy water interception to reduce canopy evaporation and increase soil moisture, and modification of soil column gradient of saturated hydraulic conductivity to increase water flow into deeper soil layers.

The CLM3.1BGC code includes a capability to switch off the effects of nitrogen limitation, producing model behavior that is more comparable with the current generation of carbon-only land biogeochemistry components in coupled climate-carbon cycle models (e.g. Friedlingstein et al., 2006). This behavior was used to examine the influence of carbon-nitrogen coupling on CO_2 fertilization and climate variability responses in global offline simulations (Thornton et al., in press). CLM3.1BGC was also used as the land component in a series of fully-coupled climate-biogeochemistry simulations currently being analyzed by the CCSM BGCWG, as originally envisioned in 2001.

1.1.5 CLM4 and CLM-CN

In response to initial studies identifying weaknesses in the structure and parameterization of CLM3.0, a community effort developed around the identification and evaluation of a number of potential modifications, mainly dealing with improvements to the hydrology of CLM3.0. This project resulted in the development of a new model, CLM4, released to the community in April 2010. CLM4 adopts the canopy integration scheme of Thornton and Zimmermann (2007) as the default behavior for both diagnostic and prognostic canopy modes. The hydrology modifications from CLM3.1BGC are replaced in CLM4 with a more comprehensive revision of the model structure and parameterization, including canopy interception, frozen soil, soil water availability, soil evaporation, surface and sub-surface runoff, and a groundwater model to determine water table depth. CLM4 includes a new parameterization to simulate nitrogen limitation on plant productivity when the prognostic carbon-nitrogen component is switched off (i.e. in diagnostic canopy mode). Oleson et al. (in press) evaluate results from offline experiments and describe how the diagnostic canopy version of CLM4 differs from CLM3.0, while Stöckli et al. (in press) show that the new model has smaller biases when compared to eddy covariance flux observations from multiple sites.

In addition to the standard diagnostic canopy model, CLM4 also includes the full prognostic carbon-nitrogen cycle capability, referred to as CLM-CN. Because full technical description for CLM-CN was not available at the time, this capability is not referenced in the May 2007 community release materials for CLM4. This Technical Note provides complete details on the implementation of CLM-CN as released with CESM1. The definitive background document for this description is the CLM4.0 Technical Note (Oleson et al., 2010). Complete technical detail is provided in the following sections for all aspects of the model where logic or implementation for CLM-CN expands upon or differs from this previous description.

1.2 Model Overview

1.2.1 Relationship to Previous Technical Descriptions

This Technical Note provides complete details on the implementation of CLM-CN as released with CLM3.5. The definitive background documents for this description are the CLM3.0 Technical Note (Oleson et al., 2004) and the CLM3.5 modifications described in the appendices of Oleson et al. (in press). Complete technical detail is provided in the following sections for all aspects of the model where logic or implementation for CLM-CN differs from these previous descriptions.

1.2.2 Surface Heterogeneity and Hierarchical Structure

[this section still needs some work] The hierarchical sub-grid structure and enumeration of plant functional types (PFTs) described for CLM3.0 (Oleson et al., 2004) is retained for CLM-CN, but while the default behavior in diagnostic canopy mode is to allow up to 4 of the 16 possible PFTs (15 vegetation types plus bare ground), CLM-CN by default allocates space in the model data structures for all 16 PFTs, then uses weights (which can be zero) to identify the fractional coverage of each PFT on the vegetated soil column. These weights can change during the course of the run (Chapter 11). Vegetation carbon and nitrogen state and flux calculations are performed independently for each PFT, except where specifically noted otherwise. It is assumed, in other words, that the multiple PFTs occupying space on a single vegetated soil column have a spatial arrangement that is patchy enough that canopy processes can be estimated as though each

patch consists of a single PFT. This is obviously not the case in many vegetation communities, and representation of realistic mixtures of PFTs at the individual scale remains an area for future model development and improvement.

1.2.3 State Variables

1.2.4 Process Representation

2 Canopy Structure

Although the canopy integration scheme introduced by Thornton and Zimmermann (2007) is used in the diagnostic canopy mode for CLM3.5, the current technical description of CLM3.5 (Oleson et al., in press) does not provide detailed equations. Complete details on the connection between canopy vertical gradient in leaf thickness, total canopy leaf carbon, and canopy leaf area index are provided in this Chapter. Details on how this integration scheme influences the calculation of photosynthesis are provided in Chapter 3. Thornton and Zimmermann (2007) provide additional details on the rationale for introducing a new canopy integration scheme, and how it relates to the scheme employed in CLM3.0.

2.1 Specific Leaf Area

Specific leaf area measures the one-sided area of a leaf per unit mass of leaf carbon, and can be thought of in general as an inverse metric of leaf thickness, with thick leaves having low and thin leaves high specific leaf area. Specific leaf area is commonly observed to increase from the top to the bottom of forest canopies. A central assumption of the canopy integration model is that, at the species level, the vertical gradient in specific leaf area (*SLA*, m^2 one-sided leaf area gC^{-1}) can be represented as a linear function *SLA(x)*, where *x* is the overlying leaf area index (m^2 one-sided leaf area / m^2 ground area) at a particular vertical canopy position, while the mass-based leaf nitrogen concentration remains constant with *x*. This assumption has been shown to be true for a range of temperate forest canopies (Thornton and Zimmermann, 2007). $SLA(x)$ is therefore given as

$$SLA(x) = SLA_0 + m\,x \tag{2.1}$$

where SLA_0 (m^2 one-sided leaf area gC^{-1}) is a fixed value of *SLA* at the top of the canopy, *m* is a linear slope coefficient, and *x* is the canopy depth expressed as overlying leaf area index (m^2 overlying one-sided leaf area m^{-2} ground area). SLA_0 and *m* both vary by plant functional type (Table XX).

2.2 Leaf and Stem Area Index

Integrating $1/SLA(x)$ vertically over the canopy gives total canopy leaf carbon (C_L, gC m^{-2} ground area) as

$$C_L = \int_0^L \frac{1}{SLA(x)}\,dx = \frac{\ln\left(\left(m\,L + SLA_0\right) - \ln\left(SLA_0\right)\right)}{m} \tag{2.2}$$

where L is the canopy leaf area index (m^2 one-sided leaf area / m^2 ground area). Equation (2.2) can be rearranged as follows to solve for L when C_L is given as a model prognostic variable:

$$L = \begin{cases} \dfrac{SLA_0\left(\exp\left(m\,C_L\right) - 1\right)}{m} & m > 0 \\ SLA_0\,C_L & m = 0 \end{cases} \tag{2.3}$$

Following the logic in Levis et al. (2004) stem area index (S, m^2 one-sided stem area / m^2 ground area) depends on L and on whether the PFT is woody or non-woody (see Table XX), as

$$S = \begin{cases} 0.25L & \text{(woody PFT)} \\ 0.05L & \text{(non-woody PFT)} \end{cases} \tag{2.4}$$

2.3 Canopy Height

The height of the top of the canopy (z_{top}, m) depends on prognostic dead stem carbon (C_{DS}, gC / m^2 ground area) and a simple allometric relationship assuming conical stems and a fixed stocking density for woody PFTs, and on L for non-woody PFTs

$$z_{top} = \begin{cases} 0.01 < \left(\dfrac{3C_{DS}\,a_{taper}{}^2}{\pi\,a_{stock}\,\rho_{wood}}\right)^{1/3} < z_{top,\max} & \text{(woody PFT)} \\ 0.25 < \;\; 0.25L \qquad\qquad < z_{top,\max} & \text{(non-woody PFT)} \end{cases} \tag{2.5}$$

where a_{taper} is the ratio height:radius for the conical stem (set to 200 for all woody PFTs), a_{stock} is the stocking density (stems m^{-2}), and ρ_{wood} is the carbon density of wood (gC m^{-3}, set to 250,000 for all woody PFTs). The parameter $z_{top,max}$ is defined as

$$z_{top,\max} = \left(\frac{z_{atm}}{R_d + R_{z0m}}\right) - 3 \tag{2.6}$$

where z_{atm} (m) is the reference height for windspeed, and R_d and R_{z0m} are the ratios of displacement height and momentum roughness length to canopy top height, respectively. This sets an upper limit to z_{top} that prevents numerical instability when z_{top} is close to z_{atm}. The height of the bottom of the canopy (z_{bot}, m) is defined as

$$z_{bot} = \begin{cases} 0 < z_{top} - 1.0 < 3.0 & \text{(woody PFT)} \\ 0 < z_{top} - 0.2 < 0.05 & \text{(non-woody PFT)} \end{cases} \tag{2.7}$$

3 Canopy Processes

This chapter provides details on processes within the vegetation canopy which differ from descriptions provided previously in Oleson et al. (2004) and Oleson et al. (in press).

3.1 Canopy Radiation Interception

CLM3.0 treats the interception of radiation in the sunlit and shaded canopy fractions in an unusual way. Detailed calculations of sunlit and shaded canopy fraction and direct and diffuse radiation interception in visible and near-infrared wavebands are performed (Dai et al., 2004), but all visible waveband intercepted radiation is then assigned to the sunlit portion of the canopy for the purpose of calculating photosynthesis, with no photosynthetically active radiation in the shaded canopy fraction (Oleson et al., 2004, p. 40, Eq. 4.9). One consequence of this treatment is that absorbed photosynthetically active radiation in the sunlit canopy fraction is frequently in the light-saturated range for leaf-scale photosynthesis, producing an underestimate of canopy photosynthesis (Thornton and Zimmermann, 2007). That behavior has been replaced in CLM3.5 and CLM-CN with a scheme that provides a more realistic distribution of absorbed radiation in the sunlit and shaded canopy fractions.

The fraction of sunlit leaves at canopy depth x, $F_{sun}(x)$, and the canopy total fractions of sunlit and shaded leaf area (f_{sun} and f_{sha}) are calculated assuming that canopy architecture favors the exposure to direct beam radiation of leaves over stems, giving

$$F_{sun}(x) = e^{-Kx} \tag{3.1}$$

$$f_{sun} = \begin{cases} \dfrac{\int_0^L F_{sun}(x)\,dx}{L} = \dfrac{1-e^{-KL}}{KL} & \text{for } L > 0.01 \\ 1 & \text{for } L \le 0.01 \end{cases} \tag{3.2}$$

$$f_{sha} = 1 - f_{sun} \tag{3.3}$$

where K is the direct beam extinction coefficient of the canopy, and

$$K = \frac{G(\mu)}{\mu} \tag{3.4}$$

where $G(\mu)$ is the relative projected area of leaf and stem elements in the direction $\cos^{-1}\mu$, and μ is the cosine of the zenith angle of the incident beam. Eq. (3.4) differs from the description given for CLM3.0 (Oleson et al., 2004, p. 40, Eq. 4.8) in that the additional multiplicative term $\sqrt{1-\omega_{vis}^{veg}}$ has been left out, following the simpler form in Dai et al. (2004). With this change, K is now defined identically in the calculation of two-stream albedos (Oleson et al., 2004, p. 23), and in the calculation of fraction sunlit leaf area.

Total shortwave radiation absorbed by the sunlit canopy (W m^{-2}) in waveband Λ is

$$\vec{S}_{sun,\Lambda} = \vec{S}_{sun,\Lambda}^{\mu\to\mu} + \vec{S}_{sun,\Lambda}^{\mu\to i} + \vec{S}_{sun,\Lambda}^{i} \tag{3.5}$$

where $\vec{S}_{sun,\Lambda}^{\mu\to\mu}$ is the portion of the incident direct beam absorbed as direct radiation in the sunlit canopy, $\vec{S}_{sun,\Lambda}^{\mu\to i}$ is the portion of the incident direct beam scattered and absorbed as diffuse radiation in the sunlit canopy, $\vec{S}_{sun,\Lambda}^{i}$ is the portion of the incident diffuse radiation absorbed in the sunlit canopy, and Λ denotes either the visible (<0.7μm) or near-infrared (≥0.7μm) waveband. Total shortwave radiation absorbed by the shaded canopy (W m^{-2}) in waveband Λ is

$$\vec{S}_{sha,\Lambda} = \vec{S}_{sha,\Lambda}^{\mu\to i} + \vec{S}_{sha,\Lambda}^{i} \tag{3.6}$$

where $\vec{S}_{sha,\Lambda}^{\mu\to i}$ is the portion of the incident direct beam absorbed as diffuse radiation in the shaded canopy and $\vec{S}_{sha,\Lambda}^{i}$ is the portion of the incident diffuse radiation absorbed in the shaded canopy.

Components of $\vec{S}_{sun,\Lambda}$ and $\vec{S}_{sha,\Lambda}$ are calculated as

$$\vec{S}_{sun,\Lambda}^{\mu\to\mu} = S_{atm}\downarrow_{\Lambda}^{\mu}\left(1-e^{-K(L+S)}\right)\left(1-\omega_{\Lambda}\right) \tag{3.7}$$

$$\vec{S}_{sun,\Lambda}^{\mu\to i} = \left(\left(S_{atm}\downarrow_{\Lambda}^{\mu}\vec{I}_{\Lambda}^{\mu}\right) - \vec{S}_{sun,\Lambda}^{\mu\to\mu}\right) f_{sun} \tag{3.8}$$

$$\vec{S}_{sun,\Lambda}^{i} = S_{atm}\downarrow_{\Lambda}\vec{I}_{\Lambda} f_{sun} \tag{3.9}$$

$$\vec{S}_{sha,\Lambda}^{\mu\to i} = \left(\left(S_{atm}\downarrow_{\Lambda}^{\mu}\vec{I}_{\Lambda}^{\mu}\right) - \vec{S}_{sun,\Lambda}^{\mu\to\mu}\right) f_{sha} \tag{3.10}$$

$$\vec{S}_{sha,\Lambda}^{i} = S_{atm}\downarrow_{\Lambda}\vec{I}_{\Lambda} f_{sha} \tag{3.11}$$

where $S_{atm}\downarrow_{\Lambda}^{\mu}$ and $S_{atm}\downarrow_{\Lambda}$ are incident direct and diffuse radiation in waveband Λ, respectively, ω_{Λ} is the fraction of incident radiation in waveband Λ that is scattered by the canopy (CLM3.0, Eqs. 3.5 and 3.8), and $\vec{I}_{\Lambda}^{\mu}$ and $\vec{I}_{\Lambda}$ are the fractions of incident direct and diffuse radiation, respectively, absorbed by the canopy (CLM3.0, Eqs. 4.1 and 4.2).

For sunlit leaf area index $L_{sun} = L\, f_{sun}$ and shaded leaf area index $L_{sha} = L\, f_{sha}$, shortwave radiation absorbed per unit leaf area are given for the sunlit and shaded canopy fractions as

$$\overline{S}_{sun,\Lambda} = \frac{\vec{S}_{sun,\Lambda}\dfrac{L}{L+S}}{L_{sun}} = \frac{\vec{S}_{sun,\Lambda}}{(L+S)\, f_{sun}} \tag{3.12}$$

and

$$\overline{S}_{sha,\Lambda} = \frac{\vec{S}_{sha,\Lambda}\dfrac{L}{L+S}}{L_{sha}} = \frac{\vec{S}_{sha,\Lambda}}{(L+S)\, f_{sha}}, \tag{3.13}$$

respectively.

3.2 Sunlit and Shaded Canopy Photosynthesis

The visible waveband of absorbed shortwave radiation (Λ=vis) is assumed to represent the photosynthetically active radiation (PAR) for the purpose of calculating leaf-level carbon assimilation fluxes, and the PAR flux per unit leaf area in the sunlit and shaded canopy fractions are given as $\phi^{sun} = \overline{S}_{sun,vis}$ and $\phi^{sha} = \overline{S}_{sha,vis}$, respectively (replacing CLM3.0 Eq. 4.9).

The overall form for the photosynthesis and stomatal conductance calculations in CLM3.0 (Oleson et al., 2004, Section 8) is retained for CLM3.5 and CLM-CN. In addition to the changes in sunlit and shaded canopy radiation interception, described above, CLM3.5 introduces a vertical canopy gradient in maximum rate of carboxylation per unit leaf area (V_{max}, μmol CO_2 m^{-2} one-sided leaf area s^{-1}), based on the canopy integration scheme in Thornton and Zimmermann (2007).

Following Niinemets and Tenhunen (1997), V_{max} can be expressed as

$$V_{\max} = N_a F_{LNR} \frac{1}{F_{NR}} a_R \tag{3.14}$$

where N_a is the area-based leaf nitrogen concentration (gN m^{-2} one-sided leaf area), F_{LNR} is the fraction of leaf nitrogen in the Rubisco enzyme (unitless), F_{NR} is the mass ratio of nitrogen in Rubisco molecule to total molecular mass (unitless), and a_R is the specific activity of Rubisco (umol CO_2 gRubisco^{-1} s^{-1}). We calculate F_{NR} as ~0.14 on the basis of protein subunit analyses of the enzyme (Kuehn and McFadden, 1969). F_{LNR} can be estimated from leaf-scale gas exchange measurements, given the corresponding N_a for the sampled leaves. N_a is related to specific leaf area and mass-based leaf N content as

$$N_a = \frac{1}{SLA\, CN_L} \tag{3.15}$$

where CN_L is the leaf carbon:nitrogen ratio (gC gN^{-1}). Woodrow and Berry (1988) give an estimate of a_R at 25°C ($a_{R,25}$ = 60) and its dependence on temperature

$$a_R' = a_{R,25}(2.4)^{\frac{T_v - 25}{10}} \tag{3.16}$$

where T_v is the leaf temperature. This is further modified by functions for high temperature degradation of the enzyme ($f(T_v)$, CLM3.0 Eq. 8.9) and for the effects of low soil moisture (β_t, CLM3.0 Eq. 8.10), giving

$$a_R = a_R' \, f\left(T_v\right) \beta_t . \tag{3.17}$$

F_{NR} and a_R are assumed to be fundamental properties of the Rubisco enzyme, and we treat them as constants for all plant types. Both F_{LNR} and CN_L are known to vary among plant types (Field et al., 1983; Wullschleger, 1993), but there is evidence that they vary little with canopy depth for a given plant type (Thornton and Zimmermann, 2007). Thornton and Zimmermann (2007). Most of the variation in $V_{max}(x)$ is therefore assumed to result from variation in $SLA(x)$. The approach used here is to calculate mean values of SLA for the sunlit and shaded canopies (SLA_{sun} and SLA_{sha}), and use these to estimate N_a and then V_{max} for the sunlit and shaded canopies from Eqs. (3.15) and (3.14). SLA_{sun} and SLA_{sha} have the following analytical solutions:

$$SLA_{sun} = \frac{\int_0^L SLA(x) F_{sun}(x)\, dx}{L_{sun}} = \frac{-\left(c\, m\, K\, L + c\, m + c\, SLA_0 K - m - SLA_0 K\right)}{K^2 L_{sun}} \tag{3.18}$$

$$SLA_{sha} = \frac{\int_0^L SLA(x)(1 - F_{sun}(x))\,dx}{L_{sha}} = \frac{L\left(SLA_0 + \frac{mL}{2}\right) - SLA_{sun}L_{sun}}{L_{sha}} \qquad (3.19)$$

where $c = \exp(-KL)$. The form for Eq. (3.19) has been rearranged to take advantage of previous calculation of SLA_{sun}.

Because of the non-linear dependence of N_a on SLA, a more accurate method would be to integrate $N_a(x)$ directly to obtain $N_{a,sun}$ and $N_{a,sha}$. These integrals do not have analytical solutions. The error associated with the approximation of $N_{a,sun}$ and $N_{a,sha}$ using Eqs. (3.18), (3.19), and substituting into Eq. (3.15) is described in Thornton and Zimmermann (2007).

3.3 Nitrogen Limitation of Primary Production

CLM-CN also introduces a down-regulation of canopy total photosynthesis based on the availability of mineral nitrogen to support new growth. Downregulation (f_{dreg}) is expressed as the fraction of potential gross primary production (CF_{GPPpot}, gC m^{-2} ground area s^{-1}) which can not be allocated to new growth given the current nitrogen supply and the constraints of the allocation model (Chapters 4 and 9). After substituting V_{max} from Eq. (3.14) and introducing the other parameterization changes described in Oleson et al. (in press), the calculation of canopy total gross primary production (CF_{GPP}, gC m^{-2} ground area s^{-1}) proceeds as in CLM3.0, but is modified by nitrogen limitation as

$$CF_{GPPpot} = \left(A_{sun}L_{sun} + A_{sha}L_{sha}\right)(12.011\text{e-}6) \qquad (3.20)$$

$$CF_{GPP} = CF_{GPPpot}\left(1 - f_{dreg}\right) \qquad (3.21)$$

where the factor 12.011e-6 converts from μmol CO_2 to gC.

4 Carbon and Nitrogen Allocation

4.1 Carbon Allocation for Maintenance Respiration Costs

The carbon and nitrogen allocation routines in CLM-CN determine the fate of newly assimilated carbon, coming from the calculation of photosynthesis, and available mineral nitrogen, coming from plant uptake of mineral nitrogen in the soil or being drawn out of plant reserves. Allocation fluxes are determined in three steps: first CF_{GPPpot} is used to evaluate the potential allocation of carbon and nitrogen assuming an unlimited nitrogen supply, then the actual nitrogen supply is compared against the demand, and finally allocation of carbon and nitrogen are reduced, if necessary, to match nitrogen supply and demand.

Allocation of available carbon on each time step is prioritized, with first priority given to the demand for carbon to support maintenance respiration of live tissues (Section 5). Second priority is to replenish the internal plant carbon pool that supports maintenance respiration during times when maintenance respiration exceeds photosynthesis (e.g. at night, during winter for perennial vegetation, or during periods of drought stress) (Sprugel et al., 1995). Third priority is to support growth of new tissues, including allocation to storage pools from which new growth will be displayed in subsequent time steps.

The total maintenance respiration demand (CF_{mr}, gC m^{-2} s^{-1}) is calculated as a function of tissue mass and nitrogen concentration, and temperature (Section 5). The carbon supply to support this demand is composed of fluxes allocated from carbon assimilated in the current timestep ($CF_{GPP,mr}$, gC m^{-2} s^{-1}) and from a storage pool that is drawn down when total demand exceeds photosynthesis ($CF_{xs,mr}$, gC m^{-2} s^{-1}):

$$CF_{mr} = CF_{GPP,mr} + CF_{xs,mr} \tag{4.1}$$

$$CF_{GPP,mr} = \begin{cases} CF_{mr} & \text{for } CF_{mr} \le CF_{GPPpot} \\ CF_{GPPpot} & \text{for } CF_{mr} > CF_{GPPpot} \end{cases} \tag{4.2}$$

$$CF_{xs,mr} = \begin{cases} 0 & \text{for } CF_{mr} \le CF_{GPPpot} \\ CF_{mr} - CF_{GPPpot} & \text{for } CF_{mr} > CF_{GPPpot} \end{cases} \tag{4.3}$$

The storage pool that supplies carbon for maintenance respiration in excess of current CF_{GPPpot} (CS_{xs}, gC m^{-2}) is permitted to run a deficit (negative state), and the magnitude of this deficit determines an allocation demand which gradually replenishes CS_{xs}. The logic for allowing a negative state for this pool is to eliminate the need to know in advance what the total maintenance respiration demand will be for a particular combination of climate and plant type. Using the deficit approach, the allocation to alleviate the deficit increases as the deficit increases, until the supply of carbon into the pool balances the demand for carbon leaving the pool in a quasi-steady state, with variability driven by the seasonal cycle, climate variation, disturbance, and internal dynamics of the plant-litter-soil system. In cases where the combination of climate and plant type are not suitable to sustained growth, the deficit in this pool increases until the available carbon is being allocated mostly to alleviate the deficit, and new growth approaches zero. The allocation flux to CS_{xs} ($CF_{GPP,xs}$, gC m^{-2} s^{-1}) is given as

$$CF_{GPP,xs,pot} = \begin{cases} 0 & \text{for } CS_{xs} \geq 0 \\ -CS_{xs} / (86400\tau_{xs}) & \text{for } CS_{xs} < 0 \end{cases} \quad (4.4)$$

$$CF_{GPP,xs} = \begin{cases} CF_{GPP,xs,pot} & \text{for } CF_{GPP,xs,pot} \leq CF_{GPPpot} - CF_{GPP,mr} \\ \max(CF_{GPPpot} - CF_{GPP,mr}, 0) & \text{for } CF_{GPP,xs,pot} > CF_{GPPpot} - CF_{GPP,mr} \end{cases} \quad (4.5)$$

where τ_{xs} is the time constant (currently set to 30 days) controlling the rate of replenishment of CS_{xs}.

Note that these two top-priority carbon allocation fluxes ($CF_{GPP,mr}$ and $CF_{GPP,xs}$) are not stoichiometrically associated with any nitrogen fluxes, and so this initial allocation step can proceed without reference to (or limitation from) the available mineral nitrogen supply.

4.2 Carbon and Nitrogen Stoichiometry of New Growth

After accounting for the carbon cost of maintenance respiration, the remaining carbon flux from photosynthesis which can be allocated to new growth (CF_{avail}, gC m^{-2} s^{-1}) is

$$CF_{avail\_alloc} = CF_{GPPpot} - CF_{GPP,mr} - CF_{GPP,xs}. \quad (4.6)$$

Potential allocation to new growth is calculated for all of the plant carbon and nitrogen state variables based on specified C:N ratios for each tissue type and allometric parameters that relate allocation between various tissue types. The allometric parameters are defined as follows:

$$\begin{aligned} a_1 &= \text{ ratio of new fine root : new leaf carbon allocation} \\ a_2 &= \text{ ratio of new coarse root : new stem carbon allocation} \\ a_3 &= \text{ ratio of new stem : new leaf carbon allocation} \\ a_4 &= \text{ ratio new live wood : new total wood allocation} \\ g_1 &= \text{ratio of growth respiration carbon : new growth carbon.} \end{aligned} \tag{4.7}$$

Parameters a_1, a_2, and a_4 are defined as constants for a given PFT (Table XX), while g_1 = 0.3 (unitless) is prescribed as a constant for all PFTs, based on construction costs for a range of woody and non-woody tissues (Larcher, 1995).

The model includes a dynamic allocation scheme that can be invoked for woody vegetation by setting the parameter a_3 = -1 in the PFT physiology lookup table, in which case the ratio for carbon allocation between new stem and new leaf increases with increasing net primary production (NPP), as

$$a_3 = \max\left(0.2,\ 0.2 + 0.0025 NPP_{ann}\right) \tag{4.8}$$

where NPP_{ann} is the annual sum of NPP from the previous year. This mechanism has the effect of increasing woody allocation in favorable growth environments (Allen et al., 2005; Vanninen and Makela, 2005) and during the phase of stand growth prior to canopy closure (Axelsson and Axelsson, 1986).

Carbon to nitrogen ratios are defined for different tissue types as follows:

$$\begin{aligned} CN_{leaf} &= \text{ C:N for leaf} \\ CN_{fr} &= \text{ C:N for fine root} \\ CN_{lw} &= \text{ C:N for live wood (in stem and coarse root)} \\ CN_{dw} &= \text{ C:N for dead wood (in stem and coarse root)} \end{aligned} \tag{4.9}$$

where all C:N parameters are defined as constants for a given PFT (Table XX).

Given values for the parameters in (4.7) and (4.9), total carbon and nitrogen allocation to new growth (CF_{alloc}, gC m^{-2} s^{-1}, and NF_{alloc}, gN m^{-2} s^{-1}, respectively) can be expressed as functions of new leaf carbon allocation ($CF_{GPP,leaf}$, gC m^{-2} s^{-1}):

$$CF_{alloc} = CF_{GPP,leaf}\, C_{allom}$$
$$NF_{alloc} = CF_{GPP,leaf}\, N_{allom} \tag{4.10}$$

where

$$C_{allom} = \begin{cases} \left(1+g_1\right)\left(1+a_1+a_3\left(1+a_2\right)\right) & \text{for woody PFT} \\ 1+g_1+a_1\left(1+g_1\right) & \text{for non-woody PFT} \end{cases} \tag{4.11}$$

$$N_{allom} = \begin{cases} \dfrac{1}{CN_{leaf}} + \dfrac{a_1}{CN_{fr}} + \dfrac{a_3 a_4\left(1+a_2\right)}{CN_{lw}} + \\ \qquad \dfrac{a_3\left(1-a_4\right)\left(1+a_2\right)}{CN_{dw}} & \text{for woody PFT} \\ \dfrac{1}{CN_{leaf}} + \dfrac{a_1}{CN_{fr}} & \text{for non-woody PFT.} \end{cases} \tag{4.12}$$

Since the C:N stoichiometry for new growth allocation is defined, from Eq. (4.10), as C_{allom}/N_{allom}, the total carbon available for new growth allocation (CF_{avail_alloc}) can be used to calculate the total plant nitrogen demand for new growth (NF_{plant_demand}, gN m^{-2} s^{-1}) as:

$$NF_{plant\_demand} = CF_{avail\_alloc}\frac{N_{allom}}{C_{allom}}. \tag{4.13}$$

4.3 Deployment of retranslocated nitrogen

In many plants, some portion of the nitrogen used to construct new tissues is mobilized from senescing tissues, especially leaves, and retained within the plant when the tissues are lost as litter. This store of retranslocated nitrogen is used to supply part of the nitrogen demand for subsequent growth (Magill et al., 1997; Oikawa et al., 2005; Son and Gower, 1991). CLM-CN includes one pool of retranslocated nitrogen ($NS_{retrans}$, gN m^{-2}), and the availability of nitrogen from this pool to support new growth ($NF_{avail\_retrans}$, gN m^{-2} s^{-1}) is proportional to the plant nitrogen demand, as:

$$NF_{avail\_retrans} = \min\left(\frac{NF_{retrans\_ann}\dfrac{NF_{plant\_demand}}{NF_{plant\_demand\_ann}}}{\Delta t}, \frac{NS_{retrans}}{\Delta t}\right) \tag{4.14}$$

where $NF_{retrans\_ann}$ (gN m^{-2} y^{-1}) is the previous year's annual sum of retranslocated nitrogen extracted from senescing tissues, $NF_{plant\_demand\_ann}$ (gN m^{-2} y^{-1}) is the previous year's annual sum of NF_{plant_demand}, and Δt (s) is the model's biogeochemistry time step. This formulation produces an annual cycle in the extraction of nitrogen from $NS_{retrans}$ which corresponds to the annual cycle of plant nitrogen demand, and which is scaled to give $NS_{retrans}$ approximately a one-year turnover time. The minimum function prevents extraction of more than the remaining pool of retranslocated nitrogen, which can be an important constraint under conditions where high rates of mortality are modifying the size of the pool. During the first year of an initial simulation, before $NF_{plant\_demand\_ann}$ and $NF_{retrans\_ann}$ have valid values, $NF_{avail\_retrans}$ is set to 0.0.

The actual flux of nitrogen from the retranslocated N pool into allocation of new growth ($NF_{retrans,alloc}$, gN m^{-2} s^{-1}) is never greater than the plant demand for new nitrogen:

$$NF_{retrans,alloc} = \min\left(NF_{plant\_demand}, NF_{avail\_retrans}\right) \tag{4.15}$$

4.4 Plant nitrogen uptake from soil mineral nitrogen pool

The total plant nitrogen demand is reduced by the nitrogen flux from $NS_{retrans}$ to give the plant demand for mineral nitrogen from the soil ($NF_{plant\_demand\_soil}$, gN m^{-2} s^{-1}):

$$NF_{plant\_demand\_soil} = NF_{plant\_demand} - NF_{retrans,alloc}\,. \tag{4.16}$$

The combined demand from all PFTs sharing space on a soil column and the demand from the heterotrophic community in the soil (nitrogen immobilization demand) compete for the available soil mineral nitrogen pool (Chapter 7). The result of this competition is passed back to the allocation algorithm as f_{plant_demand}, the fraction (from 0 to 1) of the plant nitrogen demand which can be met given the current soil mineral nitrogen supply and competition with heterotrophs. Plant uptake from the soil mineral nitrogen pool is then given as:

$$NF_{sminn,alloc} = NF_{plant\_demand\_soil}\, f_{plant\_demand} \tag{4.17}$$

4.5 Final carbon and nitrogen allocation

The total flux of allocated nitrogen is given as:

$$NF_{alloc} = NF_{retrans,alloc} + NF_{sminn,alloc} \tag{4.18}$$

From the stoichiometric relationship in Eq. (4.10), the associated carbon allocation flux is:

$$CF_{alloc} = NF_{alloc} \frac{C_{allom}}{N_{allom}}. \tag{4.19}$$

The downregulation of photosynthesis (Eq. (3.21)) can then be calculated as:

$$f_{dreg} = \frac{CF_{alloc} - CF_{avail\_alloc}}{CF_{GPPpot}}. \tag{4.20}$$

Total allocation to new leaf carbon ($CF_{alloc,leaf\_tot}$, gC m^{-2} s^{-1}) is calculated as:

$$CF_{alloc,leaf\_tot} = \frac{CF_{alloc}}{C_{allom}}. \tag{4.21}$$

As described in Chapter XX, there are two carbon pools associated with each plant tissue – one which represents the currently displayed tissue, and another which represents carbon stored for display in a subsequent growth period. The nitrogen pools follow this same organization. The model keeps track of stored carbon according to which tissue type it will eventually be displayed as, and the separation between display in the current timestep and storage for later display depends on the parameter f_{cur} (values 0 to 1). Given $CF_{alloc,leaf}$ and f_{cur}, the allocation fluxes of carbon to display and storage pools (where storage is indicated with *_stor*) for the various tissue types are given as:

$$CF_{alloc,leaf} = CF_{alloc,leaf\_tot} f_{cur} \tag{4.22}$$

$$CF_{alloc,leaf\_stor} = CF_{alloc,leaf\_tot} \left(1 - f_{cur}\right) \tag{4.23}$$

$$CF_{alloc,froot} = CF_{alloc,leaf\_tot} a_1 f_{cur} \tag{4.24}$$

$$CF_{alloc,froot\_stor} = CF_{alloc,leaf\_tot} a_1 \left(1 - f_{cur}\right) \tag{4.25}$$

$$CF_{alloc,livestem} = CF_{alloc,leaf\_tot} a_3 a_4 f_{cur} \tag{4.26}$$

$$CF_{alloc,livestem\_stor} = CF_{alloc,leaf\_tot} a_3 a_4 \left(1 - f_{cur}\right) \tag{4.27}$$

$$CF_{alloc,deadstem} = CF_{alloc,leaf\_tot} a_3 \left(1 - a_4\right) f_{cur} \tag{4.28}$$

$$CF_{alloc,deadstem\_stor} = CF_{alloc,leaf\_tot} a_3 \left(1 - a_4\right)\left(1 - f_{cur}\right) \tag{4.29}$$

$$CF_{alloc,livecroot} = CF_{alloc,leaf\_tot} a_2 a_3 a_4 f_{cur} \tag{4.30}$$

$$CF_{alloc,livecroot\_stor} = CF_{alloc,leaf\_tot} a_2 a_3 a_4 \left(1 - f_{cur}\right) \tag{4.31}$$

$$CF_{alloc,deadcroot} = CF_{alloc,leaf\_tot} a_2 a_3 (1 - a_4) f_{cur} \quad (4.32)$$

$$CF_{alloc,deadcroot\_stor} = CF_{alloc,leaf\_tot} a_2 a_3 (1 - a_4)(1 - f_{cur}). \quad (4.33)$$

The corresponding nitrogen allocation fluxes are given as:

$$NF_{alloc,leaf} = \frac{CF_{alloc,leaf\_tot}}{CN_{leaf}} f_{cur} \quad (4.34)$$

$$NF_{alloc,leaf\_stor} = \frac{CF_{alloc,leaf\_tot}}{CN_{leaf}} (1 - f_{cur}) \quad (4.35)$$

$$NF_{alloc,froot} = \frac{CF_{alloc,leaf\_tot} a_1}{CN_{fr}} f_{cur} \quad (4.36)$$

$$NF_{alloc,froot\_stor} = \frac{CF_{alloc,leaf\_tot} a_1}{CN_{fr}} (1 - f_{cur}) \quad (4.37)$$

$$NF_{alloc,livestem} = \frac{CF_{alloc,leaf\_tot} a_3 a_4}{CN_{lw}} f_{cur} \quad (4.38)$$

$$NF_{alloc,livestem\_stor} = \frac{CF_{alloc,leaf\_tot} a_3 a_4}{CN_{lw}} (1 - f_{cur}) \quad (4.39)$$

$$NF_{alloc,deadstem} = \frac{CF_{alloc,leaf\_tot} a_3 (1 - a_4)}{CN_{dw}} f_{cur} \quad (4.40)$$

$$NF_{alloc,deadstem\_stor} = \frac{CF_{alloc,leaf\_tot} a_3 (1 - a_4)}{CN_{dw}} (1 - f_{cur}) \quad (4.41)$$

$$NF_{alloc,livecroot} = \frac{CF_{alloc,leaf\_tot} a_2 a_3 a_4}{CN_{lw}} f_{cur} \quad (4.42)$$

$$NF_{alloc,livecroot\_stor} = \frac{CF_{alloc,leaf\_tot} a_2 a_3 a_4}{CN_{lw}} (1 - f_{cur}) \quad (4.43)$$

$$NF_{alloc,deadcroot} = \frac{CF_{alloc,leaf\_tot} a_2 a_3 (1 - a_4)}{CN_{dw}} f_{cur} \quad (4.44)$$

$$NF_{alloc,deadcroot\_stor} = \frac{CF_{alloc,leaf} a_2 a_3 (1 - a_4)}{CN_{dw}} (1 - f_{cur}). \quad (4.45)$$

5 Autotrophic Respiration

The model treats maintenance and growth respiration fluxes separately, even though it is difficult to measure them as separate fluxes (Lavigne and Ryan, 1997; Sprugel et al., 1995). Maintenance respiration is defined as the carbon cost to support the metabolic activity of existing live tissue, while growth respiration is defined as the additional carbon cost for the synthesis of new growth.

5.1 Maintenance Respiration

Under the assumption that tissue nitrogen content is a suitable index of cellular metabolic rate, maintenance respiration costs for live tissues (leaf, live stem, live coarse root, and fine root) are calculated as functions tissue nitrogen content and the relevant temperature, following the empirical relationship reported by Ryan (1991):

$$CF_{mr\_leaf} = NS_{leaf} MR_{base} MR_{Q10}^{(T_{2m}-20)/10} \tag{5.1}$$

$$CF_{mr\_livestem} = NS_{livestem} MR_{base} MR_{Q10}^{(T_{2m}-20)/10} \tag{5.2}$$

$$CF_{mr\_livecroot} = NS_{livecroot} MR_{base} MR_{Q10}^{(T_{2m}-20)/10} \tag{5.3}$$

$$CF_{mr\_froot} = \sum_{j=1}^{nlevsoi} NS_{froot} rootfr_j MR_{base} MR_{Q10}^{(Ts_j-20)/10} \tag{5.4}$$

where MR_{base} (= 2.525e^{-6} gC gN^{-1} s^{-1}) is the base rate of maintenance respiration per unit nitrogen content, MR_{q10} (= 2.0) is the temperature sensitivity for maintenance respiration, T_{2m} (°C) is the air temperature at 2m height, Ts_j (°C) is the soil temperature at level j, and $rootfr_j$ is the fraction of fine roots distributed in soil level j.

Note that, for woody vegetation, maintenance respiration costs are not calculated for the dead stem and dead coarse root components. These components are assumed to consist of dead xylem cells, with no metabolic function. By separating the small live component of the woody tissue (ray parenchyma, phloem, and sheathing lateral meristem cells) from the larger fraction of dead woody tissue, it is reasonable to assume a common base maintenance respiration rate for all live tissue types.

The total maintenance respiration cost is then given as:

$$CF_{mr} = CF_{mr\_leaf} + CF_{mr\_froot} + CF_{mr\_livestem} + CF_{mr\_livecroot}. \tag{5.5}$$

5.2 Growth Respiration

Growth respiration is calculated as a factor of 0.3 times the total carbon in new growth on a given timestep, based on construction costs for a range of woody and non-woody tissues (Larcher, 1995). For new carbon and nitrogen allocation that enters storage pools for subsequent display, it is not clear what fraction of the associated growth respiration should occur at the time of initial allocation, and what fraction should occur later, at the time of display of new growth from storage. Eddy covariance estimates of carbon fluxes in forest ecosystems suggest that the growth respiration associated with transfer of allocated carbon and nitrogen from storage into displayed tissue is not significant (Churkina et al., 2003), and so it is assumed in CLM-CN that all of the growth respiration cost is incurred at the time of initial allocation, regardless of the fraction of allocation that is displayed immediately (i.e. regardless of the value of f_{cur}, Section 4.5). This behavior is parameterized in such a way that if future research suggests that some fraction of the growth respiration cost should be incurred at the time of display from storage, a simple parameter modification will effect the change.[1]

[1] Parameter *grpnow* in routines CNGResp and CNAllocation, currently set to 1.0, could be changed to a smaller value to transfer some portion (1-*grpnow*) of the growth respiration forward in time to occur at the time of growth display from storage.

6 Phenology

The CLM-CN phenology model consists of several algorithms, operating at seasonal timescales, controlling transfers of stored carbon and nitrogen out of storage pools for display as new growth and losses of displayed growth to litter pools. Three distinct phenological types are represented by separate algorithms: an evergreen type, for which some fraction of annual leaf growth persists in the displayed pool for longer than one year; a seasonal-deciduous type with a single growing season per year, controlled mainly by temperature and daylength; and a stress-deciduous type with the potential for multiple growing seasons per year, controlled by temperature and soil moisture conditions.

The three phenology types share a common set of control variables. The final resolution of phenology fluxes is generalized, operating identically for all three phenology types, given a specification of the common control variables. The following sections describe first the general flux parameterization, then the algorithms for setting the control parameters for the three phenology types.

6.1 General Phenology Flux Parameterization

Fluxes of carbon and nitrogen from storage pools and into displayed tissue pools pass through a special transfer pool (denoted *_xfer*), maintained as a separate state variable for each tissue type. Storage (*_stor*) and transfer (*_xfer*) pools are maintained separately to reduce the complexity of accounting for transfers into and out of storage over the course of a single growing season.

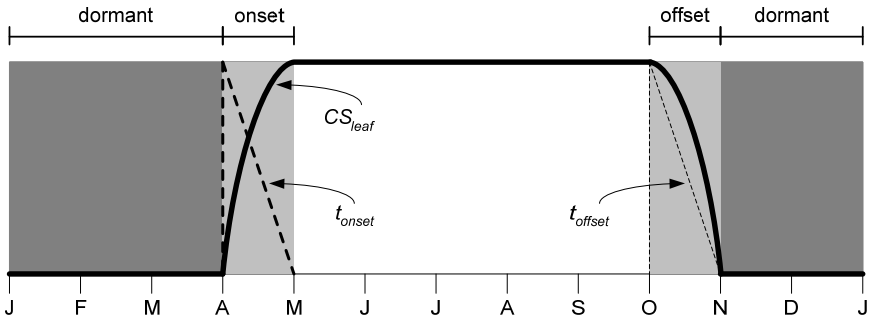

Figure XX. Example (placeholder for now) of annual phenology cycle for seasonal deciduous. From Visio: phenology1.vsd.

6.1.1 Onset Periods

The deciduous phenology algorithms specify the occurrence of onset growth periods. Carbon fluxes from the transfer pools into displayed growth are calculated during these periods as:

$$CF_{leaf\_xfer,leaf} = r_{xfer} CS_{leaf\_xfer} \tag{6.1}$$

$$CF_{froot\_xfer,froot} = r_{xfer} CS_{froot\_xfer} \tag{6.2}$$

$$CF_{livestem\_xfer,livestem} = r_{xfer} CS_{livestem\_xfer} \tag{6.3}$$

$$CF_{deadstem\_xfer,deadstem} = r_{xfer} CS_{deadstem\_xfer} \tag{6.4}$$

$$CF_{livecroot\_xfer,livecroot} = r_{xfer} CS_{livecroot\_xfer} \tag{6.5}$$

$$CF_{deadcroot\_xfer,deadcroot} = r_{xfer} CS_{deadcroot\_xfer}, \tag{6.6}$$

with corresponding nitrogen fluxes:

$$NF_{leaf\_xfer,leaf} = r_{xfer\_on} NS_{leaf\_xfer} \tag{6.7}$$

$$NF_{froot\_xfer,froot} = r_{xfer\_on} NS_{froot\_xfer} \tag{6.8}$$

$$NF_{livestem\_xfer,livestem} = r_{xfer\_on} NS_{livestem\_xfer} \tag{6.9}$$

$$NF_{deadstem\_xfer,deadstem} = r_{xfer\_on} NS_{deadstem\_xfer} \tag{6.10}$$

$$NF_{livecroot\_xfer,livecroot} = r_{xfer\_on} NS_{livecroot\_xfer} \tag{6.11}$$

$$NF_{deadcroot\_xfer,deadcroot} = r_{xfer\_on} NS_{deadcroot\_xfer}, \tag{6.12}$$

where r_{xfer_on} (s^{-1}) is a time-varying rate coefficient controlling flux out of the transfer pool:

$$r_{xfer\_on} = \begin{cases} 2/t_{onset} & \text{for } t_{onset} \neq \Delta t \\ 1/\Delta t & \text{for } t_{onset} = \Delta t \end{cases}, \tag{6.13}$$

and t_{onset} (s) is the number of seconds remaining in the current phenology onset growth period (Figure XX). The form of Eq. (6.13) produces a flux from the transfer pool which declines linearly over the onset growth period, approaching zero flux in the final timestep. An example of the flux rate out of the transfer pool and the corresponding changes in the transfer and display state variables is shown in Figure XX.

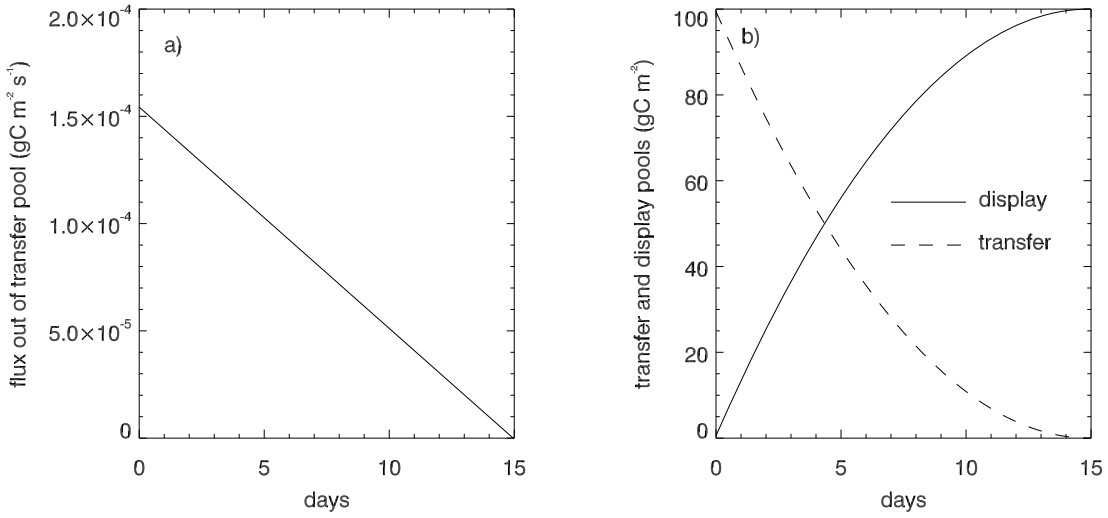

Figure XX. Example fluxes and pools sizes for an onset growth period of 15 days, with initial transfer pool size of 100 gC m^{-2} and a timestep of one hour. a) Flux leaving transfer pool (e.g. $CF_{leaf\_xfer,leaf}$). b) Carbon content of transfer pool and its associated display pool (e.g. CS_{leaf_xfer} and CS_{leaf}, respectively).

6.1.2 Offset Periods

The deciduous phenology algorithms also specify the occurrence of litterfall, or offset, periods. In contrast to the onset periods, only leaf and fine root state variables are subject to litterfall fluxes. Carbon fluxes from display pools into litter are calculated during these periods as:

$$CF_{leaf,litter}^{n} = \begin{cases} CF_{leaf,litter}^{n-1} + r_{xfer\_off}\left(CS_{leaf} - CF_{leaf,litter}^{n-1} t_{offset}\right) & \text{for } t_{offset} \neq \Delta t \\ \left(CS_{leaf} / \Delta t\right) + CF_{alloc,leaf} & \text{for } t_{offset} = \Delta t \end{cases} \quad (6.14)$$

$$CF_{froot,litter}^{n} = \begin{cases} CF_{froot,litter}^{n-1} + r_{xfer\_off}\left(CS_{froot} - CF_{froot,litter}^{n-1} t_{offset}\right) & \text{for } t_{offset} \neq \Delta t \\ CS_{froot} / \Delta t + CF_{alloc,froot} & \text{for } t_{offset} = \Delta t \end{cases} \quad (6.15)$$

$$r_{xfer\_off} = \frac{2\Delta t}{t_{offset}^{2}} \quad (6.16)$$

where superscripts *n* and *n-1* refer to fluxes on the current and previous timesteps, respectively. The rate coefficient r_{xfer_off} varies with time to produce a linearly increasing litterfall rate throughout the offset period, and the special case for fluxes in the final

litterfall timestep ($t_{offset} = \Delta t$) ensures that all of the displayed growth is sent to the litter pools for deciduous plant types.

Corresponding nitrogen fluxes during litterfall take into account retranslocation of nitrogen out of the displayed leaf pool prior to litterfall ($NF_{leaf,retrans}$, gN m^{-2} s^{-1}). Retranslocation of nitrogen out of fine roots is assumed to be negligible. The fluxes are:

$$NF_{leaf,litter} = CF_{leaf,litter} / CN_{leaf\_litter} \tag{6.17}$$

$$NF_{froot,litter} = CF_{leaf,litter} / CN_{froot} \tag{6.18}$$

$$NF_{leaf,retrans} = \left(CF_{leaf,litter} / CN_{leaf} \right) - NF_{leaf,litter} . \tag{6.19}$$

An example of the litterfall carbon flux rate and corresponding changes in display and litter carbon pool sizes over the course of an offset period is shown in Figure XX.

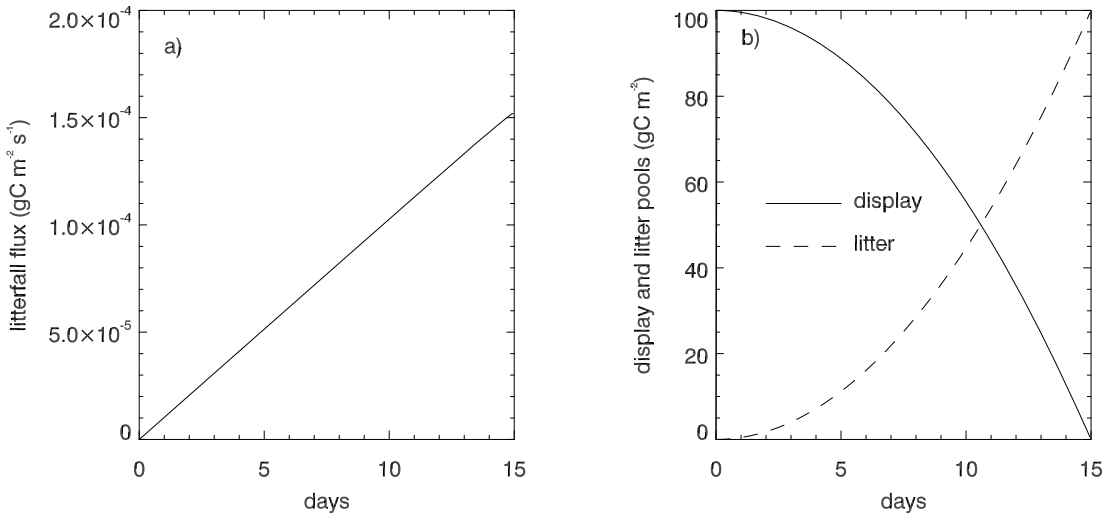

Figure XX. Example fluxes and pool sizes for an offset (litterfall) period of 15 days, with initial display pool size of 100 gC m^{-2} and a timestep of one hour. a) Litterfall flux (e.g $CF_{leaf,litter}$). b) Carbon content of display pool and litter pool through the litterfall period, ignoring the losses from litter pool due to decomposition during this period.

6.1.3 Background Onset Growth

The stress-deciduous phenology algorithm includes a provision for the case when stress signals are absent, and the vegetation shifts from a deciduous habit to an evergreen habit, until the next occurrence of an offset stress trigger (see section XX). In that case,

the regular onset flux mechanism is switched off and a background onset growth algorithm is invoked ($r_{bgtr} > 0$, see Section XX.X). During this period, small fluxes of carbon and nitrogen from the storage pools into the associated transfer pools are calculated on each time step, and the entire contents of the transfer pool is added to the associated displayed growth pool on each time step. The carbon fluxes from transfer to display pools under these conditions are:

$$CF_{leaf\_xfer,leaf} = CS_{leaf\_xfer} / \Delta t \tag{6.20}$$

$$CF_{froot\_xfer,froot} = CS_{froot\_xfer} / \Delta t \tag{6.21}$$

$$CF_{livestem\_xfer,livestem} = CS_{livestem\_xfer} / \Delta t \tag{6.22}$$

$$CF_{deadstem\_xfer,deadstem} = CS_{deadstem\_xfer} / \Delta t \tag{6.23}$$

$$CF_{livecroot\_xfer,livecroot} = CS_{livecroot\_xfer} / \Delta t \tag{6.24}$$

$$CF_{deadcroot\_xfer,deadcroot} = CS_{deadcroot\_xfer} / \Delta t\,, \tag{6.25}$$

and the corresponding nitrogen fluxes are:

$$NF_{leaf\_xfer,leaf} = NS_{leaf\_xfer} / \Delta t \tag{6.26}$$

$$NF_{froot\_xfer,froot} = NS_{froot\_xfer} / \Delta t \tag{6.27}$$

$$NF_{livestem\_xfer,livestem} = NS_{livestem\_xfer} / \Delta t \tag{6.28}$$

$$NF_{deadstem\_xfer,deadstem} = NS_{deadstem\_xfer} / \Delta t \tag{6.29}$$

$$NF_{livecroot\_xfer,livecroot} = NS_{livecroot\_xfer} / \Delta t \tag{6.30}$$

$$NF_{deadcroot\_xfer,deadcroot} = NS_{deadcroot\_xfer} / \Delta t\,. \tag{6.31}$$

6.1.4 Background Litterfall

Both evergreen and stress-deciduous phenology algorithms can specify a litterfall flux that is not associated with a specific offset period, but which occurs instead at a slow rate over an extended period of time, referred to as background litterfall. For evergreen types the background litterfall is the only litterfall flux. For stress-deciduous types either the offset period litterfall or the background litterfall mechanism may be active, but not both at once (see section XX). Given a specification of the background litterfall rate (r_{bglf}, s^{-1}), litterfall carbon fluxes are calculated as

$$CF_{leaf,litter} = r_{bglf} CS_{leaf} \tag{6.32}$$

$$CS_{froot,litter} = r_{bglf} CS_{froot}, \tag{6.33}$$

with corresponding nitrogen litterfall and retranslocation fluxes:

$$NF_{leaf,litter} = CF_{leaf,litter} / CN_{leaf\_litter} \tag{6.34}$$

$$NF_{froot,litter} = CF_{froot,litter} / CN_{froot} \tag{6.35}$$

$$NF_{leaf,retrans} = \left(CF_{leaf,litter} / CN_{leaf} \right) - NF_{leaf,litter}. \tag{6.36}$$

6.1.5 Livewood Turnover

The conceptualization of live wood vs. dead wood fractions for stem and coarse root pools is intended to capture the difference in maintenance respiration rates between these two physiologically distinct tissue types (Section 5.1). Unlike displayed pools for leaf and fine root, which are lost to litterfall, live wood cells reaching the end of their lifespan are retained as a part of the dead woody structure of stems and coarse roots. A mechanism is therefore included in the phenology routine to effect the transfer of live wood to dead wood pools, and which also takes into account the different nitrogen concentrations typical of these tissue types.

A live wood turnover rate (r_{lwt}, s^{-1}) is defined as

$$r_{lwt} = p_{lwt} / \left(365 \cdot 86400 \right) \tag{6.37}$$

where $p_{lwt} = 0.7$ is the assumed annual live wood turnover fraction. Carbon fluxes from live to dead wood pools are:

$$CF_{livestem,deadstem} = CS_{livestem} r_{lwt} \tag{6.38}$$

$$CF_{livecroot,deadcroot} = CS_{livecroot} r_{lwt}, \tag{6.39}$$

and the associated nitrogen fluxes, including retranslocation of nitrogen out of live wood during turnover, are:

$$NF_{livestem,deadstem} = CF_{livestem,deadstem} / CN_{dw} \tag{6.40}$$

$$NF_{livestem,retrans} = \left(CF_{livestem,deadstem} / CN_{lw} \right) - NF_{livestem,deadstem} \tag{6.41}$$

$$NF_{livecroot,deadcroot} = CF_{livecroot,deadcroot} / CN_{dw} \tag{6.42}$$

$$NF_{livecroot,retrans} = \left(CF_{livecroot,deadcroot} / CN_{lw} \right) - NF_{livecroot,deadcroot}. \tag{6.43}$$

6.2 Evergreen Phenology

The evergreen phenology algorithm is by far the simplest of the three possible types. It is assumed for all evergreen types that all carbon and nitrogen allocated for new growth in the current timestep goes immediately to the displayed growth pools (i.e. f_{cur} = 1.0 (Section 4)). As such, there is never an accumulation of carbon or nitrogen in the storage or transfer pools, and so the onset growth and background onset growth mechanisms are never invoked for this type. Litterfall is specified to occur only through the background litterfall mechanism – there are no distinct periods of litterfall for evergreen types, but rather a continuous (slow) shedding of foliage and fine roots. This is an obvious area for potential improvements in the model, since it is known, at least for evergreen needleleaf trees in the temperate and boreal zones, that there are distinct periods of higher and lower leaf litterfall (Ferrari, 1999; Gholz et al., 1985). The rate of background litterfall (r_{bglf}, Section 6.1.4) depends on the specified leaf longevity (τ_{leaf}, y), as

$$r_{bglf} = \frac{1}{\tau_{leaf} \cdot 365 \cdot 86400} . \qquad (6.44)$$

Values for τ_{leaf} are given in Table XX.

6.3 Seasonal-Deciduous Phenology

The seasonal-deciduous phenology algorithm in CLM-CN derives directly from the treatment used in the offline model Biome-BGC v. 4.1.2, (Thornton et al., 2002), which in turn is based on the parameterizations for leaf onset and offset for temperate deciduous broadleaf forest from White et al. (1997). Initiation of leaf onset is triggered when a common degree-day summation exceeds a critical value, and leaf litterfall is initiated when daylength is shorter than a critical value. Because of the dependence on daylength, the seasonal deciduous phenology algorithm is only valid for latitudes outside of the tropical zone, defined here as $|\text{latitude}| > 19.5°$. Neither the background onset nor background litterfall mechanism is invoked for the seasonal-deciduous phenology algorithm. The algorithm allows a maximum of one onset period and one offset period each year.

The algorithms for initiation of onset and offset periods use the winter and summer solstices as coordination signals. The period between winter and summer solstice is identified as $dayl_n > dayl_{n-1}$, and the period between summer and winter solstice is identified as $dayl_n < dayl_{n-1}$, where $dayl_n$ and $dayl_{n-1}$ are the daylength (s) calculated for the current and previous timesteps, respectively, using

$$dayl = 2 \cdot 13750.9871 \cdot \text{acos}\left(\frac{-\sin(lat)\sin(decl)}{\cos(lat)\cos(decl)} \right), \tag{6.45}$$

where *lat* and *decl* are the latitude and solar declination (radians), respectively, and the factor 13750.9871 is the number of seconds per radian of hour-angle.

6.3.1 Seasonal-Deciduous Onset Trigger

The onset trigger for the seasonal-deciduous phenology algorithm is based on an accumulated growing-degree-day approach (White et al., 1997). The growing-degree-day summation (GDD_{sum}) is initiated ($GDD_{sum} = 0$) when the phenological state is dormant and the model timestep crosses the winter solstice. Once these conditions are met, GDD_{sum} is updated on each timestep as

$$GDD_{sum}^{n} = \begin{cases} GDD_{sum}^{n-1} + \left(T_{s,3} - TKFRZ\right) f_{day} & \text{for } T_{s,3} > TKFRZ \\ GDD_{sum}^{n-1} & \text{for } T_{s,3} \le TKFRZ \end{cases} \tag{6.46}$$

where $T_{s,3}$ (K) is the temperature of the third soil layer, and $f_{day} = \Delta t / 86400$. The onset period is initiated if $GDD_{sum} > GDD_{sum\_crit}$, where

$$GDD_{sum\_crit} = \exp\left(4.8 + 0.13\left(T_{2m,ann\_avg} - TKFRZ\right)\right) \tag{6.47}$$

and where T_{2m,ann_avg} (K) is the annual average of the 2m air temperature, and TKFRZ is the freezing point of water (273.15 K). The following control variables are set when a new onset growth period is initiated:

$$GDD_{sum} = 0 \tag{6.48}$$

$$t_{onset} = 86400 \cdot n_{days\_on}, \tag{6.49}$$

where n_{days_on} is set to a constant value of 30 days. Fluxes from storage into transfer pools occur in the timestep when a new onset growth period is initiated. Carbon fluxes are:

$$CF_{leaf\_stor,leaf\_xfer} = f_{stor,xfer} CS_{leaf\_stor} / \Delta t \quad (6.50)$$

$$CF_{froot\_stor,froot\_xfer} = f_{stor,xfer} CS_{froot\_stor} / \Delta t \quad (6.51)$$

$$CF_{livestem\_stor,livestem\_xfer} = f_{stor,xfer} CS_{livestem\_stor} / \Delta t \quad (6.52)$$

$$CF_{deadstem\_stor,deadstem\_xfer} = f_{stor,xfer} CS_{deadstem\_stor} / \Delta t \quad (6.53)$$

$$CF_{livecroot\_stor,livecroot\_xfer} = f_{stor,xfer} CS_{livecroot\_stor} / \Delta t \quad (6.54)$$

$$CF_{deadcroot\_stor,deadcroot\_xfer} = f_{stor,xfer} CS_{deadcroot\_stor} / \Delta t \quad (6.55)$$

$$CF_{gresp\_stor,gresp\_xfer} = f_{stor,xfer} CS_{gresp\_stor} / \Delta t \quad (6.56)$$

and the associated nitrogen fluxes are:

$$NF_{leaf\_stor,leaf\_xfer} = f_{stor,xfer} NS_{leaf\_stor} / \Delta t \quad (6.57)$$

$$NF_{froot\_stor,froot\_xfer} = f_{stor,xfer} NS_{froot\_stor} / \Delta t \quad (6.58)$$

$$NF_{livestem\_stor,livestem\_xfer} = f_{stor,xfer} NS_{livestem\_stor} / \Delta t \quad (6.59)$$

$$NF_{deadstem\_stor,deadstem\_xfer} = f_{stor,xfer} NS_{deadstem\_stor} / \Delta t \quad (6.60)$$

$$NF_{livecroot\_stor,livecroot\_xfer} = f_{stor,xfer} NS_{livecroot\_stor} / \Delta t \quad (6.61)$$

$$NF_{deadcroot\_stor,deadcroot\_xfer} = f_{stor,xfer} NS_{deadcroot\_stor} / \Delta t \quad (6.62)$$

where $f_{stor,xfer}$ is the fraction of current storage pool moved into the transfer pool for display over the incipient onset period. This fraction is set to 0.5, based on the observation that seasonal deciduous trees are capable of replacing their canopies from storage reserves in the event of a severe early-season disturbance such as frost damage or defoliation due to insect herbivory.

If the onset criteria ($GDD_{sum} > GDD_{sum\_crit}$) is not met before the summer solstice, then GDD_{sum} is set to 0.0 and the growing-degree-day accumulation will not start again until the following winter solstice. This mechanism prevents the initiation of very short growing seasons late in the summer in cold climates. The onset counter is decremented on each time step after initiation of the onset period, until it reaches zero, signaling the end of the onset period:

$$t_{onfset}^{n} = t_{onfset}^{n-1} - \Delta t \quad (6.63)$$

6.3.2 Seasonal-Deciduous Offset Trigger

After the completion of an onset period, and once past the summer solstice, the offset (litterfall) period is triggered when daylength is shorter than 39300 s. The offset counter is set at the initiation of the offset period: $t_{offset} = 86400 \cdot n_{days\_off}$, where n_{days_off} is set to a constant value of 15 days. The offset counter is decremented on each time step after initiation of the offset period, until it reaches zero, signaling the end of the offset period:

$$t_{offset}^{n} = t_{offset}^{n-1} - \Delta t \tag{6.64}$$

6.4 Stress-Deciduous Phenology

The stress-deciduous phenology algorithm has been developed specifically for CLM-CN, but it is based in part on the grass phenology model proposed by White et al. (1997). The algorithm handles phenology for vegetation types such as grasses and tropical drought-deciduous trees that respond to both cold and drought-stress signals, and that can have multiple growing seasons per year. The algorithm also allows for the possibility that leaves might persist year-round in the absence of a suitable stress trigger. In that case the phenology switches to an evergreen habit, maintaining a marginally-deciduous leaf longevity (one year) until the occurrence of the next stress trigger.

6.4.1 Stress-Deciduous Onset Triggers

In relatively warm climates, onset triggering depends on soil water availability. At the beginning of a dormant period (end of previous offset period), an accumulated soil water index (SWI_{sum}, d) is initialized ($SWI_{sum} = 0$), with subsequent accumulation calculated as:

$$SWI_{sum}^{n} = \begin{cases} SWI_{sum}^{n-1} + f_{day} & \text{for } \Psi_{s,3} \geq \Psi_{onset} \\ SWI_{sum}^{n-1} & \text{for } \Psi_{s,3} < \Psi_{onset} \end{cases} \tag{6.65}$$

where $\Psi_{s,3}$ is the soil water potential (MPa) in the third soil layer and Ψ_{onset} = -2 MPa is the onset soil water potential threshold. Onset triggering is possible once $SWI_{sum} > 15$. If the cold climate growing degree-day accumulator is not active at the time when this threshold is reached (see below), and if the daylength is greater than 6 hours, then onset is

triggered. Except as noted below, SWI_{sum} continues to accumulate according to Eq. (6.65) during the dormant period if the daylength criteria is preventing onset triggering, and onset is then triggered at the timestep when daylength exceeds 6 hours.

In cold climates, onset triggering depends on both accumulated soil temperature summation and adequate soil moisture. At the beginning of a dormant period a freezing day accumulator (FD_{sum}, d) is initialized ($FD_{sum} = 0$), with subsequent accumulation calculated as:

$$FD_{sum}^{n} = \begin{cases} FD_{sum}^{n-1} + f_{day} & \text{for } T_{s,3} > TKFRZ \\ FD_{sum}^{n-1} & \text{for } T_{s,3} \le TKFRZ \end{cases} . \tag{6.66}$$

If $FD_{sum} > 15$ during the dormant period, then a cold-climate onset triggering criteria is introduced, following exactly the growing degree-day summation (GDD_{sum}) logic of Eqs. (6.46) and (6.47). When the cold-climate onset triggering criteria is introduced SWI_{sum} is reset ($SWI_{sum} = 0$). Onset triggering under these conditions depends on meeting all three of the following criteria: $SWI_{sum} > 15$, $GDD_{sum} > GDD_{sum\_crit}$, and daylength greater than 6 hrs.

The following control variables are set when a new onset growth period is initiated: $SWI_{sum} = 0$, $FD_{sum} = 0$, $GDD_{sum} = 0$, $n_{days\_active} = 0$, and $t_{onset} = 86400 \cdot n_{days\_on}$, where n_{days_on} is set to a constant value of 30 days. Fluxes from storage into transfer pools occur in the timestep when a new onset growth period is initiated, and are handled identically to Eqs. (6.50) - (6.56) for carbon fluxes, and to Eqs. (6.57) - (6.62) for nitrogen fluxes. The onset counter is decremented on each time step after initiation of the onset period, until it reaches zero, signaling the end of the onset period:

$$t_{onfset}^{n} = t_{onfset}^{n-1} - \Delta t \tag{6.67}$$

6.4.2 Stress-Deciduous Offset Triggers

Any one of the following three conditions is sufficient to trigger the initiation of an offset period for the stress-deciduous phenology algorithm: sustained period of dry soil, sustained period of cold temperature, or daylength shorter than 6 hours. Offset triggering due to dry soil or cold temperature conditions is only allowed once the most

recent onset period is complete. Dry soil condition is evaluated with an offset soil water index accumulator ($OSWI_{sum}$, d). To test for a sustained period of dry soils, this control variable can increase or decrease, as follows:

$$OSWI_{sum}^{n} = \begin{cases} OSWI_{sum}^{n-1} + f_{day} & \text{for } \Psi_{s,3} \le \Psi_{offset} \\ \max\left(OSWI_{sum}^{n-1} - f_{day}, 0\right) & \text{for } \Psi_{s,3} > \Psi_{onset} \end{cases} \tag{6.68}$$

where Ψ_{offset} = -2 MPa is the offset soil water potential threshold. An offset period is triggered if the previous onset period is complete and $OSWI_{sum} \ge OSWI_{sum\_crit}$, where $OSWI_{sum\_crit}$ = 15.

Cold temperature condition is evaluated with an offset freezing day accumulator (OFD_{sum}, d). To test for a sustained period of cold temperature, this variable can increase or decrease, as follows:

$$OFD_{sum}^{n} = \begin{cases} OFD_{sum}^{n-1} + f_{day} & \text{for } T_{s,3} \le TKFRZ \\ \max\left(OFD_{sum}^{n-1} - f_{day}, 0\right) & \text{for } T_{s,3} > TKFRZ \end{cases} \tag{6.69}$$

An offset period is triggered if the previous onset period is complete and $OFD_{sum} > OFD_{sum\_crit}$, where OFD_{sum_crit} = 15.

The offset counter is set at the initiation of the offset period: $t_{offset} = 86400 \cdot n_{days\_off}$, where n_{days_off} is set to a constant value of 15 days. The offset counter is decremented on each time step after initiation of the offset period, until it reaches zero, signaling the end of the offset period:

$$t_{offset}^{n} = t_{offset}^{n-1} - \Delta t \tag{6.70}$$

6.4.3 Stress-Deciduous: Long Growing Season

Under conditions when the stress-deciduous conditions triggering offset are not met for one year or longer, the stress-deciduous algorithm shifts toward the evergreen behavior. This can happen in cases where a stress-deciduous vegetation type is assigned in a climate where suitably strong stresses occur irregularly or not at all. This condition is evaluated by tracking the number of days since the beginning of the most recent onset period (n_{days_active}, d). At the end of an offset period n_{days_active} is reset to 0. A long growing season control variable (LGS, range 0 to 1) is calculated as:

$$LGS = \begin{cases} 0 & \text{for } n_{days\_active} < 365 \\ \left(n_{days\_active} / 365\right) - 1 & \text{for } 365 \le n_{days\_active} < 730 \\ 1 & \text{for } n_{days\_active} \ge 730 \end{cases}. \quad (6.71)$$

The rate coefficient for background litterfall (r_{bglf}, s^{-1}) is calculated as a function of *LGS*:

$$r_{bglf} = \frac{LGS}{\tau_{leaf} \cdot 365 \cdot 86400} \quad (6.72)$$

where τ_{leaf} is the leaf longevity (Table XX). The result is a shift to continuous litterfall as n_{days_active} increases from 365 to 730. When a new offset period is triggered r_{bglf} is set to 0.

The rate coefficient for background onset growth from the transfer pools (r_{bgtr}, s^{-1}) (Section XX.X) also depends on *LGS*, as:

$$r_{bgtr} = \frac{LGS}{365 \cdot 86400}. \quad (6.73)$$

On each timestep with $r_{bgtr} \neq 0$, carbon fluxes from storage to transfer pools are calculated as:

$$CF_{leaf\_stor,leaf\_xfer} = CS_{leaf\_stor} r_{bgtr} \quad (6.74)$$

$$CF_{froot\_stor,froot\_xfer} = CS_{froot\_stor} r_{bgtr} \quad (6.75)$$

$$CF_{livestem\_stor,livestem\_xfer} = CS_{livestem\_stor} r_{bgtr} \quad (6.76)$$

$$CF_{deadstem\_stor,deadstem\_xfer} = CS_{deadstem\_stor} r_{bgtr} \quad (6.77)$$

$$CF_{livecroot\_stor,livecroot\_xfer} = CS_{livecroot\_stor} r_{bgtr} \quad (6.78)$$

$$CF_{deadcroot\_stor,deadcroot\_xfer} = CS_{deadcroot\_stor} r_{bgtr}, \quad (6.79)$$

with corresponding nitrogen fluxes:

$$NF_{leaf\_stor,leaf\_xfer} = NS_{leaf\_stor} r_{bgtr} \quad (6.80)$$

$$NF_{froot\_stor,froot\_xfer} = NS_{froot\_stor} r_{bgtr} \quad (6.81)$$

$$NF_{livestem\_stor,livestem\_xfer} = NS_{livestem\_stor} r_{bgtr} \quad (6.82)$$

$$NF_{deadstem\_stor,deadstem\_xfer} = NS_{deadstem\_stor} r_{bgtr} \quad (6.83)$$

$$NF_{livecroot\_stor,livecroot\_xfer} = NS_{livecroot\_stor} r_{bgtr} \quad (6.84)$$

$$NF_{deadcroot\_stor,deadcroot\_xfer} = NS_{deadcroot\_stor} r_{bgtr}. \quad (6.85)$$

The result, in conjunction with the treatment of background onset growth described in Section XX.X, is a shift to continuous transfer from storage to display pools at a rate that would result in complete turnover of the storage pools in one year at steady state, once *LGS* reaches 1 (i.e. after two years without stress-deciduous offset conditions). If and when conditions cause stress-dicduous triggering again, r_{bgtr} is rest to 0.

6.5 Litterfall Fluxes Merged to the Column Level

CLM-CN uses three litter pools, defined on the basis of commonly measured chemical fractionation of fresh litter into labile (LIT1 = hot water and alcohol soluble fraction), cellulose/hemicellulose (LIT2 = acid soluble fraction) and remaining material, referred to here for convenience as lignin (LIT3 = acid insoluble fraction) (Aber et al., 1990; Taylor et al., 1989). A characteristic of the hierarchical structure of CLM-CN is that multiple plant functional types can coexist on a single soil column, while each soil column includes a single instance of the litter pools. Fluxes entering the litter pools due to litterfall are calculated using a weighted average of the fluxes originating at the PFT level. Carbon fluxes are calculated as:

$$CF_{leaf,lit1} = \sum_{p=0}^{npfts} CF_{leaf,litter} f_{lab\_leaf,p} wcol_p \tag{6.86}$$

$$CF_{leaf,lit2} = \sum_{p=0}^{npfts} CF_{leaf,litter} f_{cel\_leaf,p} wcol_p \tag{6.87}$$

$$CF_{leaf,lit3} = \sum_{p=0}^{npfts} CF_{leaf,litter} f_{lig\_leaf,p} wcol_p \tag{6.88}$$

$$CF_{froot,lit1} = \sum_{p=0}^{npfts} CF_{froot,litter} f_{lab\_froot,p} wcol_p \tag{6.89}$$

$$CF_{froot,lit2} = \sum_{p=0}^{npfts} CF_{froot,litter} f_{cel\_froot,p} wcol_p \tag{6.90}$$

$$CF_{froot,lit3} = \sum_{p=0}^{npfts} CF_{froot,litter} f_{lig\_froot,p} wcol_p \,, \tag{6.91}$$

where $f_{lab\_leaf,p}$, $f_{cel\_leaf,p}$, and $f_{lig\_leaf,p}$ are the labile, cellulose/hemicellulose, and lignin fractions of leaf litter for PFT p, $f_{lab\_froot,p}$, $f_{cel\_froot,p}$, and $f_{lig\_froot,p}$ are the labile, cellulose/hemicellulose, and lignin fractions of fine root litter for PFT p, $wtcol_p$ is the

weight relative to the column for PFT p, and p is an index through the plant functional types occurring on a column. Values for labile, cellulose, and lignin fractions for leaf and fine root litter are given in Table XX. Nitrogen fluxes to the litter pools are assumed to follow the C:N of the senescent tissue, and so are distributed using the same fractions used for carbon fluxes:

$$NF_{leaf,lit1} = \sum_{p=0}^{npfts} NF_{leaf,litter} f_{lab\_leaf,p} wcol_p \tag{6.92}$$

$$NF_{leaf,lit2} = \sum_{p=0}^{npfts} NF_{leaf,litter} f_{cel\_leaf,p} wcol_p \tag{6.93}$$

$$NF_{leaf,lit3} = \sum_{p=0}^{npfts} NF_{leaf,litter} f_{lig\_leaf,p} wcol_p \tag{6.94}$$

$$NF_{froot,lit1} = \sum_{p=0}^{npfts} NF_{froot,litter} f_{lab\_froot,p} wcol_p \tag{6.95}$$

$$NF_{froot,lit2} = \sum_{p=0}^{npfts} NF_{froot,litter} f_{cel\_froot,p} wcol_p \tag{6.96}$$

$$NF_{froot,lit3} = \sum_{p=0}^{npfts} NF_{froot,litter} f_{lig\_froot,p} wcol_p \ . \tag{6.97}$$

7 Decomposition

Decomposition of fresh litter material into progressively more recalcitrant forms of soil organic matter is represented in CLM-CN using three state variables for fresh litter and four state variables for soil organic matter (SOM). The masses of carbon and nitrogen in the live microbial community are not modeled explicitly, but the activity of these organisms is represented by decomposition fluxes transferring mass between the litter and SOM pools, and heterotrophic respiration losses associated with these transformations. The litter and SOM pools in CLM-CN are arranged as a converging cascade (Figure XX), derived directly from the implementation in Biome-BGC v4.1.2 (Thornton et al., 2002; Thornton and Rosenbloom, 2005).

7.1 Rate Constants and Parameters

Model parameters are estimated based on a synthesis of microcosm decomposition studies using radio-labeled substrates (Degens and Sparling, 1996; Ladd et al., 1992; Martin et al., 1980; Mary et al., 1993; Saggar et al., 1994; Sørensen, 1981; van Veen et al., 1984). Multiple exponential models are fitted to data from the microcosm studies to estimate exponential decay rates and respiration fractions (Thornton, 1998). The microcosm experiments used for parameterization were all conducted at constant temperature and under moist conditions with relatively high mineral nitrogen concentrations, and so the resulting rate constants are assumed not limited by the availability of water or mineral nitrogen. Table XX lists the base decomposition rates for each litter and SOM pool, as well as a base rate for physical fragmentation for the coarse woody debris pool (CWD).

Table XX. Decomposition rate constants for litter and SOM pools

	Biome-BGC	CLM-CN
	k_{disc1} (d^{-1})	k_{disc2} (hr^{-1})
k_{Lit1}	0.7	0.04892
k_{Lit2}	0.07	0.00302
k_{Lit3}	0.014	0.00059
k_{SOM1}	0.07	0.00302

k_{SOM2}	0.014	0.00059
k_{SOM3}	0.0014	0.00006
k_{SOM4}	0.0001	0.000004
k_{CWD}	0.001	0.00004

The first column of Table XX gives the rates as used for the Biome-BGC model, which uses a discrete-time model with a daily timestep. The second column of Table XX shows the rates transformed for a one-hour discrete timestep typical of CLM-CN. The transformation is based on the conversion of the initial discrete-time value (k_{disc1}) first to a continuous time value (k_{cont}), then to the new discrete-time value with a different timestep (k_{disc2}) , following Olson (1963):

$$k_{cont} = -\log\left(1 - k_{disc1}\right) \tag{7.1}$$

$$k_{disc2} = 1 - \exp\left(-k_{cont}\frac{\Delta t_2}{\Delta t_1}\right) \tag{7.2}$$

where Δt_1 (s) and Δt_2 (s) are the time steps of the initial and new discrete-time models, respectively.

These base rates are modified on each timestep by functions of soil temperature and soil water potential, based on averages of these quantities over the top five soil layers (top 29 cm of soil column). A rate scalar for temperature (r_{tsoil}, unitless) is calculated using a relationship from Lloyd and Taylor (1994):

$$r_{tsoil} = \sum_{j=1}^{5} \begin{cases} \exp\left(308.56\left(\frac{1}{71.02} - \frac{1}{T_{soil,j} - TKFRZ}\right)\right) w_{soil,j} & \text{for } T_{soil,j} \geq TKFRZ - 10 \\ 0 & \text{for } T_{soil,j} < TKFRZ - 10 \end{cases} \tag{7.3}$$

where j is the soil layer index, $T_{soil,j}$ (K) is the temperature of soil level j, and $w_{soil,j}$ is the fraction of the total soil depth in the top five layers accounted for by layer j. A rate scalar for soil water potential (r_{water}, unitless) is calculated using a relationship from Andrén and Paustian (1987) and supported by additional data in Orchard and Cook (1983):

$$r_{water} = \sum_{j=1}^{5} \begin{cases} 0 & \text{for } \Psi_j < \Psi_{min} \\ \dfrac{\log\left(\Psi_{min}/\Psi_j\right)}{\log\left(\Psi_{min}/\Psi_{max}\right)} w_{soil,j} & \text{for } \Psi_{min} \le \Psi_j \le \Psi_{max} \\ 1 & \text{for } \Psi_j > \Psi_{max} \end{cases} \quad (7.4)$$

where Ψ_j is the soil water potential in layer j, Ψ_{min} is a lower limit for soil water potential control on decomposition rate (set to -10 MPa). $\Psi_{sat,j}$ (MPa) is the saturated soil water potential, calculated using the multivariate regression model from Cosby et al. (1984):

$$\Psi_{sat,j} = -(9.8\text{e-}5)\exp\left(\left(1.54 - 0.0095P_{sand,j} + 0.0063\left(100 - P_{sand,j} - P_{clay,j}\right)\right)\log(10)\right) \quad (7.5)$$

where $P_{sand,j}$ and $P_{clay,j}$ are the volume percentages of sand and clay in soil layer j. The combined decomposition rate scalar (r_{total}, unitless) is:

$$r_{total} = r_{tsoil} r_{water} . \quad (7.6)$$

Respiration fractions are parameterized for decomposition fluxes out of each litter and SOM pool. The respiration fraction (*rf*, unitless) is the fraction of the decomposition carbon flux leaving one of the litter or SOM pools that is released as CO_2 due to heterotrophic respiration. Respiration fractions and exponential decay rates are estimated simultaneously from the results of microcosm decomposition experiments (Thornton, 1998). The same values are used in CLM-CN and Biome-BGC (Table XX).

Table XX. Respiration fractions for litter and SOM pools

Pool	*rf*
rf_{Lit1}	0.39
rf_{Lit2}	0.55
rf_{Lit3}	0.29
rf_{SOM1}	0.28
rf_{SOM2}	0.46
rf_{SOM3}	0.55
rf_{SOM4}	1.0[a]

[a] The respiration fraction for pool SOM4 is 1.0 by definition: since there is no pool downstream of SOM4, the entire carbon flux leaving this pool is assumed to be respired as CO_2.

7.2 Potential Decomposition Fluxes

Decomposition rates can also be limited by the availability of mineral nitrogen, but calculation of this limitation depends on first estimating the potential rates of decomposition, assuming an unlimited mineral nitrogen supply. The general case is described here first, referring to a generic decomposition flux from an "upstream" pool (*u*) to a "downstream" pool (*d*), with an intervening loss due to respiration. The potential carbon flux out of the upstream pool ($CF_{pot,u}$, gC m^{-2} s^{-1}) is:

$$CF_{pot,u} = CS_u k_u \tag{7.7}$$

where CS_u (gC m^{-2}) is the initial mass in the upstream pool and k_u is the decay rate constant (s^{-1}) for the upstream pool, adjusted for temperature and moisture conditions. Depending on the C:N ratios of the upstream and downstream pools and the amount of carbon lost in the transformation due to respiration (the respiration fraction), the execution of this potential carbon flux can generate either a source or a sink of new mineral nitrogen ($NF_{pot\_min,u\to d}$, gN m^{-2} s^{-1}). The governing equation (Thornton and Rosenbloom, 2005) is:

$$NF_{pot\_min,u\to d} = \frac{CF_{pot,u}\left(1 - rf_u - \frac{CN_d}{CN_u}\right)}{CN_d} \tag{7.8}$$

where rf_u is the respiration fraction for fluxes leaving the upstream pool, CN_u and CN_d are the C:N ratios for upstream and downstream pools, respectively. Negative values of $NF_{pot\_min,u\to d}$ indicate that the decomposition flux results in a source of new mineral nitrogen, while positive values indicate that the potential decomposition flux results in a sink (demand) for mineral nitrogen.

Following from the general case, potential carbon fluxes leaving individual pools in the decomposition cascade are given as:

$$CF_{pot,Lit1} = CS_{Lit1} k_{Lit1} r_{total} / \Delta t \tag{7.9}$$

$$CF_{pot,Lit2} = CS_{Lit2} k_{Lit2} r_{total} / \Delta t \tag{7.10}$$

$$CF_{pot,Lit3} = CS_{Lit3} k_{Lit3} r_{total} / \Delta t \tag{7.11}$$

$$CF_{pot,SOM1} = CS_{SOM1} k_{SOM1} r_{total} / \Delta t \tag{7.12}$$

$$CF_{pot,SOM2} = CS_{SOM2} k_{SOM2} r_{total} / \Delta t \tag{7.13}$$

$$CF_{pot,SOM3} = CS_{SOM3} k_{SOM3} r_{total} / \Delta t \tag{7.14}$$

$$CF_{pot,SOM4} = CS_{SOM4} k_{SOM4} r_{total} / \Delta t \tag{7.15}$$

where the factor ($1/\Delta t$) is included because the rate constant is calculated for the entire timestep (Eqs. (7.1) and (7.2)), but the convention is to express all fluxes on a per-second basis. Potential mineral nitrogen fluxes associated with these decomposition steps are:

$$NF_{pot\_min,Lit1 \rightarrow SOM1} = CF_{pot,Lit1} \left(1 - rf_{Lit1} - \frac{CN_{SOM1}}{CN_{Lit1}} \right) \Big/ CN_{SOM1} \tag{7.16}$$

$$NF_{pot\_min,Lit2 \rightarrow SOM2} = CF_{pot,Lit2} \left(1 - rf_{Lit2} - \frac{CN_{SOM2}}{CN_{Lit2}} \right) \Big/ CN_{SOM2} \tag{7.17}$$

$$NF_{pot\_min,Lit3 \rightarrow SOM3} = CF_{pot,Lit3} \left(1 - rf_{Lit3} - \frac{CN_{SOM3}}{CN_{Lit3}} \right) \Big/ CN_{SOM3} \tag{7.18}$$

$$NF_{pot\_min,SOM1 \rightarrow SOM2} = CF_{pot,SOM1} \left(1 - rf_{SOM1} - \frac{CN_{SOM2}}{CN_{SOM1}} \right) \Big/ CN_{SOM2} \tag{7.19}$$

$$NF_{pot\_min,SOM2 \rightarrow SOM3} = CF_{pot,SOM2} \left(1 - rf_{SOM2} - \frac{CN_{SOM3}}{CN_{SOM2}} \right) \Big/ CN_{SOM3} \tag{7.20}$$

$$NF_{pot\_min,SOM3 \rightarrow SOM4} = CF_{pot,SOM3} \left(1 - rf_{SOM3} - \frac{CN_{SOM4}}{CN_{SOM3}} \right) \Big/ CN_{SOM4} \tag{7.21}$$

$$NF_{pot\_min,SOM4} = -CF_{pot,SOM4} / CN_{SOM4} \tag{7.22}$$

where the special form of Eq. (7.22) arises because there is no SOM pool downstream of SOM4 in the converging cascade: all carbon fluxes leaving that pool are assumed to be in the form of respired CO_2, and all nitrogen fluxes leaving that pool are assumed to be sources of new mineral nitrogen.

Steps in the decomposition cascade that result in release of new mineral nitrogen (mineralization fluxes) are allowed to proceed at their potential rates, without modification for nitrogen availability. Steps that result in an uptake of mineral nitrogen (immobilization fluxes) are subject to rate limitation, depending on the availability of mineral nitrogen, the total immobilization demand, and the total demand for soil mineral nitrogen to support new plant growth. The potential mineral nitrogen fluxes from Eqs.

(7.16) - (7.22) are evaluated, summing all the positive fluxes to generate the total potential nitrogen immobilization flux (NF_{immob_demand}, gN m^{-2} s^{-1}), and summing absolute values of all the negative fluxes to generate the total nitrogen mineralization flux (NF_{gross_nmin}, gN m^{-2} s^{-1}). Since NF_{griss_nmin} is a source of new mineral nitrogen to the soil mineral nitrogen pool it is not limited by the availability of soil mineral nitrogen, and is therefore an actual as opposed to a potential flux.

7.3 Resolution of Nitrogen Limitation

Once NF_{immob_demand} is known, the competition between plant and microbial nitrogen demand can be resolved. Mineral nitrogen in the soil pool (NS_{sminn}, gN m^{-2}) at the beginning of the timestep is considered the available supply. Total demand for mineral nitrogen from this pool (NF_{total_demand}, gN m^{-2} s^{-1}) is:

$$NF_{total\_demand} = NF_{immob\_demand} + NF_{plant\_demand\_soil} \tag{7.23}$$

If $NF_{total\_demand}\Delta t < NS_{sminn}$, then the available pool is large enough to meet both plant and microbial demand, and neither plant growth nor immobilization steps in the decomposition cascade are limited by nitrogen availability in the timestep. In that case, the signaling variables f_{plant_demand} and f_{immob_demand} are both set to 1.0, where f_{plant_demand} is defined and used in Section 4, and f_{immob_demand} is the fraction of potential immobilization demand that can be met given current supply of mineral nitrogen.

If $NF_{total\_demand}\Delta t \geq NS_{sminn}$, then there is not enough mineral nitrogen to meet the combined demands for plant growth and heterotrophic immobilization, and both of these processes proceed at lower-than-potential rates, defined by the fractions f_{plant_demand} and f_{immob_demand}, where:

$$f_{plant\_demand} = f_{immob\_demand} = \frac{NS_{sminn}}{\Delta t\, NF_{total\_demand}} \tag{7.24}$$

This treatment of competition for nitrogen as a limiting resource is referred to a demand-based competition, where the fraction of the available resource that eventually flows to a particular process depends on the demand from that process in comparison to the total demand from all processes. Processes expressing a greater demand acquire a larger fraction of the available resource.

7.4 Final Decomposition Fluxes

With f_{immob_demand} known, final decomposition fluxes can be calculated. Actual carbon fluxes leaving the individual litter and SOM pools are calculated as:

$$CF_{Lit1} = \begin{cases} CF_{pot,Lit1}\, f_{immob\_demand} & \text{for } NF_{pot\_min,Lit1\rightarrow SOM1} > 0 \\ CF_{pot,Lit1} & \text{for } NF_{pot\_min,Lit1\rightarrow SOM1} \le 0 \end{cases} \tag{7.25}$$

$$CF_{Lit2} = \begin{cases} CF_{pot,Lit2}\, f_{immob\_demand} & \text{for } NF_{pot\_min,Lit2\rightarrow SOM2} > 0 \\ CF_{pot,Lit2} & \text{for } NF_{pot\_min,Lit2\rightarrow SOM2} \le 0 \end{cases} \tag{7.26}$$

$$CF_{Lit3} = \begin{cases} CF_{pot,Lit3}\, f_{immob\_demand} & \text{for } NF_{pot\_min,Lit3\rightarrow SOM3} > 0 \\ CF_{pot,Lit3} & \text{for } NF_{pot\_min,Lit3\rightarrow SOM3} \le 0 \end{cases} \tag{7.27}$$

$$CF_{SOM1} = \begin{cases} CF_{pot,SOM1}\, f_{immob\_demand} & \text{for } NF_{pot\_min,SOM1\rightarrow SOM2} > 0 \\ CF_{pot,SOM1} & \text{for } NF_{pot\_min,SOM1\rightarrow SOM2} \le 0 \end{cases} \tag{7.28}$$

$$CF_{SOM2} = \begin{cases} CF_{pot,SOM2}\, f_{immob\_demand} & \text{for } NF_{pot\_min,SOM2\rightarrow SOM3} > 0 \\ CF_{pot,SOM2} & \text{for } NF_{pot\_min,SOM2\rightarrow SOM3} \le 0 \end{cases} \tag{7.29}$$

$$CF_{SOM3} = \begin{cases} CF_{pot,SOM3}\, f_{immob\_demand} & \text{for } NF_{pot\_min,SOM3\rightarrow SOM4} > 0 \\ CF_{pot,SOM3} & \text{for } NF_{pot\_min,SOM3\rightarrow SOM4} \le 0 \end{cases} \tag{7.30}$$

$$CF_{SOM4} = CF_{pot,SOM4} \tag{7.31}$$

Heterotrophic respiration fluxes (losses of carbon as CO_2 to the atmosphere) are:

$$CF_{Lit1,HR} = CF_{Lit1} rf_{Lit1} \tag{7.32}$$

$$CF_{Lit2,HR} = CF_{Lit2} rf_{Lit2} \tag{7.33}$$

$$CF_{Lit3,HR} = CF_{Lit3} rf_{Lit3} \tag{7.34}$$

$$CF_{SOM1,HR} = CF_{SOM1} rf_{SOM1} \tag{7.35}$$

$$CF_{SOM2,HR} = CF_{SOM2} rf_{SOM2} \tag{7.36}$$

$$CF_{SOM3,HR} = CF_{SOM3} rf_{SOM3} \tag{7.37}$$

$$CF_{SOM4,HR} = CF_{SOM4} rf_{SOM4} \tag{7.38}$$

Transfers of carbon from upstream to downstream pools in the decomposition cascade are given as:

$$CF_{Lit1,SOM1} = CF_{Lit1}\left(1 - rf_{Lit1}\right) \tag{7.39}$$

$$CF_{Lit2,SOM2} = CF_{Lit2}\left(1 - rf_{Lit2}\right) \tag{7.40}$$

$$CF_{Lit3,SOM3} = CF_{Lit3}\left(1 - rf_{Lit3}\right) \tag{7.41}$$

$$CF_{SOM1,SOM2} = CF_{SOM1}\left(1 - rf_{SOM1}\right) \tag{7.42}$$

$$CF_{SOM2,SOM3} = CF_{SOM2}\left(1 - rf_{SOM2}\right) \tag{7.43}$$

$$CF_{SOM3,SOM4} = CF_{SOM3}\left(1 - rf_{SOM3}\right) \tag{7.44}$$

In accounting for the fluxes of nitrogen between pools in the decomposition cascade and associated fluxes to or from the soil mineral nitrogen pool, the model first calculates a flux of nitrogen from an upstream pool to a downstream pool, then calculates a flux either from the soil mineral nitrogen pool to the downstream pool (immobilization) or from the downstream pool to the soil mineral nitrogen pool (mineralization). Transfers of nitrogen from upstream to downstream pools in the decomposition cascade are given as:

$$NF_{Lit1,SOM1} = CF_{Lit1} / CN_{Lit1} \tag{7.45}$$

$$NF_{Lit2,SOM2} = CF_{Lit2} / CN_{Lit2} \tag{7.46}$$

$$NF_{Lit3,SOM3} = CF_{Lit3} / CN_{Lit3} \tag{7.47}$$

$$NF_{SOM1,SOM2} = CF_{SOM1} / CN_{SOM1} \tag{7.48}$$

$$NF_{SOM2,SOM3} = CF_{SOM2} / CN_{SOM2} \tag{7.49}$$

$$NF_{SOM3,SOM4} = CF_{SOM3} / CN_{SOM3} \tag{7.50}$$

Corresponding fluxes to or from the soil mineral nitrogen pool depend on whether the decomposition step is an immobilization flux or a mineralization flux:

$$NF_{sminn,Lit1\to SOM1} = \begin{cases} NF_{pot\_min,Lit1\to SOM1}\, f_{immob\_demand} & \text{for } NF_{pot\_min,Lit1\to SOM1} > 0 \\ NF_{pot\_min,Lit1\to SOM1} & \text{for } NF_{pot\_min,Lit1\to SOM1} \le 0 \end{cases} \tag{7.51}$$

$$NF_{sminn,Lit2\to SOM2} = \begin{cases} NF_{pot\_min,Lit2\to SOM2}\, f_{immob\_demand} & \text{for } NF_{pot\_min,Lit2\to SOM2} > 0 \\ NF_{pot\_min,Lit2\to SOM2} & \text{for } NF_{pot\_min,Lit2\to SOM2} \le 0 \end{cases} \tag{7.52}$$

$$NF_{sminn,Lit3\to SOM3} = \begin{cases} NF_{pot\_min,Lit3\to SOM3}\, f_{immob\_demand} & \text{for } NF_{pot\_min,Lit3\to SOM3} > 0 \\ NF_{pot\_min,Lit3\to SOM3} & \text{for } NF_{pot\_min,Lit3\to SOM3} \le 0 \end{cases} \tag{7.53}$$

$$NF_{sminn,SOM1\rightarrow SOM2} = \begin{cases} NF_{pot\_min,SOM1\rightarrow SOM2}\, f_{immob\_demand} & \text{for } NF_{pot\_min,SOM1\rightarrow SOM2} > 0 \\ NF_{pot\_min,SOM1\rightarrow SOM2} & \text{for } NF_{pot\_min,SOM1\rightarrow SOM2} \leq 0 \end{cases} \quad (7.54)$$

$$NF_{sminn,SOM2\rightarrow SOM3} = \begin{cases} NF_{pot\_min,SOM2\rightarrow SOM3}\, f_{immob\_demand} & \text{for } NF_{pot\_min,SOM2\rightarrow SOM3} > 0 \\ NF_{pot\_min,SOM2\rightarrow SOM3} & \text{for } NF_{pot\_min,SOM2\rightarrow SOM3} \leq 0 \end{cases} \quad (7.55)$$

$$NF_{sminn,SOM3\rightarrow SOM4} = \begin{cases} NF_{pot\_min,SOM3\rightarrow SOM4}\, f_{immob\_demand} & \text{for } NF_{pot\_min,SOM3\rightarrow SOM4} > 0 \\ NF_{pot\_min,SOM3\rightarrow SOM4} & \text{for } NF_{pot\_min,SOM3\rightarrow SOM4} \leq 0 \end{cases} \quad (7.56)$$

$$NF_{sminn,SOM4} = NF_{pot\_min,SOM4} \quad (7.57)$$

8 External Nitrogen Cycle

In addition to the relatively rapid cycling of nitrogen within the plant – litter – soil organic matter system, CLM-CN also represents several slow processes which couple the internal nitrogen cycle to external sources and sinks. Inputs of new mineral nitrogen are from atmospheric deposition and biological nitrogen fixation. Losses of mineral nitrogen are due to denitrification, leaching, and losses in fire. While the short-term dynamics of nitrogen limitation depend on the behavior of the internal nitrogen cycle, establishment of total ecosystem nitrogen stocks depends on the balance between sources and sinks in the external nitrogen cycle.

8.1 Atmospheric Nitrogen Deposition

CLM-CN uses a single variable to represent the total deposition of mineral nitrogen onto the land surface, combining wet and dry deposition of NO_y and NH_x as a single flux (NF_{ndep_sminn}, gN m^{-2} s^{-1}). This flux is intended to represent total reactive nitrogen deposited to the land surface which originates from the following natural and anthropogenic sources (Galloway et al., 2004): formation of NO_x during lightning, NO_x and NH_3 emission from wildfire, NO_x emission from natural soils, NH_3 emission from natural soils, vegetation, and wild animals, NO_x and NH_3 emission during fossil fuel combustion (both thermal and fuel NO_x production), NO_x and NH_3 emission from other industrial processes, NO_x and NH_3 emission from fire associated with deforestation, NO_x and NH_3 emission from agricultural burning, NO_x emission from agricultural soils, NH_3 emission from agricultural crops, NH_3 emission from agricultural animal waste, and NH_3 emission from human waste and waste water. The deposition flux is provided as a spatially and (potentially) temporally varying dataset (see Section XX for a description of the default input dataset).

The nitrogen deposition flux is assumed to enter the soil mineral nitrogen pool (NS_{sminn}) directly, although real pathways for wet and dry nitrogen deposition can be more complex, including release from melting snowpack and direct foliar uptake of deposited NO_y (e.g. Tye et al., 2005; Vallano and Sparks, 2007).

8.2 Biological Nitrogen Fixation

The fixation of new reactive nitrogen from atmospheric N_2 by soil microorganisms is an important component of both preindustrial and modern-day nitrogen budgets, but a mechanistic understanding of global-scale controls on biological nitrogen fixation (BNF) is still only poorly developed (Cleveland et al., 1999; Galloway et al., 2004). Cleveland et al. (1999) suggested empirical relationships that predict BNF as a function of either evapotranspiration rate or net primary productivity for natural vegetation. CLM-CN assumes that BNF is a function of annual net primary production (CF_{ann_NPP}, gC m^{-2} y^{-1}). The rationale for choosing net primary production over evapotranspiration as the predictor is that the two are well-correlated (Parton et al., 1993; Running et al., 1989), and the use of primary production also introduces a known dependence of BNF on the carbon supply to nitrogen fixing microorganisms (Cleveland et al., 1999). The expression used is:

$$NF_{nfix,sminn} = 1.8\left(1 - \exp\left(-0.003 CF_{ann\_NPP}\right)\right) \Big/ \left(86400 \cdot 365\right) \qquad (8.1)$$

where $NF_{nfix,sminn}$ (gN m^{-2} s^{-1}) is the rate of BNF. Eq. (8.1) is plotted over a range of annual NPP in Figure XX.

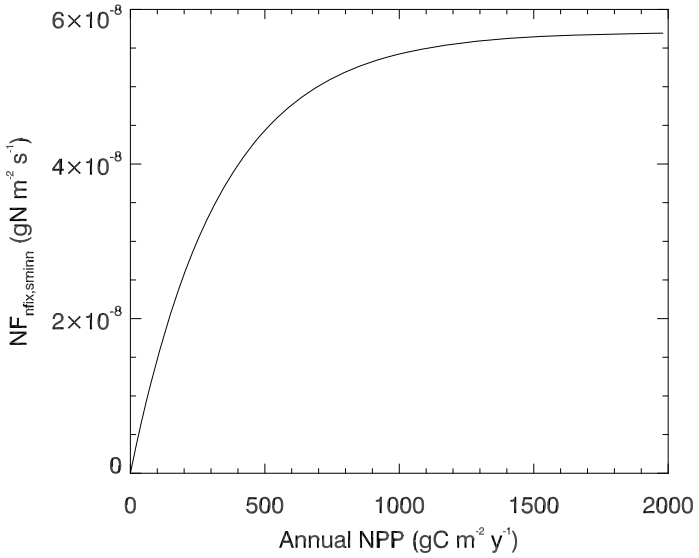

Figure XX. Biological nitrogen fixation as a function of annual net primary production.

8.3 Denitrification Losses of Nitrogen

Under aerobic conditions in the soil oxygen is the preferred electron acceptor supporting the metabolism of heterotrophs, but anaerobic conditions favor the activity of soil heterotrophs which use nitrate as an electron acceptor (e.g. *Pseudomonas* and *Clostridium*) supporting respiration. This process, known as denitrification, results in the transformation of nitrate to gaseous N_2, with smaller associated production of NO_x and N_2O. It is typically assumed that nitrogen fixation and denitrification were approximately balanced in the preindustrial biosphere (Galloway et al., 2004). It is likely that denitrification can occur within anaerobic microsites within an otherwise aerobic soil environment, leading to large global denitrification fluxes even when fluxes per unit area are rather low (Galloway et al., 2004).

Because the vertical distribution of soil organic matter is not resolved explicitly in CLM-CN, a simple denitrification parameterization is used that treats denitrification as a constant fraction of gross nitrogen mineralization. At each step in the decomposition cascade, if the transformation from an upstream to a downstream pool is predicted to mineralize (as opposed to immobilize) nitrogen, then a constant fraction of the nitrogen mineralization flux is assumed to be lost via denitrification. Due to large uncertainties in the mechanistic understanding of the environmental controls on denitrification, no modifications to the denitrification fraction are made for different soil moisture conditions. This is identified as a high-priority area for future model development.

Denitrification fluxes associated with gross mineralization in the decomposition cascade are calculated as follows:

$$NF_{denit,Lit1\rightarrow SOM1} = \begin{cases} 0 & \text{for } NF_{pot\_min,Lit1\rightarrow SOM1} > 0 \\ -NF_{pot\_min,Lit1\rightarrow SOM1}\, f_{denit} & \text{for } NF_{pot\_min,Lit1\rightarrow SOM1} \le 0 \end{cases} \quad (8.2)$$

$$NF_{denit,Lit2\rightarrow SOM2} = \begin{cases} 0 & \text{for } NF_{pot\_min,Lit2\rightarrow SOM2} > 0 \\ -NF_{pot\_min,Lit2\rightarrow SOM2}\, f_{denit} & \text{for } NF_{pot\_min,Lit2\rightarrow SOM2} \le 0 \end{cases} \quad (8.3)$$

$$NF_{denit,Lit3\rightarrow SOM3} = \begin{cases} 0 & \text{for } NF_{pot\_min,Lit3\rightarrow SOM3} > 0 \\ -NF_{pot\_min,Lit3\rightarrow SOM3}\, f_{denit} & \text{for } NF_{pot\_min,Lit3\rightarrow SOM3} \le 0 \end{cases} \quad (8.4)$$

$$NF_{denit,SOM1\rightarrow SOM2} = \begin{cases} 0 & \text{for } NF_{pot\_min,SOM1\rightarrow SOM2} > 0 \\ -NF_{pot\_min,SOM1\rightarrow SOM2}\, f_{denit} & \text{for } NF_{pot\_min,SOM1\rightarrow SOM2} \le 0 \end{cases} \quad (8.5)$$

$$NF_{denit,SOM2\rightarrow SOM3} = \begin{cases} 0 & \text{for } NF_{pot\_min,SOM2\rightarrow SOM3} > 0 \\ -NF_{pot\_min,SOM2\rightarrow SOM3}\, f_{denit} & \text{for } NF_{pot\_min,SOM2\rightarrow SOM3} \le 0 \end{cases} \quad (8.6)$$

$$NF_{denit,SOM3\rightarrow SOM4} = \begin{cases} 0 & \text{for } NF_{pot\_min,SOM3\rightarrow SOM4} > 0 \\ -NF_{pot\_min,SOM3\rightarrow SOM4}\, f_{denit} & \text{for } NF_{pot\_min,SOM3\rightarrow SOM4} \le 0 \end{cases} \quad (8.7)$$

$$NF_{denit,SOM4} = -NF_{pot\_min,SOM4} \quad (8.8)$$

where f_{denit} = 0.01 is the constant denitrification fraction of gross mineralization, and the denitrification fluxes are assumed to be leaving the soil mineral nitrogen pool (NS_{sminn}) and entering the atmosphere. The speciation of gaseous nitrogen fluxes entering the atmosphere (e.g. N_2 vs. NO_x or N_2O) is not specified. Providing an explicit speciation of these nitrogen losses is another high-priority area for future model development.

The model includes one other denitrification pathway, intended to represent the observed losses of mineral nitrogen in systems experiencing nitrogen saturation. One reason this mechanism has been included is in anticipation of an agricultural fertilization flux, provided either through a prescribed dataset or through a prognostic agricultural management routine. The model does not currently include an explicit representation of the fertilization flux, but when it is introduced, it will be necessary to account for the substantial denitrification losses associated with high nitrate concentrations in some heavily fertilized agricultural soils. Nitrogen saturation can also occur in natural vegetation systems, especially under conditions of high atmospheric nitrogen deposition, and so this mechanism plays a useful role even prior to the introduction within the model of agricultural fertilization.

For the purpose of this calculation, nitrogen saturation is evaluated on each timestep, by comparing the total demand for new mineral nitrogen from plants and immobilization with the available soil mineral nitrogen pool. The denitrification of excess soil mineral nitrogen is non-zero whenever the supply of mineral nitrogen exceeds the demand:

$$NF_{sminn,denit} = \begin{cases} \left(\frac{NS_{sminn}}{\Delta t}\right) - NF_{total\_demand}\, f_{dnx} & \text{for } NF_{total\_demand}\Delta t < NS_{sminn} \\ 0 & \text{for } NF_{total\_demand}\Delta t \ge NS_{sminn} \end{cases} \quad (8.9)$$

where f_{dnx} (unitless) is the fraction of excess soil mineral nitrogen subject to denitrification on each timestep. This fraction is parameterized such that 50% of any excess soil mineral nitrogen would be lost to denitrification per day:

$$f_{dnx} = 0.5\frac{\Delta t}{86400} \tag{8.10}$$

8.4 Leaching Losses of Nitrogen

Soil mineral nitrogen remaining after plant uptake, immobilization, and denitrification is subject to loss as a dissolved component of hydrologic outflow from the soil column (leaching). This leaching loss ($NF_{leached}$, gN m^{-2} s^{-1}) depends on the concentration of dissolved mineral (inorganic) nitrogen in soil water solution (DIN, gN kgH_2O), and the rate of hydrologic discharge from the soil column to streamflow (Q_{dis}, kgH_2O m^{-2} s^{-1}, Section x.x of Oleson et al., 2004), as

$$NF_{leached} = DIN \cdot Q_{dis}. \tag{8.11}$$

DIN is calculated assuming that a constant fraction (sf, proportion) of the remaining soil mineral N pool is in soluble form, and that this entire fraction is dissolved in the total soil water. It is further assumed that $sf = 0.1$, representing an estimated 10% of the total NS_{sminn} pool as soluble nitrate, with the remaining 90% as less soluble ammonia. DIN is then given as

$$DIN = \frac{NS_{sminn}sf}{WS_{tot\_soil}} \tag{8.12}$$

where WS_{tot_soil} (kgH_2O m^{-2}) is the total mass of soil water content integrated over the column. The total mineral nitrogen leaching flux is limited on each time step to not exceed the soluble fraction of NS_{sminn}

$$NF_{leached} = \min\left(NF_{leached}, \frac{NS_{sminn}sf}{\Delta t} \right). \tag{8.13}$$

This parameterization of the soluble fraction is poorly constrained by observations. fraction of total soil mineral N pool present as nitrate will vary spatially and temporally, depending on oxygen status of soils and rates of nitrification. A calibration of this

parameterization against observations of dissolved nitrate in headwater streams might be an effective method for imposing better observational constraints at broad spatial scales.

8.5 Losses of Nitrogen Due to Fire

The final pathway for nitrogen loss is through combustion, also known as pyrodenitrification. Detailed equations are provided, together with the effects of fire on the carbon budget, in Chapter 9. It is assumed in CLM-CN that losses of N due to fire are restricted to vegetation and litter pools (including coarse woody debris). Loss rates of N are determined by the fraction of biomass lost to combustion, assuming that most of the nitrogen in the burned biomass is lost to the atmosphere (Schlesinger, 1997; Smith et al., 2005). It is assumed that soil organic matter pools of carbon and nitrogen are not directly affected by fire (Neff et al., 2005).

9 Plant Mortality

Plant mortality as described here applies to perennial vegetation types, and is intended to represent the death of individuals from a stand of plants due to the aggregate of processes such as wind throw, insect attack, disease, extreme temperatures or drought, and age-related decline in vigor. These processes are referred to in aggregate as "gap-phase" mortality, following [ref]. Mortality due to fire and anthropogenic land cover change are treated separately (see Sections 10 and 11, respectively).

9.1 Mortality Fluxes Leaving Vegetation Pools

Whole-plant mortality is parameterized very simply, assuming a mortality rate of 2% yr^{-1} for all vegetation types. This is clearly a gross oversimplification of an important process, and additional work is required to better constrain this process in different climate zones (Keller et al., 2004; Sollins, 1982), for different species mixtures (Gomes et al., 2003), and for different size and age classes (Busing, 2005; Law et al., 2003). Literature values for forest mortality rates range from at least 0.7% to 3.0% yr^{-1}. Taking the annual rate of mortality (*am*, proportion yr^{-1}) as 0.02, a rate per second (*m*) is calculated as $m = am/(365 \cdot 86400)$. All vegetation carbon and nitrogen pools for display, storage, and transfer are affected at rate *m*, with mortality fluxes out of vegetation pools eventually merged to the column level and deposited in litter pools. Mortality fluxes out of displayed vegetation carbon and nitrogen pools are

$$CF_{leaf\_mort} = CS_{leaf} m \tag{9.1}$$

$$CF_{froot\_mort} = CS_{froot} m \tag{9.2}$$

$$CF_{livestem\_mort} = CS_{livestem} m \tag{9.3}$$

$$CF_{deadstem\_mort} = CS_{deadstem} m \tag{9.4}$$

$$CF_{livecroot\_mort} = CS_{livecroot} m \tag{9.5}$$

$$CF_{deadcroot\_mort} = CS_{deadcroot} m \tag{9.6}$$

$$NF_{leaf\_mort} = NS_{leaf} m \tag{9.7}$$

$$NF_{froot\_mort} = NS_{froot} m \tag{9.8}$$

$$NF_{livestem\_mort} = NS_{livestem} m \quad (9.9)$$

$$NF_{deadstem\_mort} = NS_{deadstem} m \quad (9.10)$$

$$NF_{livecroot\_mort} = NS_{livecroot} m \quad (9.11)$$

$$NF_{deadcroot\_mort} = NS_{deadcroot} m \quad (9.12)$$

$$NF_{retrans\_mort} = NS_{retrans} m \; . \quad (9.13)$$

Mortality fluxes out of carbon and nitrogen storage pools are

$$CF_{leaf\_stor\_mort} = CS_{leaf\_stor} m \quad (9.14)$$

$$CF_{froot\_stor\_mort} = CS_{froot\_stor} m \quad (9.15)$$

$$CF_{livestem\_stor\_mort} = CS_{livestem\_stor} m \quad (9.16)$$

$$CF_{deadstem\_stor\_mort} = CS_{deadstem\_stor} m \quad (9.17)$$

$$CF_{livecroot\_stor\_mort} = CS_{livecroot\_stor} m \quad (9.18)$$

$$CF_{deadcroot\_stor\_mort} = CS_{deadcroot\_stor} m \quad (9.19)$$

$$CF_{gresp\_stor\_mort} = CS_{gresp\_stor} m \quad (9.20)$$

$$NF_{leaf\_stor\_mort} = NS_{leaf\_stor} m \quad (9.21)$$

$$NF_{froot\_stor\_mort} = NS_{froot\_stor} m \quad (9.22)$$

$$NF_{livestem\_stor\_mort} = NS_{livestem\_stor} m \quad (9.23)$$

$$NF_{deadstem\_stor\_mort} = NS_{deadstem\_stor} m \quad (9.24)$$

$$NF_{livecroot\_stor\_mort} = NS_{livecroot\_stor} m \quad (9.25)$$

$$NF_{deadcroot\_stor\_mort} = NS_{deadcroot\_stor} m \quad (9.26)$$

Mortality fluxes out of carbon and nitrogen transfer growth pools are

$$CF_{leaf\_xfer\_mort} = CS_{leaf\_xfer} m \quad (9.27)$$

$$CF_{froot\_xfer\_mort} = CS_{froot\_xfer} m \quad (9.28)$$

$$CF_{livestem\_xfer\_mort} = CS_{livestem\_xfer} m \quad (9.29)$$

$$CF_{deadstem\_xfer\_mort} = CS_{deadstem\_xfer} m \quad (9.30)$$

$$CF_{livecroot\_xfer\_mort} = CS_{livecroot\_xfer} m \quad (9.31)$$

$$CF_{deadcroot\_xfer\_mort} = CS_{deadcroot\_xfer} m \quad (9.32)$$

$$CF_{gresp\_xfer\_mort} = CS_{gresp\_xfer} m \quad (9.33)$$

$$NF_{leaf\_xfer\_mort} = NS_{leaf\_xfer} m \quad (9.34)$$

$$NF_{froot\_xfer\_mort} = NS_{froot\_xfer} m \quad (9.35)$$

$$NF_{livestem\_xfer\_mort} = NS_{livestem\_xfer} m \quad (9.36)$$

$$NF_{deadstem\_xfer\_mort} = NS_{deadstem\_xfer} m \quad (9.37)$$

$$NF_{livecroot\_xfer\_mort} = NS_{livecroot\_xfer} m \quad (9.38)$$

$$NF_{deadcroot\_xfer\_mort} = NS_{deadcroot\_xfer} m \quad (9.39)$$

9.2 Mortality Fluxes Merged to the Column Level

Analogous to the treatment of litterfall fluxes (Section 6.5), mortality fluxes leaving the vegetation pools are merged to the column level according to the weighted distribution of PFTs on the column, and deposited in litter and coarse woody debris pools, which are defined at the column level. Carbon and nitrogen fluxes from mortality of displayed leaf and fine root into litter pools are calculated as

$$CF_{leaf\_mort,lit1} = \sum_{p=0}^{npfts} CF_{leaf\_mort} f_{lab\_leaf,p} wcol_p \quad (9.40)$$

$$CF_{leaf\_mort,lit2} = \sum_{p=0}^{npfts} CF_{leaf\_mort} f_{cel\_leaf,p} wcol_p \quad (9.41)$$

$$CF_{leaf\_mort,lit3} = \sum_{p=0}^{npfts} CF_{leaf\_mort} f_{lig\_leaf,p} wcol_p \quad (9.42)$$

$$CF_{froot\_mort,lit1} = \sum_{p=0}^{npfts} CF_{froot\_mort} f_{lab\_froot,p} wcol_p \quad (9.43)$$

$$CF_{froot\_mort,lit2} = \sum_{p=0}^{npfts} CF_{froot\_mort} f_{cel\_froot,p} wcol_p \quad (9.44)$$

$$CF_{froot\_mort,lit3} = \sum_{p=0}^{npfts} CF_{froot\_mort} f_{lig\_froot,p} wcol_p \quad (9.45)$$

$$NF_{leaf\_mort,lit1} = \sum_{p=0}^{npfts} NF_{leaf\_mort} f_{lab\_leaf,p} wcol_p \quad (9.46)$$

$$NF_{leaf\_mort,lit2} = \sum_{p=0}^{npfts} NF_{leaf\_mort} f_{cel\_leaf,p} wcol_p \quad (9.47)$$

$$NF_{leaf\_mort,lit3} = \sum_{p=0}^{npfts} NF_{leaf\_mort} f_{lig\_leaf,p} wcol_p \quad (9.48)$$

$$NF_{froot\_mort,lit1} = \sum_{p=0}^{npfts} NF_{froot\_mort} f_{lab\_froot,p} wcol_p \quad (9.49)$$

$$NF_{froot\_mort,lit2} = \sum_{p=0}^{npfts} NF_{froot\_mort} f_{cel\_froot,p} wcol_p \quad (9.50)$$

$$NF_{froot\_mort,lit3} = \sum_{p=0}^{npfts} NF_{froot\_mort} f_{lig\_froot,p} wcol_p \ . \quad (9.51)$$

Carbon and nitrogen mortality fluxes from displayed live and dead stem and coarse root pools are merged to the column level and deposited in the coarse woody debris pools:

$$CF_{livestem\_mort,cwd} = \sum_{p=0}^{npfts} CF_{livestem\_mort} wcol_p \quad (9.52)$$

$$CF_{deadstem\_mort,cwd} = \sum_{p=0}^{npfts} CF_{deadstem\_mort} wcol_p \quad (9.53)$$

$$CF_{livecroot\_mort,cwd} = \sum_{p=0}^{npfts} CF_{livecroot\_mort} wcol_p \quad (9.54)$$

$$CF_{deadcroot\_mort,cwd} = \sum_{p=0}^{npfts} CF_{deadcroot\_mort} wcol_p \quad (9.55)$$

$$NF_{livestem\_mort,cwd} = \sum_{p=0}^{npfts} NF_{livestem\_mort} wcol_p \quad (9.56)$$

$$NF_{deadstem\_mort,cwd} = \sum_{p=0}^{npfts} NF_{deadstem\_mort} wcol_p \quad (9.57)$$

$$NF_{livecroot\_mort,cwd} = \sum_{p=0}^{npfts} NF_{livecroot\_mort} wcol_p \quad (9.58)$$

$$NF_{deadcroot\_mort,cwd} = \sum_{p=0}^{npfts} NF_{deadcroot\_mort} wcol_p \quad (9.59)$$

All vegetation storage and transfer pools for carbon and nitrogen are assumed to exist as labile pools within the plant (e.g. as carbohydrate stores, in the case of carbon

pools). This assumption applies to storage and transfer pools for both non-woody and woody tissues. The mortality fluxes from these pools are therefore assumed to be deposited in the labile litter pools (CS_{lit1}, NS_{lit1}), after being merged to the column level. Carbon mortality fluxes out of storage and transfer pools are:

$$CF_{leaf\_stor\_mort,lit1} = \sum_{p=0}^{npfts} CF_{leaf\_stor\_mort} wcol_p \tag{9.60}$$

$$CF_{froot\_stor\_mort,lit1} = \sum_{p=0}^{npfts} CF_{froot\_stor\_mort} wcol_p \tag{9.61}$$

$$CF_{livestem\_stor\_mort,lit1} = \sum_{p=0}^{npfts} CF_{livestem\_stor\_mort} wcol_p \tag{9.62}$$

$$CF_{deadstem\_stor\_mort,lit1} = \sum_{p=0}^{npfts} CF_{deadstem\_stor\_mort} wcol_p \tag{9.63}$$

$$CF_{livecroot\_stor\_mort,lit1} = \sum_{p=0}^{npfts} CF_{livecroot\_stor\_mort} wcol_p \tag{9.64}$$

$$CF_{deadcroot\_stor\_mort,lit1} = \sum_{p=0}^{npfts} CF_{deadcroot\_stor\_mort} wcol_p \tag{9.65}$$

$$CF_{gresp\_stor\_mort,lit1} = \sum_{p=0}^{npfts} CF_{gresp\_stor\_mort} wcol_p \tag{9.66}$$

$$CF_{leaf\_xfer\_mort,lit1} = \sum_{p=0}^{npfts} CF_{leaf\_xfer\_mort} wcol_p \tag{9.67}$$

$$CF_{froot\_xfer\_mort,lit1} = \sum_{p=0}^{npfts} CF_{froot\_xfer\_mort} wcol_p \tag{9.68}$$

$$CF_{livestem\_xfer\_mort,lit1} = \sum_{p=0}^{npfts} CF_{livestem\_xfer\_mort} wcol_p \tag{9.69}$$

$$CF_{deadstem\_xfer\_mort,lit1} = \sum_{p=0}^{npfts} CF_{deadstem\_xfer\_mort} wcol_p \tag{9.70}$$

$$CF_{livecroot\_xfer\_mort,lit1} = \sum_{p=0}^{npfts} CF_{livecroot\_xfer\_mort} wcol_p \tag{9.71}$$

$$CF_{deadcroot\_xfer\_mort,lit1} = \sum_{p=0}^{npfts} CF_{deadcroot\_xfer\_mort} wcol_p \tag{9.72}$$

$$CF_{gresp\_xfer\_mort,lit1} = \sum_{p=0}^{npfts} CF_{gresp\_xfer\_mort} wcol_p \ . \tag{9.73}$$

Nitrogen mortality fluxes out of storage and transfer pools, including the storage pool for retranslocated nitrogen, are calculated as:

$$NF_{leaf\_stor\_mort,lit1} = \sum_{p=0}^{npfts} NF_{leaf\_stor\_mort} wcol_p \tag{9.74}$$

$$NF_{froot\_stor\_mort,lit1} = \sum_{p=0}^{npfts} NF_{froot\_stor\_mort} wcol_p \tag{9.75}$$

$$NF_{livestem\_stor\_mort,lit1} = \sum_{p=0}^{npfts} NF_{livestem\_stor\_mort} wcol_p \tag{9.76}$$

$$NF_{deadstem\_stor\_mort,lit1} = \sum_{p=0}^{npfts} NF_{deadstem\_stor\_mort} wcol_p \tag{9.77}$$

$$NF_{livecroot\_stor\_mort,lit1} = \sum_{p=0}^{npfts} NF_{livecroot\_stor\_mort} wcol_p \tag{9.78}$$

$$NF_{deadcroot\_stor\_mort,lit1} = \sum_{p=0}^{npfts} NF_{deadcroot\_stor\_mort} wcol_p \tag{9.79}$$

$$NF_{retrans\_mort,lit1} = \sum_{p=0}^{npfts} NF_{retrans\_mort} wcol_p \tag{9.80}$$

$$NF_{leaf\_xfer\_mort,lit1} = \sum_{p=0}^{npfts} NF_{leaf\_xfer\_mort} wcol_p \tag{9.81}$$

$$NF_{froot\_xfer\_mort,lit1} = \sum_{p=0}^{npfts} NF_{froot\_xfer\_mort} wcol_p \tag{9.82}$$

$$NF_{livestem\_xfer\_mort,lit1} = \sum_{p=0}^{npfts} NF_{livestem\_xfer\_mort} wcol_p \tag{9.83}$$

$$NF_{deadstem\_xfer\_mort,lit1} = \sum_{p=0}^{npfts} NF_{deadstem\_xfer\_mort} wcol_p \tag{9.84}$$

$$NF_{livecroot\_xfer\_mort,lit1} = \sum_{p=0}^{npfts} NF_{livecroot\_xfer\_mort} wcol_p \tag{9.85}$$

$$NF_{deadcroot\_xfer\_mort,lit1} = \sum_{p=0}^{npfts} NF_{deadcroot\_xfer\_mort} wcol_p \ . \tag{9.86}$$

10 Fire

Predictions of area affected by fire and fire fluxes from the affected area are based on the algorithms given in Thonicke et al. (2001), with modifications to translate from the original annual time step to the sub-daily time step used for carbon and nitrogen calculations in CLM-CN. The algorithm has two steps. First, an estimate is generated of the fractional area of the column affected by fire during the time step, and then the fluxes for combustion and fire-related mortality are calculated. Combustion affects live vegetation pools of carbon and nitrogen, and also litter and coarse woody debris pools. Soil organic matter is assumed to be unaffected by fire (Neff et al., 2005). Fire-related mortality is represented as a transfer of some affected but uncombusted fraction of the vegetation carbon and nitrogen pools to the appropriate litter pools.

10.1 Fire Probability and Fractional Area Affected by Fire

Prediction of fire occurrence depends only on fuel availability and inferred fuel moisture condition (Thonicke et al., 2001). Ignition is assumed to occur if suitably dry fuels are present, an assumption that takes into account the large area represented by each grid cell in a typical simulation. This logic would need to be modified for predictions of fire occurrence at high spatial resolution.

Fuel availability is assessed as a simple binary threshold, with fire occurrence in each time step dependent on fuel density ≥ 200 gC m^{-2}. CLM-CN uses the sum of total litter carbon and coarse woody debris carbon to calculate fuel density. An alternative formulation would be to include live aboveground biomass in the calculation of fuel density, which would generate larger total land area exposed to fire in each time step, and larger global fire emissions.

Fuel moisture condition is evaluated on the basis of fuel moisture content, defined as the fraction of fuel water holding capacity at saturation. A threshold for fuel moisture content above which ignition and fire spread are suppressed is termed the "moisture of extinction" (m_e, proportion), calculated as a weighted average of values $m_{e,p}$ where subscript p refers to the value of m_e for a specific PFT:

$$m_e = \sum_{p=0}^{npfts} m_{e,p} wtcol_p \ . \tag{10.1}$$

In practice, the model includes only two different values for $m_{e,p}$, one for woody vegetation ($m_{e,woody} = 0.3$) and another for herbaceous (all other) vegetation ($m_{e,herb} = 0.2$), following Thonicke et al. (2001).

As a surrogate for tracking fuel moisture content, CLM-CN uses the soil moisture as a fraction of plant-available volumetric water content in the top 50 cm of the soil column (m, proportion), similar to the implementation in Thonicke et al. (2001). This is calculated as:

$$m = \frac{\dfrac{\sum_{i=1}^{i_{50}} \left(\theta_i - \theta_{dry,i}\right) \Delta z_i}{\sum_{i=1}^{i_{50}} \Delta z_i}}{\dfrac{\sum_{i=1}^{i_{50}} \left(\theta_{sat,i} - \theta_{dry,i}\right) \Delta z_i}{\sum_{i=1}^{i_{50}} \Delta z_i}}, \tag{10.2}$$

where θ_i is the volumetric soil water content in soil layer i (from Eq. 7.115, Oleson et al. 2004), $\theta_{sat,i}$ is the saturated volumetric water content in soil layer i (from Eq. 7.72, Oleson et al. 2004), Δz_i is the thickness of soil layer i and i_{50} is the index of the last soil layer for which the lower boundary is <= 50 cm from the soil surface (from Eqs. 6.6 and 6.7, Oleson et al. 2004). Equation (10.2) could be simplified to eliminate the denominators, but is left in expanded form to correspond better with the calculation steps in the source code. Rearranging Eq. 7.74 from Oleson et al. (2004), $\theta_{dry,i}$ is calculated as:

$$\theta_{dry,i} = \theta_{sat,i} \left(\frac{\psi_{dry}}{\psi_{sat,i}} \right)^{-1/B} , \tag{10.3}$$

where $\psi_{sat,i}$ and B are given by Eqs. 7.75 and 7.73, respectively, in Oleson et al. (2004), and ψ_{dry} is defined as 316230 mm or, equivalently, -3.1 MPa.

A final condition for fire occurrence is that ground surface temperature (T_g, K, from section 6.1 of Oleson et al. 2004) be above freezing. The probability of at least one fire in a day on a column (fp), based on Thonicke et al. (2001) is

$$fp = \begin{cases} \exp\left(-\pi\left(\frac{m}{m_e}\right)^2\right) & \text{for: } fuel\ density \geq 200 gC m^{-2}, m \leq m_e, \text{and } T_{grnd} > TKFRZ \\ 0 & \text{otherwise} \end{cases} \quad (10.4)$$

Figure XX shows the variability in *fp* over a range of *m*, for the two endpoints of m_e (0.3 for woody, 0.2 for herbaceous).

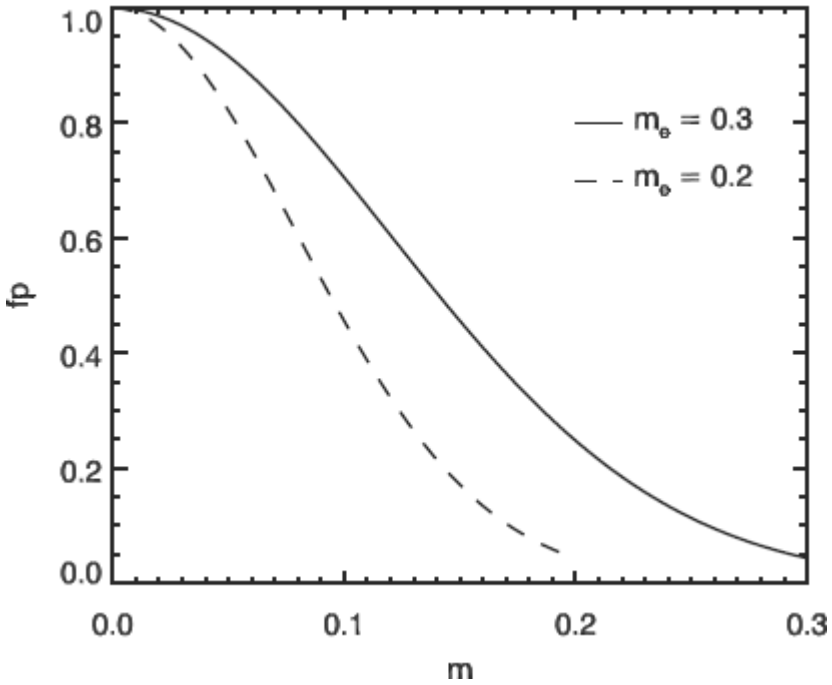

In the Thonicke et al. (2001) implementation of the fire algorithm, fire season length (*N*, days yr^{-1}) is estimated by taking an annual sum of daily values of *fp*, with *N* updated once each year. This approach is modified in CLM-CN so that *N* is updated on each time step using an e-folding approximation to the annual sum of *fp*. This allows for seasonal variation in the estimation of fire intensity at the grid cell level, effectively translating the original annual time step model of Thonicke et al. (2001) into a sub-daily time step model. This should allow the model to capture interannual variation in fire dynamics, as in Thonicke et al. (2001), as well as seasonal dynamics.

The e-folding method approximates an *n*-time step running mean at time step *i* ($\overline{x}_n^i$) of a variable *x* by calculating the following weighted sum

$$\overline{x}_n^i = \overline{x}_n^{i-1}\frac{n-1}{n} + x^i\frac{1}{n}. \quad (10.5)$$

For consistency with Thonicke et al. (2001), CLM-CN approximates an annual running mean by setting the number of e-folding time-steps (n) to

$$n = \frac{365 \cdot 86400}{\Delta t}, \tag{10.6}$$

then calculating N (fire season length, days yr^{-1}) as

$$N = s \cdot 365 \tag{10.7}$$

where

$$s = \overline{fp}_n^i = \overline{fp}_n^{i-1} \frac{n-1}{n} + fp^i \frac{1}{n} \tag{10.8}$$

and $\overline{fp}_n^i$ (one-year e-folding mean of daily fire probability) is equivalent to the variable s from Thonicke et al. (2001).

Following directly from Thonicke et al. (2001), s is used to estimate the annual fractional area burned for a grid cell (A_{ann}, fraction burned yr^{-1}) as

$$A_{ann} = s \cdot \exp\left(\frac{s-1}{0.45(s-1)^3 + 2.83(s-1)^2 + 2.96(s-1) + 1.04} \right). \tag{10.9}$$

This annual fraction burned is updated on every time step as s evolves, and is converted to a fraction area burned per time step ($A_{\Delta t}$) as follows

$$A_{\Delta t} = \begin{cases} \frac{fp}{N} A_{ann} \frac{\Delta t}{86400} & \text{for} \quad N \neq 0 \\ 0 & \text{for} \quad N = 0 \end{cases}. \tag{10.10}$$

When $A_{\Delta t}$ is summed over all time steps in a year this approach gives a total fractional area burned close to A_{ann}, with the seasonal distribution of burned area following the temporal dynamics of fp.

10.2 Combustion Losses and Fire-Related Mortality

The column-level estimate of fractional area burned for the timestep ($A_{\Delta t}$) is converted to a fractional area affected per second, and further reduced according to a PFT-specific "fire resistivity" factor ($resist_p$) (Thonicke et al., 2001) to give the PFT-level fraction of biomass affected by fire (f, fraction affected s^{-1})

$$f = \frac{A_{\Delta t}}{\Delta t}\left(1 - resist_p\right). \tag{10.11}$$

This treatment makes the assumption that all PFTs sharing space on a column will be subject to the same fractional area of fire ($A_{\Delta t}$), while different PFTs will have potentially different levels of resistance to the same fire exposure.

Carbon and nitrogen in leaves, fine roots, live stem and coarse root (cambial tissue) and all storage and transfer pools for the fire-affected proportion of each PFT is assumed to be lost to the atmosphere through combustion, while only a fraction of the dead stem and dead coarse root pools in the fire-affected fraction is assumed to be lost to combustion (*wcf*, the woody combustion fraction), with the remainder (1-*wcf*) being transferred from vegetation to coarse woody debris pools. The model uses $wcf = 0.2$ as a global constant (R. Keane, personal communication). The model currently ignores the generation and fate of charcoal or black carbon during and after fire. Further development of the fire module should explore a dynamic treatment of *wcf*, and a more realistic treatment of black carbon dynamics. PFT-level carbon fluxes to the atmosphere due to combustion are calculated as:

$$CF_{leaf\_fire} = CS_{leaf}\, f \tag{10.12}$$

$$CF_{leaf\_stor\_fire} = CS_{leaf\_stor}\, f \tag{10.13}$$

$$CF_{leaf\_xfer\_fire} = CS_{leaf\_xfer}\, f \tag{10.14}$$

$$CF_{froot\_fire} = CS_{froot}\, f \tag{10.15}$$

$$CF_{froot\_stor\_fire} = CS_{froot\_stor}\, f \tag{10.16}$$

$$CF_{froot\_xfer\_fire} = CS_{froot\_xfer}\, f \tag{10.17}$$

$$CF_{livestem\_fire} = CS_{livestem}\, f \tag{10.18}$$

$$CF_{livestem\_stor\_fire} = CS_{livestem\_stor}\, f \tag{10.19}$$

$$CF_{livestem\_xfer\_fire} = CS_{livestem\_xfer}\, f \tag{10.20}$$

$$CF_{deadstem\_fire} = CS_{deadstem}\, f \cdot wcf \tag{10.21}$$

$$CF_{deadstem\_stor\_fire} = CS_{deadstem\_stor}\, f \tag{10.22}$$

$$CF_{deadstem\_xfer\_fire} = CS_{deadstem\_xfer}\, f \tag{10.23}$$

$$CF_{livecroot\_fire} = CS_{livecroot}\, f \tag{10.24}$$

$$CF_{livecroot\_stor\_fire} = CS_{livecroot\_stor}\, f \tag{10.25}$$

$$CF_{livecroot\_xfer\_fire} = CS_{livecroot\_xfer}\, f \tag{10.26}$$

$$CF_{deadcroot\_fire} = CS_{deadcroot}\, f \cdot wcf \tag{10.27}$$

$$CF_{deadcroot\_stor\_fire} = CS_{deadcroot\_stor}\, f \tag{10.28}$$

$$CF_{deadcroot\_xfer\_fire} = CS_{deadcroot\_xfer}\, f \tag{10.29}$$

$$CF_{gresp\_stor\_fire} = CS_{gresp\_stor}\, f \tag{10.30}$$

$$CF_{gresp\_xfer\_fire} = CS_{gresp\_xfer}\, f \tag{10.31}$$

PFT-level nitrogen fluxes to the atmosphere due to combustion are calculated as:

$$NF_{leaf\_fire} = NS_{leaf}\, f \tag{10.32}$$

$$NF_{leaf\_stor\_fire} = NS_{leaf\_stor}\, f \tag{10.33}$$

$$NF_{leaf\_xfer\_fire} = NS_{leaf\_xfer}\, f \tag{10.34}$$

$$NF_{froot\_fire} = NS_{froot}\, f \tag{10.35}$$

$$NF_{froot\_stor\_fire} = NS_{froot\_stor}\, f \tag{10.36}$$

$$NF_{froot\_xfer\_fire} = NS_{froot\_xfer}\, f \tag{10.37}$$

$$NF_{livestem\_fire} = NS_{livestem}\, f \tag{10.38}$$

$$NF_{livestem\_stor\_fire} = NS_{livestem\_stor}\, f \tag{10.39}$$

$$NF_{livestem\_xfer\_fire} = NS_{livestem\_xfer}\, f \tag{10.40}$$

$$NF_{deadstem\_fire} = NS_{deadstem}\, f \cdot wcf \tag{10.41}$$

$$NF_{deadstem\_stor\_fire} = NS_{deadstem\_stor}\, f \tag{10.42}$$

$$NF_{deadstem\_xfer\_fire} = NS_{deadstem\_xfer}\, f \tag{10.43}$$

$$NF_{livecroot\_fire} = NS_{livecroot}\, f \tag{10.44}$$

$$NF_{livecroot\_stor\_fire} = NS_{livecroot\_stor}\, f \tag{10.45}$$

$$NF_{livecroot\_xfer\_fire} = NS_{livecroot\_xfer}\, f \tag{10.46}$$

$$NF_{deadcroot\_fire} = NS_{deadcroot}\, f \cdot wcf \tag{10.47}$$

$$NF_{deadcroot\_stor\_fire} = NS_{deadcroot\_stor}\, f \tag{10.48}$$

$$NF_{deadcroot\_xfer\_fire} = NS_{deadcroot\_xfer}\, f \tag{10.49}$$

$$NF_{retrans\_fire} = NS_{retrans}\, f \tag{10.50}$$

Non-combustion PFT-level carbon and nitrogen fluxes due to fire-induced mortality are calculated as:

$$CF_{deadstem\_fire\_mort} = CS_{deadstem}\ f\left(1 - wcf\right) \tag{10.51}$$

$$CF_{deadcroot\_fire\_mort} = CS_{deadcroot}\ f\left(1 - wcf\right) \tag{10.52}$$

$$NF_{deadstem\_fire\_mort} = NS_{deadstem}\ f\left(1 - wcf\right) \tag{10.53}$$

$$NF_{deadcroot\_fire\_mort} = NS_{deadcroot}\ f\left(1 - wcf\right) \tag{10.54}$$

Analogous to the treatment of non-fire mortality fluxes (Section 9.2), fire-induced mortality fluxes leaving the dead stem and dead coarse root vegetation pools are merged to the column level according to the weighted distribution of PFTs on the column, and deposited in coarse woody debris pools. Carbon and nitrogen fluxes into coarse woody debris pools from fire-induced mortality are calculated as:

$$CF_{deadstem\_fire,cwd} = \sum_{p=0}^{npfts} CF_{deadstem\_fire\_mort}\, wcol_p \tag{10.55}$$

$$CF_{deadcroot\_fire,cwd} = \sum_{p=0}^{npfts} CF_{deadcroot\_fire\_mort}\, wcol_p \tag{10.56}$$

$$NF_{deadstem\_fire,cwd} = \sum_{p=0}^{npfts} NF_{deadstem\_fire\_mort}\, wcol_p \tag{10.57}$$

$$NF_{deadcroot\_fire,cwd} = \sum_{p=0}^{npfts} NF_{deadcroot\_fire\_mort}\, wcol_p \tag{10.58}$$

Litter and coarse woody debris pools are also subject to combustion losses based on the column-level estimate of fractional area burned per time step. Litter pools in the affected fraction are assumed to be completely lost to combustion, while coarse woody debris combustion losses in the affected fraction are subject to the same woody combustion fraction (*wcf*) used for woody vegetation pools. The column-level fractional area affected by fire per second (f_c) is

$$f_c = \frac{A_{\Delta t}}{\Delta t}\,. \tag{10.59}$$

Carbon and nitrogen losses to the atmosphere from combustion of litter and coarse woody debris pools are

$$CF_{litr1\_fire} = CS_{litr1} f_c \tag{10.60}$$

$$CF_{litr2\_fire} = CS_{litr2} f_c \tag{10.61}$$

$$CF_{litr3\_fire} = CS_{litr3} f_c \tag{10.62}$$

$$CF_{cwd\_fire} = CS_{cwd} f_c \cdot wcf \tag{10.63}$$

$$NF_{litr1\_fire} = NS_{litr1} f_c \tag{10.64}$$

$$NF_{litr2\_fire} = NS_{litr2} f_c \tag{10.65}$$

$$NF_{litr3\_fire} = NS_{litr3} f_c \tag{10.66}$$

$$NF_{cwd\_fire} = NS_{cwd} f_c \cdot wcf \tag{10.67}$$

11 Dynamic Land Cover

Changes in land use and land cover due to human activity exert a significant influence on the global climate system through the effects of land use and land cover change (LULCC) on long-lived greenhouse gases, and on surface energy balance (changes in albedo and partitioning between sensible and latent heat fluxes) (Forster et al., 2007). Understanding the spatial and temporal patterns of historical and present-day LULCC and the influence of these on net fluxes of greenhouse gases remains an active area of research (Feddema et al., 2005; Hurtt et al., 2006; Stephens et al., 2007). Predictions of future LULCC under various socio-economic scenarios is also an active research area (Nakicenovic and Swart, 2000; Smith and Wigley, 2006; Van Vuuren et al., 2007) with important consequences for future trajectories of climate change.

CLM-CN includes a prognostic treatment of mass and energy fluxes associated with prescribed spatial and temporal variability in LULCC patterns. Provided with an annual time series of the spatial distribution of PFTs, CLM-CN diagnoses the implied increases and decreases in area for individual PFTs at each model time step, then imposes the necessary modifications to the fractional area occupied by each PFT on a grid cell, and performs all the mass and energy balance accounting necessary to represent the expansion and contraction of PFT area. The general approaches used in CLM-CN for handling expansion and contraction of PFT area are presented first, followed by a detailed description of the algorithms.

11.1 Overview of Dynamic Land Cover Approach

The two main cases to consider are expansion and contraction of area for a given PFT. Within these, there are special considerations for the initiation of a new PFT (expansion from zero previous area), and disappearance of an existing PFT (contraction to zero area) within a given grid cell.

The following discussion pertains to the case where all PFTs for a particular grid cell coexist on a single soil/snow column, sharing space and competing for water and nutrients within the column. This is the default sub-grid configuration for CLM-CN, and is a necessary condition for successful implementation of the LULCC dynamics

described here. Other implementations are anticipated which will require additional mechanisms to ensure the conservation of mass and energy during LULCC transistions. For example, a new implementation of crops is already under development which places the crop PFTs within their own landunit, sharing space on a single column but separate from the natural vegetation landunit. Transfer of area from one soil/snow column to another requires new mechanisms to handle conservation of water and energy within the soil/snow columns, and also conservation of carbon and nitrogen stored in litter and soil organic matter pools. This is a high priority area for further model development.

For the case of a PFT which is expanding, conservation of mass is maintained by assuming that the original total mass for the PFT (density x original area) is retained under the expanded area. In other words, the density of all the PFT state variables is reduced to account for the increase in area. Since the incremental changes in area on each time step are typically very small, this modification of carbon and nitrogen density has a minor influence on the physiological behavior of the PFT. Discrete physiological variables such as flags for the phenology routines are not affected by the incremental expansion of PFT area.

For the case of a PFT initiating from zero area in the previous timestep, it is necessary to introduce a very small amount of seed material (carbon and nitrogen) to allow the initiation of a non-zero leaf area. For consistency, the same seeding approach is applied to all new area added to a PFT during expansion. Mass balance is maintained by keeping track of this seed carbon and nitrogen as additional inputs to the land system. A more mechanistic approach would be to include carbon and nitrogen in reproductive tissue as part of the primary production allocation routine, then to draw seed carbon and nitrogen from these pools to initiate growth in the expanded PFT area. This is identified as a medium priority topic for future model development.

For the case where the area for a PFT is decreasing, biomass from the lost PFT area is distributed between litter pools, wood product pools, and land cover conversion fluxes which are assumed to be released immediately to the atmosphere. Carbon and nitrogen densities and all physiological variables are unchanged for the remaining area. In the special case where a PFT is reduced to zero area, some clean-up mechanisms are implemented to reset the physiological parameters to be ready when and if the PFT

returns with non-zero weight in a subsequent time step. The disaggregation of biomass during reduction of PFT area into litter, wood product pools, and immediate conversion losses follows generally from the methods of Houghton et al. (1983), and from more recent implementation of those methods in modeling studies such as McGuire et al. (2001).

11.2 Dynamic Land Cover Forcing Data and Interpolation

While the fluxes of carbon, nitrogen, water, and energy associated with land cover dynamics are prognostic in CLM-CN, the changes in area over time associated with individual PFTs are diagnostic – these changes in area are prescribed through a forcing dataset, referred to here as the "dynpft" dataset. The dynpft dataset consists of an annual time series of global grids, where each annual time step includes information describing the sub-grid fractional area occupied by all the PFTs within each grid cell. Changes in area for a given PFT within a given grid cell for a given model time step are inferred from a time-interpolation of the area information for that PFT from the two bracketing annual time slices in the dynpft dataset.

As a special case, when the time dimension of the dynpft dataset starts at a later year than the current model time step, the first time slice from the dynpft dataset is used to represent the current time step PFT fractional area distributions. Similarly, when the time dimension of the dynpft dataset stops at an earlier year than the current model time step, the last time slice of the dynpft dataset is used. So when a dynpft dataset is used the simulation will have invariant representations of PFT distributions through time for the periods prior to and following the time duration of the dynpft dataset, with dynamic PFT distributions during the period covered by the dynpft dataset.

The following equations captures this logic, where $year_{cur}$ is the calendar year for the current timestep, *dynpft_year*(1) and *dynpft_year*(*nyears*) are the first and last calendar years in the dynpft dataset, respectively, *nyears* is the number of years in the dynpft dataset, nt_1 and nt_2 are the early and late bracketing years used in the interpolation algorithm, and *n* is the index value for the *dynpft_years* array corresponding to *dynpft_years*(*n*) = $year_{cur}$:

$$nt_1 = \begin{cases} 1 & \text{for} \quad year_{cur} < dynpft\_year(1) \\ n & \text{for} \quad dynpft\_year(1) \le year_{cur} < dynpft\_year(nyears) \\ nyears & \text{for} \quad year_{cur} \ge dynpft\_year(nyears) \end{cases} \tag{11.1}$$

$$nt_2 = \begin{cases} 1 & \text{for} \quad year_{cur} < dynpft\_year(1) \\ n+1 & \text{for} \quad dynpft\_year(1) \le year_{cur} < dynpft\_year(nyears) \\ nyears & \text{for} \quad year_{cur} \ge dynpft\_year(nyears) \end{cases}. \tag{11.2}$$

Interpolation of PFT weights between annual time slices in the dynpft dataset uses a simple linear algorithm, based on the conversion of the current time step information into a floating-point value for the number of calendar days since January 1 of the current model year (*cday*). The interpolation weight for the current time step tw_{cday} is

$$tw_{cday} = \frac{366 - cday}{365}. \tag{11.3}$$

where the numerator of Eq. (11.3) uses 366 instead of 365 because the time manager function for CLM returns a value of *cday* = 1.0 for a time of 0Z on January 1. Given weights $w_p(nt_1)$ and $w_p(nt_2)$ from the dynpft dataset for PFT *p* at the bracketing annual time slices nt_1 and nt_2, the interpolated PFT weight for the current time step ($w_{p,t}$) is

$$w_{p,t} = tw_{cday}\left(w_p(nt_1) - w_p(nt_2)\right) + w_p(nt_2). \tag{11.4}$$

The form of Eq. (11.4) is designed to improve roundoff accuracy performance, and guarantees $w_{p,t}$ stays in the range [0,1]. Note that values for $w_p(nt_1)$, $w_p(nt_2)$, and $w_{p,t}$ are fractional weights at the column level of the subgrid hierarchy.

11.3 Carbon and Nitrogen Mass Balance Associated with Increases in PFT Area

Fluxes of carbon and nitrogen associated with dynamic land cover are driven by the change in weight for a given PFT between the current and previous time steps (Δw_p), where

$$\Delta w_p = w_p^t - w_p^{t-\Delta t} \tag{11.5}$$

and by the initial carbon and nitrogen state of the PFT.

For the case of $\Delta w_p > 0$ (PFT area increasing) the PFT-level carbon state variables from the previous time step are modified to apply the previous column-level mass to the

new column-level area, and accounting for the addition of seed carbon to the leaf and, if a woody PFT, dead stem carbon pools:

$$CS^{t}_{leaf} = CS^{t-\Delta t}_{leaf}\, r_1 + seedC_{leaf}\, fC_{disp} r_2 \tag{11.6}$$

$$CS^{t}_{leaf\_stor} = CS^{t-\Delta t}_{leaf\_stor} r_1 + seedC_{leaf}\, fC_{stor} r_2 \tag{11.7}$$

$$CS^{t}_{leaf\_xfer} = CS^{t-\Delta t}_{leaf\_xfer} r_1 + seedC_{leaf}\, fC_{xfer} r_2 \tag{11.8}$$

$$CS^{t}_{froot} = CS^{t-\Delta t}_{froot}\, r_1 \tag{11.9}$$

$$CS^{t}_{froot\_stor} = CS^{t-\Delta t}_{froot\_stor}\, r_1 \tag{11.10}$$

$$CS^{t}_{froot\_xfer} = CS^{t-\Delta t}_{froot\_xfer}\, r_1 \tag{11.11}$$

$$CS^{t}_{livestem} = CS^{t-\Delta t}_{livestem}\, r_1 \tag{11.12}$$

$$CS^{t}_{livestem\_stor} = CS^{t-\Delta t}_{livestem\_stor}\, r_1 \tag{11.13}$$

$$CS^{t}_{livestem\_xfer} = CS^{t-\Delta t}_{livestem\_xfer}\, r_1 \tag{11.14}$$

$$CS^{t}_{deadstem} = CS^{t-\Delta t}_{deadstem}\, r_1 + seedC_{deadstem} r_2 \tag{11.15}$$

$$CS^{t}_{deadstem\_stor} = CS^{t-\Delta t}_{deadstem\_stor}\, r_1 \tag{11.16}$$

$$CS^{t}_{deadstem\_xfer} = CS^{t-\Delta t}_{deadstem\_xfer}\, r_1 \tag{11.17}$$

$$CS^{t}_{livecroot} = CS^{t-\Delta t}_{livecroot}\, r_1 \tag{11.18}$$

$$CS^{t}_{livecroot\_stor} = CS^{t-\Delta t}_{livecroot\_stor}\, r_1 \tag{11.19}$$

$$CS^{t}_{livecroot\_xfer} = CS^{t-\Delta t}_{livecroot\_xfer}\, r_1 \tag{11.20}$$

$$CS^{t}_{deadcroot} = CS^{t-\Delta t}_{deadcroot}\, r_1 \tag{11.21}$$

$$CS^{t}_{deadcroot\_stor} = CS^{t-\Delta t}_{deadcroot\_stor}\, r_1 \tag{11.22}$$

$$CS^{t}_{deadcroot\_xfer} = CS^{t-\Delta t}_{deadcroot\_xfer}\, r_1 \tag{11.23}$$

$$CS^{t}_{gresp\_stor} = CS^{t-\Delta t}_{gresp\_stor}\, r_1 \tag{11.24}$$

$$CS^{t}_{gresp\_xfer} = CS^{t-\Delta t}_{gresp\_xfer}\, r_1 \tag{11.25}$$

$$CS^{t}_{xsmrpool} = CS^{t-\Delta t}_{xsmrpool}\, r_1 \tag{11.26}$$

where superscripts t and t-Δt indicate current and previous allocation timesteps, $seedC_{leaf}$ and $seedC_{deadstem}$ are the carbon densities for leaf and dead stem seed source on the new

PFT area, fC_{disp}, fC_{stor}, and fC_{xfer} are the fractions of leaf seed carbon to go into displayed, stored, and transfer pools, respectively, and r_1 and r_2 are ratios defined as

$$r_1 = \frac{w_p^{t-\Delta t}}{w_p^t} \tag{11.27}$$

and

$$r_2 = \frac{\Delta w_p}{w_p^t} \tag{11.28}.$$

Carbon densities for leaf and dead stem seed source are currently set as global constants, with $seedC_{leaf} = 1$ gC m^{-2}, and $seedC_{deadstem} = 0.1$ gC m^{-2} for woody PFTs or $seedC_{deadstem} = 0$ for non-woody PFTs. These seed sources are necessary for PFTs initiating from zero area on the previous allocation time step: $seedC_{leaf}$ provides a very small leaf area with which photosynthesis can be initiated, and $seedC_{deadstem}$ provides a non-zero canopy height for woody PFTs, an important condition for numerical stability in the surface energy flux calculations. The distribution of $seedC_{leaf}$ between display, storage, and transfer pools depends on the relative distribution of leaf carbon between those pools from the previous time step, as

$$fC_{disp} = \frac{CS_{leaf}^{t-\Delta t}}{CS_{leaf}^{t-\Delta t} + CS_{leaf\_stor}^{t-\Delta t} + CS_{leaf\_xfer}^{t-\Delta t}} \tag{11.29}$$

$$fC_{stor} = \frac{CS_{stor}^{t-\Delta t}}{CS_{leaf}^{t-\Delta t} + CS_{leaf\_stor}^{t-\Delta t} + CS_{leaf\_xfer}^{t-\Delta t}} \tag{11.30}$$

$$fC_{xfer} = \frac{CS_{xfer}^{t-\Delta t}}{CS_{leaf}^{t-\Delta t} + CS_{leaf\_stor}^{t-\Delta t} + CS_{leaf\_xfer}^{t-\Delta t}}, \tag{11.31}$$

unless the PFT is initiating from zero weight in the previous timestep, in which case these fractions depend only on the phenological type for the PFT, as

$$fC_{disp} = \begin{cases} 1 & \text{for evergreen type} \\ 0 & \text{for deciduous type} \end{cases} \tag{11.32}$$

$$fC_{stor} = \begin{cases} 0 & \text{for evergreen type} \\ 1 & \text{for deciduous type} \end{cases} \tag{11.33}$$

$$fC_{xfer} = 0\,. \tag{11.34}$$

PFT-level nitrogen state variables for the case of $\Delta w_p > 0$ are modified in parallel with the carbon state variables, as:

$$NS^t_{leaf} = NS^{t-\Delta t}_{leaf}\, r_1 + seedN_{leaf}\, fN_{disp} r_2 \quad (11.35)$$

$$NS^t_{leaf\_stor} = NS^{t-\Delta t}_{leaf\_stor} r_1 + seedN_{leaf}\, fN_{stor} r_2 \quad (11.36)$$

$$NS^t_{leaf\_xfer} = NS^{t-\Delta t}_{leaf\_xfer} r_1 + seedN_{leaf}\, fN_{xfer} r_2 \quad (11.37)$$

$$NS^t_{froot} = NS^{t-\Delta t}_{froot}\, r_1 \quad (11.38)$$

$$NS^t_{froot\_stor} = NS^{t-\Delta t}_{froot\_stor}\, r_1 \quad (11.39)$$

$$NS^t_{froot\_xfer} = NS^{t-\Delta t}_{froot\_xfer}\, r_1 \quad (11.40)$$

$$NS^t_{livestem} = NS^{t-\Delta t}_{livestem}\, r_1 \quad (11.41)$$

$$NS^t_{livestem\_stor} = NS^{t-\Delta t}_{livestem\_stor}\, r_1 \quad (11.42)$$

$$NS^t_{livestem\_xfer} = NS^{t-\Delta t}_{livestem\_xfer}\, r_1 \quad (11.43)$$

$$NS^t_{deadstem} = NS^{t-\Delta t}_{deadstem}\, r_1 + seedN_{deadstem} r_2 \quad (11.44)$$

$$NS^t_{deadstem\_stor} = NS^{t-\Delta t}_{deadstem\_stor}\, r_1 \quad (11.45)$$

$$NS^t_{deadstem\_xfer} = NS^{t-\Delta t}_{deadstem\_xfer}\, r_1 \quad (11.46)$$

$$NS^t_{livecroot} = NS^{t-\Delta t}_{livecroot}\, r_1 \quad (11.47)$$

$$NS^t_{livecroot\_stor} = NS^{t-\Delta t}_{livecroot\_stor}\, r_1 \quad (11.48)$$

$$NS^t_{livecroot\_xfer} = NS^{t-\Delta t}_{livecroot\_xfer}\, r_1 \quad (11.49)$$

$$NS^t_{deadcroot} = NS^{t-\Delta t}_{deadcroot}\, r_1 \quad (11.50)$$

$$NS^t_{deadcroot\_stor} = NS^{t-\Delta t}_{deadcroot\_stor}\, r_1 \quad (11.51)$$

$$NS^t_{deadcroot\_xfer} = NS^{t-\Delta t}_{deadcroot\_xfer}\, r_1 \quad (11.52)$$

$$NS^t_{retrans} = NS^{t-\Delta t}_{retrans}\, r_1, \quad (11.53)$$

where $seedN_{leaf}$ and $seedN_{deadstem}$ are the nitrogen densities for leaf and dead stem seed source on the new PFT area, fN_{disp}, fN_{stor}, and fN_{xfer} are the fractions of leaf seed nitrogen to go into displayed, stored, and transfer pools, respectively.

The $seedN_{leaf}$ and $seedN_{deadstem}$ parameters depend on the specifications for $seedC_{leaf}$ and $seedC_{deadstem}$, and on the PFT-specific C:N ratios for these pools, as

$$seedN_{leaf} = \frac{seedC_{leaf}}{CN_{leaf}} \tag{11.54}$$

and

$$seedN_{deadstem} = \begin{cases} \dfrac{seedC_{deadstem}}{CN_{dw}} & \text{for woody PFTs} \\ 0 & \text{for non-woody PFTs} \end{cases} . \tag{11.55}$$

The distribution of $seedN_{leaf}$ between display, storage, and transfer pools depends on the relative distribution of leaf nitrogen between those pools from the previous time step, as

$$fN_{disp} = \frac{NS_{leaf}^{t-\Delta t}}{NS_{leaf}^{t-\Delta t} + NS_{leaf\_stor}^{t-\Delta t} + NS_{leaf\_xfer}^{t-\Delta t}} \tag{11.56}$$

$$fN_{stor} = \frac{NS_{stor}^{t-\Delta t}}{NS_{leaf}^{t-\Delta t} + NS_{leaf\_stor}^{t-\Delta t} + NS_{leaf\_xfer}^{t-\Delta t}} \tag{11.57}$$

$$fN_{xfer} = \frac{NS_{xfer}^{t-\Delta t}}{NS_{leaf}^{t-\Delta t} + NS_{leaf\_stor}^{t-\Delta t} + NS_{leaf\_xfer}^{t-\Delta t}} , \tag{11.58}$$

unless the PFT is initiating from zero weight in the previous timestep, in which case these fractions depend only on the phenological type for the PFT, as

$$fN_{disp} = \begin{cases} 1 & \text{for evergreen type} \\ 0 & \text{for deciduous type} \end{cases} \tag{11.59}$$

$$fN_{stor} = \begin{cases} 0 & \text{for evergreen type} \\ 1 & \text{for deciduous type} \end{cases} \tag{11.60}$$

$$fN_{xfer} = 0 . \tag{11.61}$$

Total column-level fluxes of carbon into leaf and dead stem pools by way of seeding during the expansion of PFTs ($CS_{dwt\_seed,leaf}$ and $CS_{dwt\_seed,deadstem}$, respectively) are tracked for use in the verification of conservation of mass, as

$$CF_{dwt\_seed,leaf} = \sum_{p=0}^{npfts} \frac{seedC_{leaf,p} \Delta w_p}{\Delta t} \tag{11.62}$$

and

$$CF_{dwt\_seed,deadstem} = \sum_{p=0}^{npfts} \frac{seedC_{deadstem,p} \Delta w_p}{\Delta t} \tag{11.63}$$

where the subscript *p* for the *seedC* terms refers to the set of PFTs occupying space on the column following the dynpft updates. Column-level nitrogen fluxes are tracked analogously, as

$$NF_{dwt\_seed,leaf} = \sum_{p=0}^{npfts} \frac{seedN_{leaf,p} \Delta w_p}{\Delta t} \tag{11.64}$$

and

$$NF_{dwt\_seed,deadstem} = \sum_{p=0}^{npfts} \frac{seedN_{deadstem,p} \Delta w_p}{\Delta t} \tag{11.65}$$

11.4 Carbon and Nitrogen Mass Balance Associated with Decreases in PFT Area

For the case of $\Delta w_p < 0$ (PFT area decreasing) the PFT-level carbon and nitrogen state variables from the previous time step are retained unchanged, reflecting the assumption that the PFT has lost area, but on a per-unit-area basis the composition of the vegetation in the remaining area for that PFT is unaffected. Carbon and nitrogen mass lost from the PFT level through reductions in PFT area is directed to litter or wood product pools, or lost to the atmosphere during the land cover conversion. In the special case where a PFT decreases to zero area, then the state variables are all set to zero.

Leaf, live stem, and all storage and transfer pools of carbon and nitrogen from the affected fraction of the PFT area are assumed to be lost immediately to the atmosphere, referred to here as the conversion flux. The following terms give the contributions of an individual PFT to the column-level conversion flux for carbon:

$$CF_{leaf\_dwt,conv,p} = \begin{cases} CS_{leaf} \Delta w_p / \Delta t & \text{for } w_p^t > 0 \\ CS_{leaf} w_p^{t-\Delta t} / \Delta t & \text{for } w_p^t = 0 \end{cases} \tag{11.66}$$

$$CF_{leaf\_stor\_dwt,conv,p} = \begin{cases} CS_{leaf\_stor} \Delta w_p / \Delta t & \text{for } w_p^t > 0 \\ CS_{leaf\_stor} w_p^{t-\Delta t} / \Delta t & \text{for } w_p^t = 0 \end{cases} \tag{11.67}$$

$$CF_{leaf\_xfer\_dwt,conv,p} = \begin{cases} CS_{leaf\_xfer} \Delta w_p / \Delta t & \text{for } w_p^t > 0 \\ CS_{leaf\_xfer} w_p^{t-\Delta t} / \Delta t & \text{for } w_p^t = 0 \end{cases} \quad (11.68)$$

$$CF_{froot\_stor\_dwt,conv,p} = \begin{cases} CS_{froot\_stor} \Delta w_p / \Delta t & \text{for } w_p^t > 0 \\ CS_{froot\_stor} w_p^{t-\Delta t} / \Delta t & \text{for } w_p^t = 0 \end{cases} \quad (11.69)$$

$$CF_{froot\_xfer\_dwt,conv,p} = \begin{cases} CS_{froot\_xfer} \Delta w_p / \Delta t & \text{for } w_p^t > 0 \\ CS_{froot\_xfer} w_p^{t-\Delta t} / \Delta t & \text{for } w_p^t = 0 \end{cases} \quad (11.70)$$

$$CF_{livestem\_dwt,conv,p} = \begin{cases} CS_{livestem} \Delta w_p / \Delta t & \text{for } w_p^t > 0 \\ CS_{livestem} w_p^{t-\Delta t} / \Delta t & \text{for } w_p^t = 0 \end{cases} \quad (11.71)$$

$$CF_{livestem\_stor\_dwt,conv,p} = \begin{cases} CS_{livestem\_stor} \Delta w_p / \Delta t & \text{for } w_p^t > 0 \\ CS_{livestem\_stor} w_p^{t-\Delta t} / \Delta t & \text{for } w_p^t = 0 \end{cases} \quad (11.72)$$

$$CF_{livestem\_xfer\_dwt,conv,p} = \begin{cases} CS_{livestem\_xfer} \Delta w_p / \Delta t & \text{for } w_p^t > 0 \\ CS_{livestem\_xfer} w_p^{t-\Delta t} / \Delta t & \text{for } w_p^t = 0 \end{cases} \quad (11.73)$$

$$CF_{deadstem\_dwt,conv,p} = \begin{cases} CS_{deadstem} \Delta w_p \, f_{conv,p} / \Delta t & \text{for } w_p^t > 0 \\ CS_{deadstem} w_p^{t-\Delta t} \, f_{conv,p} / \Delta t & \text{for } w_p^t = 0 \end{cases} \quad (11.74)$$

$$CF_{deadstem\_stor\_dwt,conv,p} = \begin{cases} CS_{deadstem\_stor} \Delta w_p / \Delta t & \text{for } w_p^t > 0 \\ CS_{deadstem\_stor} w_p^{t-\Delta t} / \Delta t & \text{for } w_p^t = 0 \end{cases} \quad (11.75)$$

$$CF_{deadstem\_xfer\_dwt,conv,p} = \begin{cases} CS_{deadstem\_xfer} \Delta w_p / \Delta t & \text{for } w_p^t > 0 \\ CS_{deadstem\_xfer} w_p^{t-\Delta t} / \Delta t & \text{for } w_p^t = 0 \end{cases} \quad (11.76)$$

$$CF_{livectoor\_stor\_dwt,conv,p} = \begin{cases} CS_{livecroot\_stor} \Delta w_p / \Delta t & \text{for } w_p^t > 0 \\ CS_{livecroot\_stor} w_p^{t-\Delta t} / \Delta t & \text{for } w_p^t = 0 \end{cases} \quad (11.77)$$

$$CF_{livecroot\_xfer\_dwt,conv,p} = \begin{cases} CS_{livecroot\_xfer} \Delta w_p / \Delta t & \text{for } w_p^t > 0 \\ CS_{livecroot\_xfer} w_p^{t-\Delta t} / \Delta t & \text{for } w_p^t = 0 \end{cases} \quad (11.78)$$

$$CF_{deadcroot\_stor\_dwt,conv,p} = \begin{cases} CS_{deadcroot\_stor} \Delta w_p / \Delta t & \text{for } w_p^t > 0 \\ CS_{deadcroot\_stor} w_p^{t-\Delta t} / \Delta t & \text{for } w_p^t = 0 \end{cases} \quad (11.79)$$

$$CF_{deadcroot\_xfer\_dwt,conv,p} = \begin{cases} CS_{deadcroot\_xfer} \Delta w_p / \Delta t & \text{for } w_p^t > 0 \\ CS_{deadcroot\_xfer} w_p^{t-\Delta t} / \Delta t & \text{for } w_p^t = 0 \end{cases} \tag{11.80}$$

$$CF_{gresp\_stor\_dwt,conv,p} = \begin{cases} CS_{gresp\_stor} \Delta w_p / \Delta t & \text{for } w_p^t > 0 \\ CS_{gresp\_stor} w_p^{t-\Delta t} / \Delta t & \text{for } w_p^t = 0 \end{cases} \tag{11.81}$$

$$CF_{gresp\_xfer\_dwt,conv,p} = \begin{cases} CS_{gresp\_xfer} \Delta w_p / \Delta t & \text{for } w_p^t > 0 \\ CS_{gresp\_xfer} w_p^{t-\Delta t} / \Delta t & \text{for } w_p^t = 0 \end{cases} \tag{11.82}$$

$$CF_{xsmrpool\_dwt,conv,p} = \begin{cases} CS_{xsmrpool} \Delta w_p / \Delta t & \text{for } w_p^t > 0 \\ CS_{xsmrpool} w_p^{t-\Delta t} / \Delta t & \text{for } w_p^t = 0 \end{cases} \tag{11.83}$$

where $f_{conv,p}$ is a PFT-specific fraction of the affected part of the dead stem pool which is assumed to be lost immediately to the atmosphere during land cover conversion. The PFT-level total conversion flux of carbon ($CF_{conv,p}$, gC m^{-2} s^{-1}) is then given as:

$$\begin{aligned} CF_{conv,p} = {} & CF_{leaf\_dwt,conv,p} + CF_{leaf\_stor\_dwt,conv,p} + CF_{leaf\_xfer\_dwt,conv,p} + \\ & CF_{froot\_stor\_dwt,conv,p} + CF_{froot\_xfer\_dwt,conv,p} + \\ & CF_{livestem\_dwt,conv,p} + CF_{livestem\_stor\_dwt,conv,p} + CF_{livestem\_xfer\_dwt,conv,p} + \\ & CF_{deadstem\_dwt,conv,p} + CF_{deadstem\_stor\_dwt,conv,p} + CF_{deadstem\_xfer\_dwt,conv,p} + \\ & CF_{livecroot\_stor\_dwt,conv,p} + CF_{livecroot\_xfer\_dwt,conv,p} + \\ & CF_{deadcroot\_stor\_dwt,conv,p} + CF_{deadcroot\_xfer\_dwt,conv,p} + \\ & CF_{gresp\_stor\_dwt,conv,p} + CF_{gresp\_xfer\_dwt,conv,p} + \\ & CF_{xsmrpool\_dwt,conv,p}. \end{aligned} \tag{11.84}$$

The corresponding column-level conversion flux of carbon (CF_{conv}, gC m^{-2} s^{-1}) is then given as:

$$CF_{conv} = \sum_{p=0}^{npfts} CF_{conv,p} \; . \tag{11.85}$$

It should be noted that the form of Eqs. (11.66) through (11.83) produces fluxes for each PFT scaled per unit area of the column on which the PFT exists, and so the usual dependence on $wcol_p$ is missing from Eq. (11.85). The same is true for the other PFT-level fluxes associated with land cover change, described below. The reason for this difference with respect to, for example, the aggregation of PFT-level fluxes to the column

level for mortality, is that for dynamic land cover fluxes the relevant PFT-level weights are changing during the time step, while the total area of all PFTs on a column is constant. fluxesand nitrogen (NF_{conv}, gN m^{-2} s^{-1}).

The following terms give the contributions of an individual PFT to the column-level conversion flux for nitrogen:

$$NF_{leaf\_dwt,conv,p} = \begin{cases} NS_{leaf}\Delta w_p / \Delta t & \text{for } w_p^t > 0 \\ NS_{leaf} w_p^{t-\Delta t} / \Delta t & \text{for } w_p^t = 0 \end{cases} \quad (11.86)$$

$$NF_{leaf\_stor\_dwt,conv,p} = \begin{cases} NS_{leaf\_stor}\Delta w_p / \Delta t & \text{for } w_p^t > 0 \\ NS_{leaf\_stor} w_p^{t-\Delta t} / \Delta t & \text{for } w_p^t = 0 \end{cases} \quad (11.87)$$

$$NF_{leaf\_xfer\_dwt,conv,p} = \begin{cases} NS_{leaf\_xfer}\Delta w_p / \Delta t & \text{for } w_p^t > 0 \\ NS_{leaf\_xfer} w_p^{t-\Delta t} / \Delta t & \text{for } w_p^t = 0 \end{cases} \quad (11.88)$$

$$NF_{froot\_stor\_dwt,conv,p} = \begin{cases} NS_{froot\_stor}\Delta w_p / \Delta t & \text{for } w_p^t > 0 \\ NS_{froot\_stor} w_p^{t-\Delta t} / \Delta t & \text{for } w_p^t = 0 \end{cases} \quad (11.89)$$

$$NF_{froot\_xfer\_dwt,conv,p} = \begin{cases} NS_{froot\_xfer}\Delta w_p / \Delta t & \text{for } w_p^t > 0 \\ NS_{froot\_xfer} w_p^{t-\Delta t} / \Delta t & \text{for } w_p^t = 0 \end{cases} \quad (11.90)$$

$$NF_{livestem\_dwt,conv,p} = \begin{cases} NS_{livestem}\Delta w_p / \Delta t & \text{for } w_p^t > 0 \\ NS_{livestem} w_p^{t-\Delta t} / \Delta t & \text{for } w_p^t = 0 \end{cases} \quad (11.91)$$

$$NF_{livestem\_stor\_dwt,conv,p} = \begin{cases} NS_{livestem\_stor}\Delta w_p / \Delta t & \text{for } w_p^t > 0 \\ NS_{livestem\_stor} w_p^{t-\Delta t} / \Delta t & \text{for } w_p^t = 0 \end{cases} \quad (11.92)$$

$$NF_{livestem\_xfer\_dwt,conv,p} = \begin{cases} NS_{livestem\_xfer}\Delta w_p / \Delta t & \text{for } w_p^t > 0 \\ NS_{livestem\_xfer} w_p^{t-\Delta t} / \Delta t & \text{for } w_p^t = 0 \end{cases} \quad (11.93)$$

$$NF_{deadstem\_dwt,conv,p} = \begin{cases} NS_{deadstem}\Delta w_p f_{conv,p} / \Delta t & \text{for } w_p^t > 0 \\ NS_{deadstem} w_p^{t-\Delta t} f_{conv,p} / \Delta t & \text{for } w_p^t = 0 \end{cases} \quad (11.94)$$

$$NF_{deadstem\_stor\_dwt,conv,p} = \begin{cases} NS_{deadstem\_stor}\Delta w_p / \Delta t & \text{for } w_p^t > 0 \\ NS_{deadstem\_stor} w_p^{t-\Delta t} / \Delta t & \text{for } w_p^t = 0 \end{cases} \quad (11.95)$$

$$NF_{deadstem\_xfer\_dwt,conv,p} = \begin{cases} NS_{deadstem\_xfer} \Delta w_p / \Delta t & \text{for } w_p^t > 0 \\ NS_{deadstem\_xfer} w_p^{t-\Delta t} / \Delta t & \text{for } w_p^t = 0 \end{cases} \quad (11.96)$$

$$NF_{livecroot\_stor\_dwt,conv,p} = \begin{cases} NS_{livecroot\_stor} \Delta w_p / \Delta t & \text{for } w_p^t > 0 \\ NS_{livecroot\_stor} w_p^{t-\Delta t} / \Delta t & \text{for } w_p^t = 0 \end{cases} \quad (11.97)$$

$$NF_{livecroot\_xfer\_dwt,conv,p} = \begin{cases} NS_{livecroot\_xfer} \Delta w_p / \Delta t & \text{for } w_p^t > 0 \\ NS_{livecroot\_xfer} w_p^{t-\Delta t} / \Delta t & \text{for } w_p^t = 0 \end{cases} \quad (11.98)$$

$$NF_{deadcroot\_stor\_dwt,conv,p} = \begin{cases} NS_{deadcroot\_stor} \Delta w_p / \Delta t & \text{for } w_p^t > 0 \\ NS_{deadcroot\_stor} w_p^{t-\Delta t} / \Delta t & \text{for } w_p^t = 0 \end{cases} \quad (11.99)$$

$$NF_{deadcroot\_xfer\_dwt,conv,p} = \begin{cases} NS_{deadcroot\_xfer} \Delta w_p / \Delta t & \text{for } w_p^t > 0 \\ NS_{deadcroot\_xfer} w_p^{t-\Delta t} / \Delta t & \text{for } w_p^t = 0 \end{cases} \quad (11.100)$$

$$NF_{retrans\_dwt,conv,p} = \begin{cases} NS_{retrans} \Delta w_p / \Delta t & \text{for } w_p^t > 0 \\ NS_{retrans} w_p^{t-\Delta t} / \Delta t & \text{for } w_p^t = 0 \end{cases} \quad (11.101)$$

The PFT-level total conversion flux of nitrogen ($NF_{conv,p}$, gN m^{-2} s^{-1}) is:

$$\begin{aligned} NF_{conv,p} = {} & NF_{leaf\_dwt,conv,p} + NF_{leaf\_stor\_dwt,conv,p} + NF_{leaf\_xfer\_dwt,conv,p} + \\ & NF_{froot\_stor\_dwt,conv,p} + NF_{froot\_xfer\_dwt,conv,p} + \\ & NF_{livestem\_dwt,conv,p} + NF_{livestem\_stor\_dwt,conv,p} + NF_{livestem\_xfer\_dwt,conv,p} + \\ & NF_{deadstem\_dwt,conv,p} + NF_{deadstem\_stor\_dwt,conv,p} + NF_{deadstem\_xfer\_dwt,conv,p} + \\ & NF_{livecroot\_stor\_dwt,conv,p} + NF_{livecroot\_xfer\_dwt,conv,p} + \\ & NF_{deadcroot\_stor\_dwt,conv,p} + NF_{deadcroot\_xfer\_dwt,conv,p} + \\ & NF_{retrans\_dwt,conv,p}. \end{aligned} \quad (11.102)$$

The corresponding column-level conversion flux of nitrogen (NF_{conv}, gN m^{-2} s^{-1}) is then given as:

$$NF_{conv} = \sum_{p=0}^{npfts} NF_{conv,p} \; . \quad (11.103)$$

Fine root carbon and nitrogen pools on the fractional area affected by land cover change are assumed to enter the column-level litter pools, while live and dead coarse root carbon and nitrogen pools from the affected area are assumed to enter the column-level

coarse woody debris pools. Fluxes to litter from fine root carbon and nitrogen are calculated as:

$$CF_{froot\_dwt,lit,p} = \begin{cases} CS_{froot} \Delta w_p / \Delta t & \text{for } w_p^t > 0 \\ CS_{froot} w_p^{t-\Delta t} / \Delta t & \text{for } w_p^t = 0 \end{cases} \quad (11.104)$$

and

$$NF_{froot\_dwt,lit,p} = \begin{cases} NS_{froot} \Delta w_p / \Delta t & \text{for } w_p^t > 0 \\ NS_{froot} w_p^{t-\Delta t} / \Delta t & \text{for } w_p^t = 0 \end{cases} \quad (11.105)$$

These PFT-level fluxes are aggregated to the column-level and distributed among the litter pools as follows, for carbon:

$$CF_{froot\_dwt,lit1} = \sum_{p=0}^{npfts} CF_{froot\_dwt,lit,p} \, f_{lab\_leaf,p} \quad (11.106)$$

$$CF_{froot\_dwt,lit2} = \sum_{p=0}^{npfts} CF_{froot\_dwt,lit,p} \, f_{cel\_leaf,p} \quad (11.107)$$

$$CF_{froot\_dwt,lit3} = \sum_{p=0}^{npfts} CF_{froot\_dwt,lit,p} \, f_{lig\_leaf,p} \quad (11.108)$$

and for nitrogen:

$$NF_{froot\_dwt,lit1} = \sum_{p=0}^{npfts} NF_{froot\_dwt,lit,p} \, f_{lab\_leaf,p} \quad (11.109)$$

$$NF_{froot\_dwt,lit2} = \sum_{p=0}^{npfts} NF_{froot\_dwt,lit,p} \, f_{cel\_leaf,p} \quad (11.110)$$

$$NF_{froot\_dwt,lit3} = \sum_{p=0}^{npfts} NF_{froot\_dwt,lit,p} \, f_{lig\_leaf,p} \,, \quad (11.111)$$

where $f_{lab\_leaf,p}$, $f_{cel\_froot,p}$, and $f_{lig\_froot,p}$ are labile, cellulose, and lignin fractions of fine root material, as defined in Section 6.5.

PFT-level fluxes of carbon and nitrogen to coarse woody debris from live and dead coarse root pools are calculated as:

$$CF_{livecroot\_dwt,cwd,p} = \begin{cases} CS_{livecroot} \Delta w_p / \Delta t & \text{for } w_p^t > 0 \\ CS_{livecroot} w_p^{t-\Delta t} / \Delta t & \text{for } w_p^t = 0 \end{cases} \quad (11.112)$$

$$CF_{deadcroot\_dwt,cwd,p} = \begin{cases} CS_{deadcroot} \Delta w_p / \Delta t & \text{for } w_p^t > 0 \\ CS_{deadcroot} w_p^{t-\Delta t} / \Delta t & \text{for } w_p^t = 0 \end{cases} \quad (11.113)$$

and

$$NF_{livecroot\_dwt,cwd,p} = \begin{cases} NS_{livecroot} \Delta w_p / \Delta t & \text{for } w_p^t > 0 \\ NS_{livecroot} w_p^{t-\Delta t} / \Delta t & \text{for } w_p^t = 0 \end{cases} \quad (11.114)$$

$$NF_{deadcroot\_dwt,cwd,p} = \begin{cases} NS_{deadcroot} \Delta w_p / \Delta t & \text{for } w_p^t > 0 \\ NS_{deadcroot} w_p^{t-\Delta t} / \Delta t & \text{for } w_p^t = 0 \end{cases} \quad (11.115)$$

These PFT-level fluxes are aggregated to the column-level coarse woody debris pool as follows, for carbon:

$$CF_{livecroot\_dwt,cwd} = \sum_{p=0}^{npfts} CF_{livecroot\_dwt,cwd,p} \quad (11.116)$$

$$CF_{deadcroot\_dwt,cwd} = \sum_{p=0}^{npfts} CF_{deadcroot\_dwt,cwd,p} , \quad (11.117)$$

and for nitrogen:

$$NF_{livecroot\_dwt,cwd} = \sum_{p=0}^{npfts} NF_{livecroot\_dwt,cwd,p} \quad (11.118)$$

$$NF_{deadcroot\_dwt,cwd} = \sum_{p=0}^{npfts} NF_{deadcroot\_dwt,cwd,p} . \quad (11.119)$$

For the case of a woody PFT experiencing a reduction in area, a fraction of the aboveground woody biomass associated with the lost area is assumed to be converted to wood products. Two wood product pools are tracked for each column, with 10-year and 100-year lifespans, respectively. The fractions of woody biomass entering these pools are currently defined as constants for each PFT, although a more highly-resolved accounting of regional differences in forest management practices is desirable. Carbon and nitrogen fluxes at the PFT-level are given as:

$$CF_{deadstem\_dwt,prod10,p} = \begin{cases} CS_{deadstem} \Delta w_p f_{prod10,p} / \Delta t & \text{for } w_p^t > 0 \\ CS_{deadstem} w_p^{t-\Delta t} f_{prod10,p} / \Delta t & \text{for } w_p^t = 0 \end{cases} \quad (11.120)$$

$$CF_{deadstem\_dwt,prod100,p} = \begin{cases} CS_{deadstem} \Delta w_p f_{prod100,p} / \Delta t & \text{for } w_p^t > 0 \\ CS_{deadstem} w_p^{t-\Delta t} f_{prod100,p} / \Delta t & \text{for } w_p^t = 0 \end{cases} \quad (11.121),$$

and

$$NF_{deadstem\_dwt,prod10,p} = \begin{cases} NS_{deadstem} \Delta w_p f_{prod10,p} / \Delta t & \text{for } w_p^t > 0 \\ NS_{deadstem} w_p^{t-\Delta t} f_{prod10,p} / \Delta t & \text{for } w_p^t = 0 \end{cases} \quad (11.122)$$

$$NF_{deadstem\_dwt,prod100,p} = \begin{cases} NS_{deadstem} \Delta w_p f_{prod100,p} / \Delta t & \text{for } w_p^t > 0 \\ NS_{deadstem} w_p^{t-\Delta t} f_{prod100,p} / \Delta t & \text{for } w_p^t = 0 \end{cases} \quad (11.123)$$

These fluxes into wood product pools are aggregated to the column-level as:

$$CF_{deadstem\_dwt,prod10} = \sum_{p=0}^{npfts} CF_{deadstem\_dwt,prod10,p} \quad (11.124)$$

$$CF_{deadstem\_dwt,prod100} = \sum_{p=0}^{npfts} CF_{deadstem\_dwt,prod100,p} \quad (11.125)$$

and

$$NF_{deadstem\_dwt,prod10} = \sum_{p=0}^{npfts} NF_{deadstem\_dwt,prod10,p} \quad (11.126)$$

$$NF_{deadstem\_dwt,prod100} = \sum_{p=0}^{npfts} NF_{deadstem\_dwt,prod100,p} \; . \quad (11.127)$$

For each PFT, the values for $f_{conv,p}$, $f_{prod10,p}$, and $f_{prod100,p}$ sum to 1.0. Values for each of the currently defined woody PFTs are given in Table XX.

PFT#	PFT name	f_{conv}	f_{prod10}	$f_{prod100}$
1	Needleleaf evergreen temperate tree	0.6	0.3	0.1
2	Needleleaf evergreen boreal tree	0.6	0.3	0.1
3	Needleleaf deciduous boreal tree	0.6	0.3	0.1
4	Broadleaf evergreen tropical tree	0.6	0.4	0.0
5	Broadleaf evergreen temperate tree	0.6	0.3	0.1
6	Broadleaf deciduous tropical tree	0.6	0.4	0.0
7	Broadleaf deciduous temperate tree	0.6	0.3	0.1
8	Broadleaf deciduous boreal tree	0.6	0.3	0.1
9	Broadleaf evergreen shrub	0.8	0.2	0.0
10	Broadleaf deciduous temperate shrub	0.8	0.2	0.0
11	Broadleaf deciduous boreal shrub	0.8	0.2	0.0

Table XX. Aboveground wood fractions assigned to conversion flux, 10-year, and 100-year product pools during loss of PFT area due to land cover change. Values used here are based on the relative proportions of conversion flux, 10-year product pool and 100-year product pool from Houghton et al. (1983).

Losses to the atmosphere from the column-level product pools ($CF_{prod10,loss}$, $CF_{prod100,loss}$ (gC $m^{-2}s^{-1}$) and $NF_{prod10,loss}$, $NF_{prod100,loss}$ (gN m^{-2} s^{-1})) are estimated using an exponential decay algorithm:

$$CF_{prod10,loss} = CS_{prod10} k_{prod10} \quad (11.128)$$

$$CF_{prod100,loss} = CS_{prod100} k_{prod100} \quad (11.129)$$

$$NF_{prod10,loss} = NS_{prod10} k_{prod10} \quad (11.130)$$

$$NF_{prod100,loss} = NS_{prod100} k_{prod100} \quad (11.131)$$

where k_{prod10} = 7.2e-9 and $k_{prod100}$ = 7.2e-10 are parameterized to give ~90% loss of initial mass over 10 and 100 years, respectively, for the 10-year and 100-year product pools.

12 Prognostic Biogeography: Coupling a Dynamic Global Vegetation Model (DGVM) to CLM-CN

13 Prognostic Crop Model: Coupling the Agro-IBIS Crop Model to CLM-CN

14 Carbon Isotopes

CLM-CN includes a fully prognostic representation of the fluxes, storage, and isotopic discrimination of the stable carbon isotope ^{13}C. The implementation of the ^{13}C capability takes advantage of the CLM-CN hierarchical data structures, replicating the carbon state and flux variable structures at the column and PFT level to track total carbon and the ^{13}C isotope separately (see description of data structure hierarchy in Chapter XX). For the most part, fluxes and associated updates to carbon state variables for ^{13}C are calculated directly from the corresponding total C fluxes. Separate calculations are required in a few special cases, such as where isotopic discrimination occurs, or where the necessary isotopic ratios are undefined. The general approach for ^{13}C flux and state variable calculation is described here, followed by a description of all the places where special calculations are required.

14.1 General Form for Calculating ^{13}C Flux

In general, the flux of ^{13}C corresponding to a given flux of total C (CF_{13C} and CF_{totC}, respectively) is determined by CF_{totC}, the masses of ^{13}C and total C in the upstream pools (CS_{13C_up} and CS_{totC_up}, respectively, i.e. the pools *from which* the fluxes of ^{13}C and total C originate), and a fractionation factor, f_{frac}:

$$CF_{13C} = \begin{cases} CF_{totC} \dfrac{CS_{13C\_up}}{CS_{totC\_up}} f_{frac} & \text{for } CS_{totC} \neq 0 \\ 0 & \text{for } CS_{totC} = 0 \end{cases} \qquad (14.1)$$

If the f_{frac} = 1.0 (no fractionation), then the fluxes CF_{13C} and CF_{totC} will be in simple proportion to the masses CS_{13C_up} and CS_{totC_up}. Values of f_{frac} < 1.0 indicate a discrimination against the heavier isotope (^{13}C) in the flux-generating process, while f_{frac} > 1.0 would indicate a preference for the heavier isotope. Currently, in all cases where Eq. (14.1) is used to calculate a ^{13}C flux, f_{frac} is set to 1.0.

14.2 Isotope Symbols, Units, and Reference Standards

Carbon has two primary stable isotopes, ^{12}C and ^{13}C. ^{12}C is the most abundant, comprising about 99% of all carbon. The isotope ratio of a compound, R_A, is the mass ratio of the rare isotope to the abundant isotope

$$R_A = \frac{^{13}C_A}{^{12}C_A}. \tag{14.2}$$

Carbon isotope ratios are often expressed using delta notation, δ. The $\delta^{13}C$ value of a compound A, $\delta^{13}C_A$, is the difference between the isotope ratio of the compound, R_A, and that of the Pee Dee Belemnite standard, R_{PDB}, in parts per thousand

$$\delta^{13}C_A = \left(\frac{R_A}{R_{PDB}} - 1 \right) \times 1000 \tag{14.3}$$

where R_{PDB} = 0.0112372, and units of δ are per mil (‰).

Isotopic fractionation during the reaction A→B can be expressed several ways. One expression of the fractionation factor is with alpha (α) notation, where

$$\alpha_{A-B} = \frac{R_A}{R_B} = \frac{\delta_A + 1000}{\delta_B + 1000}. \tag{14.4}$$

This can also be expressed using another form of delta notation (Δ), where

$$\alpha_{A-B} = \frac{\Delta_{A-B}}{1000} + 1. \tag{14.5}$$

In other words, if $\Delta_{A\text{-}B}$=4.4‰, then $\alpha_{A\text{-}B}$=1.0044.

14.3 Carbon Isotope Discrimination During Photosynthesis

We model photosynthesis as a two-step process: diffusion of CO_2 into the stomatal cavity, followed by enzymatic fixation (Chapter 3.2). Each step is associated with a kinetic isotope effect. The kinetic isotope effect during diffusion of CO_2 through the stomatal opening is 4.4‰. The kinetic isotope effect during fixation of CO_2 with Rubisco is ~30‰; however, since about 5-10% of carbon in C3 plants reacts with phosphoenolpyruvate carboxylase (PEPC) (Melzer and O'Leary, 1987), the net kinetic isotope effect during fixation is ~27‰ for C3 plants. In C4 photosynthesis, only the diffusion effect is important

15 Mass Balance Checking

16 Numerical Implementation

17 Initialization Methods

17.1 Starting from Bare Ground (Spin-up)

17.2 Starting from Spun-up Initial Conditions

18 Input Requirements

18.1 Surface Dataset

18.2 Landcover Description

18.3 Plant Physiological Parameters

18.4 Nitrogen Deposition

18.5 CO_2 Concentration

19 Benchmark Simulation: 1984-2004

19.1 Run Description

19.1.1 Initial Conditions

19.1.2 Surface Dataset

19.1.3 Landcover Description

19.1.4 Plant Physiological Parameters

19.1.5 Nitrogen Deposition

19.1.6 CO_2 Concentration

19.2 Output Summary

19.3 Evaluation Against Observations

19.4 Benchmark Simulation Archive

20 References

Aber, J.D., Melillo, J.M. and McClaugherty, C.A., 1990. Predicting long-term patterns of mass loss, nitrogen dynamics, and soil organic matter formation from initial fime litter chemistry in temperate forest ecosystems. Canadian Journal of Botany, 68: 2201-2208.

Allen, C.B., Will, R.E. and Jacobson, M.A., 2005. Production efficiency and radiation use efficiency of four tree species receiving irrigation and fertilization. Forest Science, 51(6): 556-569.

Andrén, O. and Paustian, K., 1987. Barley straw decomposition in the field: a comparison of models. Ecology, 68(5): 1190-1200.

Axelsson, E. and Axelsson, B., 1986. Changes in carbon allocation patterns in spruce and pine trees following irrigation and fertilization. Tree Physiology, 2: 189-204.

Bonan, G.B., 1996. A Land Surface Model (LSM version 1.0) for Ecological, Hydrological, and Atmospheric Studies: Technical Description and User's Guide. NCAR/TN-417+STR, National Center for Atmospheric Research, Boulder, CO.

Bonan, G.B., 1998. The land surface climatology for the NCAR land surface model coupled to the NCAR Community Climate Model. Journal of Climate, 11: 1307-1326.

Bonan, G.B. et al., 2002. The land surface climatology of the Community Land Model coupled to the NCAR Community Climate Model. Journal of Climate, 15: 3123-3149.

Busing, R.T., 2005. Tree mortality, canopy turnover, and woody detritus in old cove forests of the southern Appalachians. Ecology, 86(1): 73-84.

Churkina, G. et al., 2003. Analyzing the ecosystem carbon dynamics of four European coniferous forests using a biogeochemistry model. Ecosystems, 6: 168-184.

Cleveland, C.C. et al., 1999. Global patterns of terrestrial biological nitrogen (N_2) fixation in natural ecosystems. Global Biogeochemical Cycles, 13(2): 623-645.

Cosby, B.J., Hornberger, G.M., Clapp, R.B. and Ginn, T.R., 1984. A statistical exploration of the relationships of soil moisture characteristics to the physical properties of soils. Water Resources Research, 20: 682-690.

Dai, Y., Dickinson, R.E. and Wang, Y.-P., 2004. A two-big-leaf model for canopy temperature, photosynthesis, and stomatal conductance. Journal of Climate, 17: 2281-2299.

Dai, Y. et al., 2003. The Common Land Model. Bulletin of the American Meteorological Society, 84: 1013-1023.

Degens, B. and Sparling, G., 1996. Changes in aggregation do not correspond with changes in labile organic C fractions in soil amended with ^{14}C-glucose. Soil Biology and Biochemistry, 28(4/5): 453-462.

Dickinson, R.E. et al., 2006. The Community Land Model and its climate statistics as a component of the Community Climate System Model. Journal of Climate, 19: 2302-2324.

Feddema, J. et al., 2005. The importance of land-cover change in simulating future climates. Science, 310(5754): 1674-1678.

Ferrari, J.B., 1999. Fine-scale patterns of leaf litterfall and nitrogen cycling in an old-growth forest. Canadian Journal of Forest Research, 29: 291-302.

Field, C., Merino, J. and Mooney, H.A., 1983. Compromises between water-use efficiency and nitrogen-use efficiency in five species of California evergreens. Oecologia, 60: 384-389.

Forster, P. et al., 2007. Changes in atmospheric constituents and in radiative forcing. In: S. Solomon et al. (Editors), Climate Change 2007: The Physical Science Basis. Contribution of Working Group I to the Fourth Assessment Report of the Intergovernmental Panel on Climate Change. Cambridge University Press, Cambridge, United Kingdom and New York, NY, U.S.A.

Friedlingstein, P. et al., 2006. Climate-carbon cycle feedback analysis: results from the C^{4}MIP model intercomparison. Journal of Climate, 19: 3337-3353.

Galloway, J.N. et al., 2004. Nitrogen cycles: past, present, and future. Biogeochemistry, 70: 153-226.

Gholz, H.L., Perry, C.S., Cropper, W.P., Jr. and Hendry, L.C., 1985. Litterfall, decomposition, and nitrogen and phosphorous dynamics in a chronosequence of slash pine (*Pinus elliottii*) plantations. Forest Science, 31(2): 463-478.

Gomes, E.P.C., Mantovani, W. and Kageyama, P.Y., 2003. Mortality and recruitment of trees in a secondary montane rain forest in southeastern Brazil. Brazilian Journal of Biology, 63(1): 47-60.

Houghton, R.A. et al., 1983. Changes in the carbon content of terrestrial biota and soils between 1860 and 1980: a net release of CO_2 to the atmosphere. Ecological Monographs, 53: 235-262.

Hunt, E.R., Jr. et al., 1996. Global net carbon exchange and intra-annual atmospheric CO_2 concentrations predicted by an ecosystem process model and three-dimensional atmospheric transport model. Global Biogeochemical Cycles, 10(3): 431-456.

Hunt, E.R., Jr. and Running, S.W., 1992. Simulated dry matter yields for aspen and spruce stands in the north american boreal forest. Canadian Journal of Remote Sensing, 18(3): 126-133.

Hurtt, G.C. et al., 2006. The underpinnings of land-use history: three centuries of global gridded land-use transitions, wood harvest activity, and resulting secondary lands. Global Change Biology, 12: 1-22.

Keller, M., Palace, M., Asner, G.P., Pereira, R., Jr. and Silva, J.N.M., 2004. Coarse woody debris in undisturbed and logged forests in the eastern Brazilian Amazon. Global Change Biology, 10: 784-795.

Kimball, J.S., Thornton, P.E., White, M.A. and Running, S.W., 1997. Simulating forest productivity and surface-atmosphere exchange in the BOREAS study region. Tree Physiology, 17: 589-599.

Kuehn, G.D. and McFadden, B.A., 1969. Ribulose 1,5-diphosphate carboxylase from *Hydrogenomonas eutropha* and *Hydrogenomonas facilis*. II. Molecular weight, subunits, composition, and sulfhydryl groups. Biochemistry Journal, 8: 2403-2408.

Ladd, J.N., Jocteur-Monrozier, L. and Amato, M., 1992. Carbon turnover and nitrogen transformations in an alfisol and vertisol amended with [U-^{14}C] glucose and [^{15}N] ammonium sulfate. Soil Biology and Biochemistry, 24(4): 359-371.

Larcher, W., 1995. Physiological Plant Ecology. Springer-Verlag, Berlin Heidelberg.

Lavigne, M.B. and Ryan, M.G., 1997. Growth and maintenance respiration rates of aspen, black spruce, and jack pine stems at northern and southern BOREAS sites. Tree Physiology, 17: 543-551.

Law, B.E., Sun, O.J., Campbell, J., Van Tuyl, S. and Thornton, P.E., 2003. Changes in carbon storage and fluxes in a chronosequence of ponderosa pine. Global Change Biology, 9(4): 510-514.

Lawrence, D.M., Thornton, P.E., Oleson, K.W. and Bonan, G.B., 2007. The partitioning of evapotranspiration into transpiration, soil evaporation, and canopy evaporation in a GCM: impacts on land-atmosphere interaction. Journal of Hydrometeorology, 8(4): 862-880.

Levis, S., Bonan, G.B., Vertenstein, M. and Oleson, K.W., 2004. The community land model's dynamic global vegetation model (CLM-DGVM): technical description and user's guide. NCAR Tech Note NCARTN-459+IA

NCAR, Boulder, CO.

Lloyd, J. and Taylor, J.A., 1994. On the temperature dependence of soil respiration. Functional Ecology, 8: 315-323.

Magill, A.H. et al., 1997. Biogeochemical response of forest ecosystems to simulated chronic nitrogen deposition. Ecological Applications, 7(2): 402-415.

Martin, J.P., Haider, K. and Kassim, G., 1980. Biodegradation and stabilization after 2 years of specific crop, lignin, and polysaccharide carbons in soils. Soil Science Society of America Journal, 44: 1250-1255.

Mary, B., Fresneau, C., Morel, J.L. and Mariotti, A., 1993. C and N cycling during decomposition of root mucilage, roots and glucose in soil. Soil Biology and Biochemistry, 25(8): 1005-1014.

McGuire, A.D. et al., 2001. Carbon balance of the terrestrial bioshpere in the twentieth century: analyses of CO_2, climate and land use effects with four process-based ecosystem models. Global Biogeochemical Cycles, 15(1): 183-206.

Melzer, E. and O'Leary, M.H., 1987. Anapleurotic CO_2 fixation by phosphoenolpyruvate carboxylase in C3 plants. Plant Physiology, 84: 58-60.

Nakicenovic, N. and Swart, R. (Editors), 2000. Special Report on Emissions Scenarios. Cambridge University Press, Cambridge, United Kingdom, 612 pp.

Neff, J.C., Harden, J.W. and Gleixner, G., 2005. Fire effects on soil organic matter content, composition, and nutrients in boreal interior Alaska. Canadian Journal of Forest Research-Revue Canadienne De Recherche Forestiere, 35(9): 2178-2187.

Niinemets, Ü. and Tenhunen, J.D., 1997. A model separating leaf structural and physiological effects on carbon gain along light gradients for the shade-tolerant species *Acer saccharum*. Plant, Cell and Environment, 20: 845-866.
Oikawa, S., Hikosaka, K. and Hirose, T., 2005. Dynamics of leaf area and nitrogen in the canopy of an annual herb, Xanthium canadense. Oecologia, 143(4): 517-526.
Oleson, K.W. et al., 2004. Technical description of the Community Land Model (CLM). NCAR Tech Note NCARTN-461+STR, NCAR, Boulder.
Oleson, K.W. et al., 2010. Technical Description of version 4.0 of the Community Land Model (CLM). NCAR Technical Note, NCAR/TN-478+STR, 257 pp.
Oleson, K.W. et al., in press. Improvements to the Community Land Model and their impact on the hydrological cycle. Journal of Geophysical Research, xx(xx): xx-xx.
Olson, J.S., 1963. Energy storage and the balance of producers and decomposers in ecological systems. Ecology, 44(2): 322-331.
Orchard, V.A. and Cook, F.J., 1983. Relationship between soil respiration and soil moisture. Soil Biology and Biochemistry, 15(4): 447-453.
Parton, W.J. et al., 1993. Observations and modeling of biomass and soil organic matter dynamics for the grassland biome worlwide. Global Biogeochemical Cycles, 7(4): 785-809.
Running, S.W. and Coughlan, J.C., 1988. A general model of forest ecosystem processes for regional applications. I. Hydrological balance, canopy gas exchange and primary production processes. Ecological Modelling, 42: 125-154.
Running, S.W. and Gower, S.T., 1991. FOREST BGC, A general model of forest ecosystem processes for regional applications. II. Dynamic carbon allocation and nitrogen budgets. Tree Physiology, 9: 147-160.
Running, S.W. and Hunt, E.R., Jr., 1993. Generalization of a forest ecosystem process model for other biomes, BIOME-BGC, and an applicationfor global-scale models. In: J.R. Ehleringer and C. Field (Editors), Scaling Physiological Processes: Leaf to Globe. Academic Press, San Diego, CA, pp. 141-158.
Running, S.W. et al., 1989. Mapping regional forest evapotranspiration and photosynthesis by coupling satellite data with ecosystem simlation. Ecology, 70(4): 1090-1101.
Ryan, M.G., 1991. A simple method for estimating gross carbon budgets for vegetation in forest ecosystems. Tree Physiology, 9: 255-266.
Saggar, S., Tate, K.R., Feltham, C.W., Childs, C.W. and Parshotam, A., 1994. Carbon turnover in a range of allophanic soils amended with ^{14}C-labelled glucose. Soil Biology and Biochemistry, 26(9): 1263-1271.
Schlesinger, W.H., 1997. Biogeochemistry: an analysis of global change. Academic Press, London, 588 pp.
Smith, A.M.S., Wooster, M.J., Drake, N.A., Dipotso, F.M. and Perry, G.L.W., 2005. Fire in African savanna: Testing the impact of incomplete combustion on pyrogenic emissions estimates. Ecological Applications, 15(3): 1074-1082.
Smith, S.J. and Wigley, T.M.L., 2006. Multi-gas forcing stabilization with the MiniCAM. Multigas Mitigation and Climate Policy. The Energy Journal Special Issue.
Sollins, P., 1982. Input and decay of coarse woody debris in coniferous stands in western Oregon and Washington. Canadian Journal of Forest Research, 12: 18-28.

Son, Y. and Gower, S.T., 1991. Aboveground nitrogen and phosphorus use by five plantation-grown trees with different leaf longevities. Biogeochemistry, 14: 167-191.

Sørensen, L.H., 1981. Carbon-nitrogen relationships during the humification of cellulose in soils containing different amounts of clay. Soil Biology and Biochemistry, 13: 313-321.

Sprugel, D.G., Ryan, M.G., Brooks, J.R., Vogt, K.A. and Martin, T.A., 1995. Respiration from the organ level to stand level. In: W.K. Smith and T.M. Hinkley (Editors), Resource Physiology of Conifers. Academic Press, San Diego,CA, pp. 255-299.

Stephens, B.B. et al., 2007. Weak northern and strong tropical land carbon uptake from vertical profiles of atmospheric CO_2. Science, 316: 1732-1735.

Stöckli, R. et al., in press. The use of FLUXNET in the Community Land Model development. Journal of Geophysical Research, xx(xx): xx-xx.

Taylor, B.R., Parkinson, D. and Parsons, W.F.J., 1989. Nitrogen and lignin content as predictors of litter decay rates: A microcosm test. Ecology, 70(1): 97-104.

Thonicke, K., Venevsky, S., Sitch, S. and Cramer, W., 2001. The role of fire disturbance for global vegetation dynamics: coupling fire into a Dynamic Global Vegetation Model. Global Ecology and Biogeography, 10: 661-667.

Thornton, P.E., 1998. Regional ecosystem simulation: combining surface- and satellite-based observations to study linkages between terrestrial energy and mass budgets. Ph.D. Thesis, The University of Montana, Missoula, 280 pp.

Thornton, P.E., Lamarque, J.-F., Rosenbloom, N.A. and Mahowald, N., in press. Influence of carbon-nitrogen cycle coupling on land model response to CO2 fertilization and climate variability. Global Biogeochemical Cycles.

Thornton, P.E. et al., 2002. Modeling and measuring the effects of disturbance history and climate on carbon and water budgets in evergreen needleleaf forests. Agricultural and Forest Meteorology, 113: 185-222.

Thornton, P.E. and Rosenbloom, N.A., 2005. Ecosystem model spin-up: estimating steady state conditions in a coupled terrestrial carbon and nitrogen cycle model. Ecological Modelling, 189(1/2): 25-48.

Thornton, P.E. and Zimmermann, N.E., 2007. An improved canopy integration scheme for a land surface model with prognostic canopy structure. Journal of Climate, 20(15): 3902-3923.

Tye, A.M. et al., 2005. The fate of N-15 added to high Arctic tundra to mimic increased inputs of atmospheric nitrogen released from a melting snowpack. Global Change Biology, 11(10): 1640-1654.

Vallano, D.M. and Sparks, J.P., 2007. Quantifying foliar uptake of gaseous itrogen dioxide using enriched foliar δ^{15}N values. New Phytologist (OnlineEarly Articles), doi: 10.1111/j.1469-8137.2007.02311.x.

van Veen, J.A., Ladd, J.N. and Frissel, M.J., 1984. Modelling C and N turnover through the microbial biomass in soil. Plant and Soil, 76: 257-274.

Van Vuuren, D.P. et al., 2007. Stabilizing greenhouse gas concentrations at low levels: an assessment of reduction strategies and costs. Climatic Change, 81: 119-159.

Vanninen, P. and Makela, A., 2005. Carbon budget for Scots pine trees: effects of size, competition and site fertility on growth allocation and production. Tree Physiology, 25(1): 17-30.

White, M.A., Thornton, P.E. and Running, S.W., 1997. A continental phenology model for monitoring vegetation responses to interannual climatic variability. Global Biogeochemical Cycles, 11(2): 217-234.

White, M.A., Thornton, P.E., Running, S.W. and Nemani, R.R., 2000. Parameterization and sensitivity analysis of the Biome-BGC terrestrial ecosystem model: net primary production controls. Earth Interactions, 4(3): 1-85.

Woodrow, I.E. and Berry, J.A., 1988. Enzymatic regulation of photosynthetic CO_2 fixation in C_3 plants. Annual Reviews of Plant Physiology and Plant Molecular Biology, 39: 533-594.

Wullschleger, S.D., 1993. Biochemical limitations to carbon assimilation in C_3 plants - A retrospective analysis of the A/C_i curves from 109 species. Journal of Experimental Botany, 44(262): 907-920.

Zeng, X., Shaikh, M., Dai, Y., Dickinson, R.E. and Myneni, R., 2002. Coupling of the Common Land Model to the NCAR Community Climate Model. Journal of Climate, 15: 1832-1854.